DRAFT TECHNICAL MEMORANDUM

OVERVIEW OF METHODS, MODELS, AND RESULTS TO DEVELOP UNIMPAIRED, IMPAIRED, and FUTURE FLOW AND TEMPERATURE ESTIMATES ALONG LOWER ALAMEDA CREEK FOR HYDROLOGIC YEARS 1996-2009

Prepared for:

Alameda Creek Fisheries Workgroup - Flows Subcommittee

Prepared by:

Amod S. Dhakal
San Francisco Water, Power and Sewer Services of the San Francisco Public Utilities Commission

Evan Buckland
Alameda County Water District

Scott McBain
McBain and Trush, Inc.

April 13, 2012

This page intentionally left blank

TABLE OF CONTENTS

Table of Contents (continued) Page

LIST OF FIGURES

List of Figures (continued) Page

List of Figures (continued) Page

LIST OF TABLES

Page

ABBREVIATIONS AND ACRONYMS

ACDD	Alameda Creek Diversion Dam
ACFCD	Alameda County Flood Control District
ACFCC	Alameda County Flood Control Channel
ACPWA	Alameda County Public Works Agency
ACWD	Alameda County Water District
ASDHM	Alameda System Daily Hydrologic Model
BO	Biological Opinion
CDFG	California Department of Fish and Game
CDRP	Calaveras Dam Replacement Project
CFS	Cubic Feet per Second
CY	Calendar Year (January 1-December 31)
DSOD	California Division of Safety of Dams
EDT	Ecosystem Diagnosis and Treatment mode
GWRF	ACWD’s Ground Water Recharge Facilities
HCP	Habitat Conservation Plan
HEC-RAS	Hydrologic Engineering Center, River Analysis System
HEC-HMS	Hydrologic Engineering Center, Hydrologic Modeling System
HHLSM	Hetch Hetchy Local Simulation Model
HY	Hydrologic year (October 1-September 30), same as Water Year
MAE	Mean Absolute Error
NGD	Number of Good Days model
NMFS	National Marine Fisheries Service
PB	Percent Bias
Q	daily average streamflow
SBA	South Bay Aqueduct, delivers water from San Joaquin Delta via State Water Project
SFPUC	San Francisco Public Utilities Commission
SMP	Surface Mining Permit
SRA	Spawning Risk Assessment model
SVTP	Sunol Valley (water) Treatment Plant
USGS	United States Geological Survey

ACKNOWLEDGEMENTS

A wide range of individuals provided important field and monitoring data to support this report. Scott Chenue and Laura Kidd of the SFPUC Natural Resources Division provided flow and water temperature measurement data critical for flow loss estimates and water temperature model calibration. Mike Webster and Stuart Hill of the USGS provided context to USGS gaging records, and valuable and timely updates to flow data for use in the ASDHM and HEC-RAS models. Frank Codd and Danli Li of the Alameda County Public Works Agency provided storm drain and drainage area information for the Niles Cone reach. Hanson Aggregates provided quarry pumping data for inclusion in the ASDHM model. Lastly, the authors express their gratitude to the Alameda Creek Fisheries Workgroup Flows Subcommittee and participating agencies for providing staff time, reviewing draft results, and making this report possible.

1 INTRODUCTION

The Alameda Creek Fisheries Workgroup, and the agencies and stakeholders that comprise the Workgroup, are attempting to recover steelhead (*Oncorhyncus mykiss*) populations in the Alameda Creek watershed. At the direction of the Workgroup, an overall Study Plan was completed in January 2008 that identified ten "Elements" to address priority management issues associated with steelhead recovery (M&T 2008). This report satisfies two of those Elements: Study Plan Element #5 and Study Plan Element #8. Study Plan Element #5 was to conduct water temperature monitoring and develop a water temperature model, and Study Plan Element #8 was to develop a water operations model and data management. Information provided by these two Elements would feed into a variety of other Elements, including Element #1 (Quantification of Steelhead Habitat), Element #2 (Adult Steelhead Passage Assessment), and others. The immediate use is intended to be the three studies underway that address Element #1 and Element #2: Ecosystem Diagnosis and Treatment (EDT), the Number of Good Days (NGD), and the Spawning Risk Assessment (SRA). The EDT analysis is being conducted by ICF International as part of the San Francisco Public Utilities Commission (SFPUC) Habitat Conservation Plan effort for Alameda Creek. The NGD and SRA analyses are being conducted by McBain & Trush, Inc. (M&T) on behalf of the Alameda Creek Fisheries Workgroup. These analyses require information on hydrology, water temperature, and channel geometry for a variety of management scenarios, and this information does not currently exist for most scenarios.

Alameda Creek has a growing amount of hydrologic and water temperature data being collected by various organizations. The U.S. Geological Survey (USGS) and Spring Valley Water District (later acquired by the City of San Francisco) had several gaging stations on Alameda Creek and Arroyo de la Laguna (and tributaries) that provide useful insights to unimpaired flows. Beginning in the late 1990's, USGS installed additional gaging stations in the upper Alameda Creek watershed, greatly improving the recent hydrologic record. Then, beginning in 2001, Alameda County Water District (ACWD), SFPUC, and the Zone 7 Water Agency (Zone 7) began conducting water temperature monitoring on Alameda Creek and Arroyo de la Laguna (and tributaries), but this monitoring was conducted mostly in the summer months rather than continuously through the entire year. The 2008 Study Plan recommended that water temperature monitoring locations be expanded and monitoring be conducted year-round. Since 2008, the SFPUC has conducted continuous, 30-minute increment water temperature monitoring at 26 locations; in addition, USGS is now collecting water temperature at most of their gaging stations, and ACWD is collecting continuous water temperature data on Vallecitos Creek.

The EDT, NGD, and SRA efforts will be analyzing a variety of scenarios that include unimpaired conditions, impaired conditions, and future conditions. Despite the wealth of available flow and water temperature data, there are many data gaps that need to be filled to analyze the range of scenarios. Specifically, flows and water temperatures are needed on a daily time step for the various flow management scenarios described in Section 1.4 between Alameda Creek Diversion Dam (ACDD) and San Francisco Bay. There are many challenges to developing these data, including:

- The Alameda Creek watershed is highly regulated, with many import (e.g., Hetch Hetchy, South Bay Aqueduct) and export locations.
- Land use and associated rainfall-runoff processes are highly variable within the Alameda Creek and Arroyo de la Laguna watersheds.
    - Rainfall-runoff patterns vary widely in the watershed due to strong rain shadow effects, and the available precipitation data do not adequately capture the spatial heterogeneity.

- Despite the large number of gages and reservoir management records, most data sources do not go back to early dates that reflect true unimpaired conditions.
- There are uncertainties about infiltration losses in the Sunol Valley, and how these losses may have evolved over time, and how they may change in the future.
- The number of currently operating USGS gaging stations is considerably less in the Arroyo de la Laguna portion of the watershed, making flow contributions from Arroyo de la Laguna less certain, particularly for the Unimpaired scenario.
- Daily average streamflow data on San Antonio Creek upstream of San Antonio Reservoir, ideally to be used for unimpaired flow estimates, do not exist, and streamflow data downstream of San Antonio Dam used for impaired flow estimates do not exist prior to 10/1/1999. Likewise, impaired streamflow data downstream of Calaveras Dam do not exist prior to 5/23/2002.
- Rainfall and other meteorological information, used for the water temperature model, is scarce in the Arroyo de la Laguna watershed, and there are gaps in the available data for many stations that limit the number of stations that can be used.

1.1 Goal and objectives

The overall goal is to develop predictive models that estimate streamflows and water temperatures at different locations along Alameda Creek on a daily time step over the hydrologic year (HY) 1996-2009 time series. In the near term (December 2011 to February 2012), these predictions will be used as input data to the EDT model, NGD model, and SRA model. Objectives and tasks to achieve this goal include:

1. Develop a robust mass balance hydrologic model to predict streamflows at different locations along Alameda Creek on a daily time step from ACDD to San Francisco Bay;
2. Develop a steady-state hydraulic model to predict hydraulic geometry relationships (width, depth, velocity, etc.) as a function of flow at all cross sections along Alameda Creek;
3. Develop a water quality model to predict water temperature on a daily time step for the 1996-2009 time series for all Scenarios.

The models should be able to help game scenarios, to understand Sunol Valley hydrology, and to evaluate future SFPUC operations, as well as predict streamflows at Niles gage, to provide input to ACWD operations model on a daily time step.

1.2 Spatial extent and analytical nodes

This effort focuses on ACDD downstream to San Francisco Bay, and computes flow and water temperature at 12 nodes between these two locations (Figure 1 and Table 1). Arroyo de la Laguna, at the confluence with Alameda Creek, is almost twice the drainage area as Alameda Creek upstream of the confluence. However, for this initial effort, Arroyo de la Laguna is treated as a single input, and no further detail (i.e., nodes) is provided within the watershed. We expect to expand into Arroyo de la Laguna with additional nodes at a later time.

1.3 Analysis period

Continuous gaging stations on Alameda Creek were expanded by USGS beginning in HY1996, and continue to expand based on efforts by the SFPUC, ACWD, Zone 7, and other agencies. Table 2 summarizes the available streamflow gaging stations and their period of record. Based on this availability of hydrologic data, the HY1996-2009 time series was chosen, and the hydrologic and water temperature models were applied to predict flows and water temperatures for the various scenarios on a daily time step. All scenarios use the HY1996-2009 time series, with the exception of the measured impaired scenario (Scenario 4), which uses the HY2000-2009 time series due to data limitations prior to HY2000.

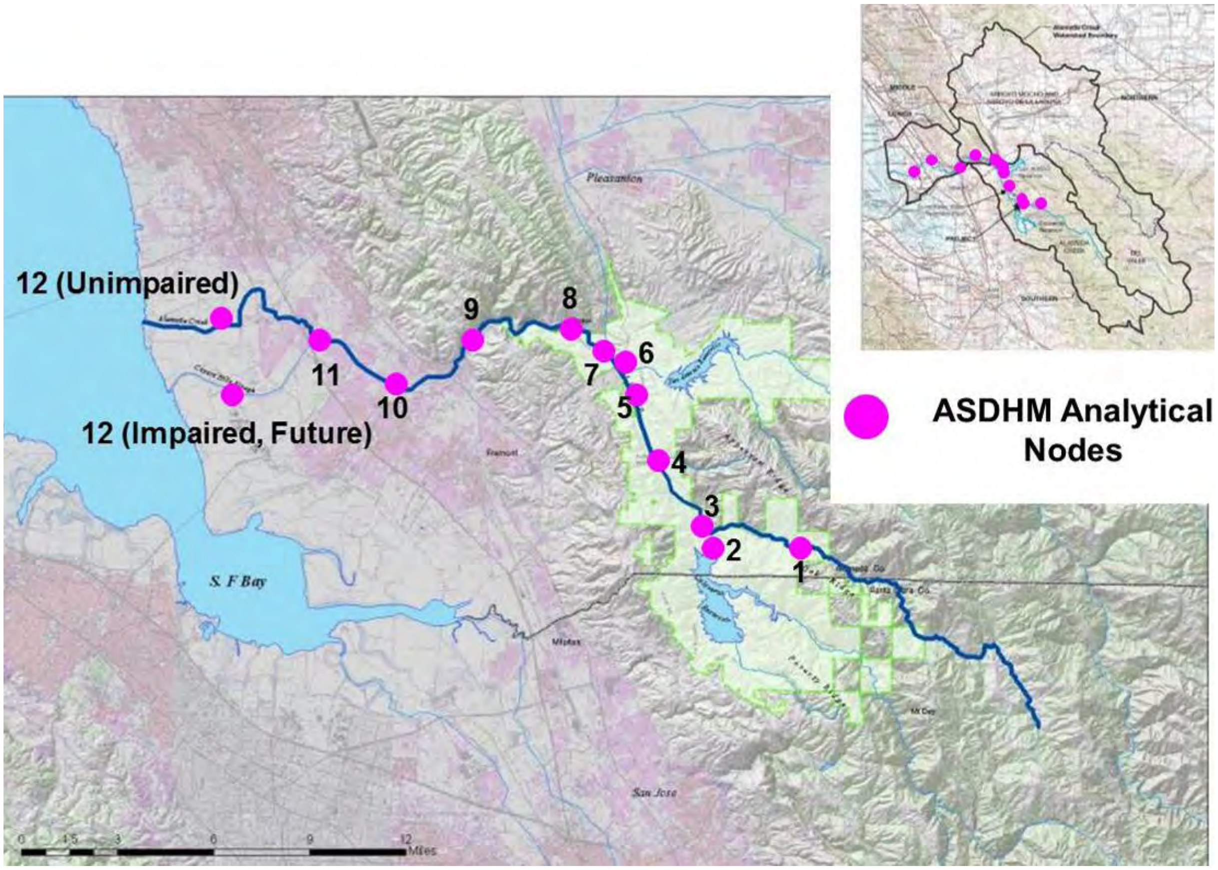

Figure 1. Spatial extent of hydrology, hydraulic, and water temperature modeling efforts, and ASDHM analytical nodes where flow computations are summarized by the various scenarios.

Table 1. Description of analytical node locations on mainstem Alameda Creek.

Node	Location (common name)
1	At ACDD and USGS gaging station above ACDD
2	At USGS Calaveras Creek gaging station (Calaveras gage)
3	At USGS Alameda Creek below Calaveras Creek gaging station (Confluence gage)
4	At USGS Alameda Creek below Welch Creek gaging station (Welch Creek gage)
5	Immediately upstream of San Antonio Creek confluence
6	Immediately downstream of San Antonio Creek confluence, upstream of gravel quarry discharge point
7	Immediately upstream of Arroyo de la Laguna confluence
8	Immediately downstream of Arroyo de la Laguna confluence
9	At USGS Alameda Creek near Niles gaging station (Niles gage)
10	At base of ACWD Rubber Dam #2
11	At USGS Alameda Creek near Union City gaging station (Flood Channel gage)
12	At Coyote Hills Regional Park

Table 2. Summary of available streamflow hydrology data used in the ASDHM model for various scenarios. Unless noted, all data are published at a daily time step.

USGS gage number	Station name (common name)	Drainage area (mi^2)	Period of record (hydrologic year)
11-172945	USGS Alameda Creek Above Diversion Dam (Above ACDD gage)	33.3	1995-present
11-173200	USGS Arroyo Hondo near San Jose (Arroyo Hondo gage)	77.1	1969-1981, 1995-present
11-173000	USGS Alameda Creek near Sunol (Sunol gage)	37.5	1912-1930
11-173500	USGS Calaveras Creek near Sunol (Calaveras gage)	98.7	1898-1908, 1910-1930, 2002-present
11-173510	USGS Alameda Creek below Calaveras Creek near Sunol (Confluence gage)	135.0	1996-present
11-173575	USGS Alameda Creek below Welch Creek near Sunol (Welch Creek gage)	145.0	2000-present
11-174000	USGS San Antonio Creek near Sunol (San Antonio Creek gage)	37.0	1912-1930, 1960-1965, 2000-present
N/A	Gravel Quarry pumping flows from Hansen Aggregates	N/A	2000-present (mixture of monthly, weekly, and daily data)
N/A	South Bay Aqueduct (SBA) deliveries to Vallecitos Creek turnout from ACWD	N/A	1996-present
11-176000	USGS Arroyo Mocho near Livermore (Arroyo Mocho gage)	38.2	1912-1930, 1964-2002
11-176900	USGS Arroyo de la Laguna near Verona (Verona gage)	403.0	1912-1919, 1921-1930, 1970-1983, 1988-present
11-179000	USGS Alameda Creek near Niles (Niles gage)	633.0	1891-present
11-180500	USGS Dry Creek at Union City (Dry Creek gage)	9.4	1917-1919, 1959-present
11-180700	USGS Alameda Creek Flood Channel at Union City (Union City gage)	639.0	1959-present

1.4 Scenarios

Six initial hydrology scenarios were developed as part of the SFPUC Habitat Conservation Plan (HCP) process (Table 3). The ASDHM modeling effort can simulate all six hydrologic scenarios; however, subsequent discussion with regulatory agencies has focused the analysis to Hydrologic Scenarios 1, 2, 5, and 6. Scenario 4 may be analyzed in the future, so model outputs for Scenario 4 have been generated from the ASDHM and HEC-RAS models. Hydrologic Scenario 3 only has output from the ASDHM model, but is not reported here. From this section forward, the term "Scenario" will refer to the hydrologic scenarios listed in Table 3.

The various scenarios have been developed for EDT and NGD to make comparisons between future conditions and various historic scenarios (impaired and unimpaired). There are two impaired scenarios (Scenario 4 and Scenario 6) to account for the California Division of Safety of Dams (DSOD) operational restrictions on Calaveras Dam. Beginning in 2001, storage volumes in Calaveras Dam have been restricted to be approximately 30% of capacity, which has resulted in higher streamflows below ACDD and Calaveras Dam than typical operations. Because the change in operations in 2001 occurred mid-way through the HY1996-2009 time series, observed impaired flows

(Scenario 4) are not reflective of what normal operations would have been without the DSOD restrictions, and thus comparisons to future flow scenarios would have produced unrealistic results. Therefore, an additional Scenario 6 was added to predict flows and water temperatures that would have occurred under actual operations without the DSOD restrictions, which would represent a more valid comparison with Scenario 5.

Table 3. Summary of Scenarios used by EDT and NGD-SRA analyses.

Scenario number	Hydrology scenarios	EDT scenarios/application	NGD and SRA application
1	Unimpaired Alameda Creek + Impaired Arroyo de la Laguna (Simulation Period: HY1996-2009)	Template: Baseline for HCP Impact Analysis	Not used
2	Unimpaired everywhere (Simulation Period: HY1996-2009)	Pre-Dam: Provide context and inform Conservation Measures	Used to compare future impaired results
3	1995 MOU flows on AC, measured impaired on Arroyo de la Laguna (Simulation Period: HY1996-2009)	Not used	Not used
4	Measured impaired everywhere (Simulation Period: HY2000-2009)	Probably not used	Not used
5	Future SFPUC Conservation Strategy + ACWD proposed flows + impaired Arroyo de la Laguna (Simulation Period: HY1996-2009)	Conservation Flows: Assess the extent to which take is mitigated by Conservation Strategy	Used to evaluate improvements over unimpaired and computed impaired
6	Computed impaired on AC + impaired Arroyo de la Laguna) (Simulation Period: HY1996-2009)*	Covered Activities: Estimate take	Used to compare future impaired results
6	Computed impaired on AC + impaired Arroyo de la Laguna) (Simulation Period: HY1996-2009)*	Unimpeded Passage: Provide context and inform Conservation Measures	N/A

* There is no difference in hydrology between the two Scenario 6 EDT Scenario/Application options.

Each scenario had unique hydrologic and operational assumptions, and the rationale for those combinations of assumptions is based on the needs of the EDT and NGD analyses. The basic assumption options are listed below, with more detailed assumptions in Appendix A:

- Whether upper Alameda Creek and/or Arroyo de la Laguna was unimpaired or impaired.
- Operations at ACDD: No diversion (unimpaired, Scenario 1 and Scenario 2), variably operational influenced by DSOD restrictions (Scenario 4), hypothetical typical diversions without DSOD restrictions (Scenario 6), and future typical diversions (Scenario 5).
- Operations at Calaveras Dam: No storage (unimpaired, Scenario 1 and Scenario 2), operations influenced by DSOD restrictions (Scenario 4), hypothetical typical operations without DSOD restrictions (Scenario 6), and future operations (Scenario 5).
- Sunol Valley loss/gain: Zero losses/gains (unimpaired, Scenario 1 and Scenario 2) and 17 cfs infiltration loss (Scenarios 4, 5, and 6) with no downstream return (Scenario 5 and Scenario 6) or downstream return represented by measured Gravel Quarry pumping (Scenario 4). Natural downstream return flow is omitted in all scenarios.
- Operations at ACWD: no diversion (unimpaired, Scenario 1), measured historic diversions (Scenario 4 and Scenario 6), and future typical diversions (Scenario 6).

The specific assumptions for each scenario are discussed in Table 4.

Table 4. Summary of hydrologic assumptions for each of the six Scenarios developed by the ASDHM model for EDT and NGD analyses.

Scenario number	Hydrology scenario	ACDD assumption[1]	Calaveras Dam assumption[2]	Sunol Valley loss/gain assumption	San Antonio Creek assumption	Arroyo de la Laguna assumption	ACWD assumption[3]
1	unimpaired Alameda Creek + impaired Arroyo de la Laguna (Simulation Period: HY1996-2009)	measured unimpaired (Above ACDD gage)	computed unimpaired	zero losses, zero gains	computed unimpaired	measured impaired (Verona gage+SBA deliveries)	measured impaired (Node 9 ➔ Node 11 ➔ Node 10)
2	unimpaired everywhere (Simulation Period: HY1996-2009)	measured unimpaired (Above ACDD gage)	computed unimpaired	zero losses, zero gains	computed unimpaired	computed unimpaired (with caveats)	computed unimpaired
3	MOU + impaired Arroyo de la Laguna (Simulation Period: HY1996-2009)	computed impaired using MOU assumptions on ACDD operational rules (650 cfs max diversion)	computed impaired using MOU assumptions	17 cfs infiltration loss, 0 cfs gravel quarry pumping[5] gain	computed impaired for HY1996-2001, measured impaired for HY2002-2009	measured impaired (Verona gage+SBA deliveries)	measured impaired (Node 9 ➔ Node 11 ➔ Node 10)
4	measured impaired everywhere (Simulation Period: HY2000-2009)	computed measured impaired using available ACDD operations records. No data for HY1996-1999.	measured impaired for HY2000-2009. No data for HY1996-1999.	17 cfs infiltration loss, average of 3 cfs gravel quarry pumping[5] gain	computed impaired for HY1996-1999, measured impaired for HY2000 - 2009	measured impaired (Verona gage+SBA deliveries)	measured impaired (Node 9 ➔ Node 11 ➔ Node 10)
5	future (SFPUC Conservation Strategy + ACWD proposed flows + impaired Arroyo de la Laguna) (Simulation Period: HY1996-2009)	computed future impaired using future instream flow requirement and operational assumptions	computed impaired using future assumptions	17 cfs infiltration loss, 0 cfs gravel quarry pumping[5] gain	computed impaired for HY1996-1999, measured impaired for HY2000 - 2009	measured impaired (Verona gage+SBA deliveries)	measured impaired or ACWD bypass, whichever is more (Node 9 ➔ Node 11 ➔ Node 10)
6	computed impaired on AC + impaired Arroyo de la Laguna) (Simulation Period: HY1996-2009)	computed measured impaired with no instream flow requirement with typical (pre-DSOD) ACDD operational rules (650 cfs max diversion)	computed impaired using typical pre-DSOD operational assumptions. No instream flow requirement.	17 cfs infiltration loss, 0 cfs gravel quarry pumping[5] gain	computed impaired for HY1996-1999, measured impaired for HY2000 - 2009	measured impaired (Verona gage+SBA deliveries)	measured impaired (Node 9 ➔ Node 11 ➔ Node 10)

[1] ACDD is at Node 1
[2] Calaveras Dam is immediately upstream of Node 2
[3] ACWD diversion and infiltration zone is between Node 9 and 10
[4] SBA=South Bay Aqueduct, which is delivered to Vallecitos Creek, which is then added to Arroyo de la Laguna just upstream of the Alameda Creek confluence.
[5] Gravel quarry pumping delivers water immediately downstream of the San Antonio Creek confluence.

1.5 Overview of modeling approach

To achieve the goal described in Section 1.1, we developed four modeling efforts that were designed to be integrative. The overall approach was to first develop the hydrology for the selected scenarios, then, using the output from the hydrology model, develop hydraulic geometry and water temperature relationships based on that hydrology (Figure 2). We investigated HEC-HMS as a tool to develop the hydrology for the various scenarios, but after some comparisons between predicted and observed hydrology, we concluded that HEC-HMS did not provide the needed accuracy for the lower flows (<100 cfs) that were the focus of the EDT and NGD analysis. Therefore, we developed a spreadsheet model, ASDHM, to predict flows on a daily time step for the scenarios shown in Table 3. Three separate spreadsheets comprise the ASDHM: one for unimpaired conditions (Scenario 2), one for measured impaired conditions (Scenario 4), and one for computed impaired and future conditions (Scenarios 1, 5, and 6). Future flow release operations for SFPUC on upper Alameda Creek and ACWD on lower Alameda Creek were incorporated into the ASDHM to develop a future flow scenario (Scenario 5). An estimate of contemporary Sunol Valley flow loss, as measured by SFPUC in 2008, was also incorporated into the ASDHM. The ASDHM future spreadsheet model can facilitate easy development of other scenarios and/or can be used for conducting sensitivity analyses related to flow loses or other processes.

In parallel, a steady-state HEC-RAS hydraulic model was developed from over 120 field-surveyed cross sections between ACDD and San Francisco Bay, and calibrated using USGS and SFPUC gaging station records. The steady-state HEC-RAS model was run for a range of flows, and cross section-specific relationships between local flow and width, depth, velocity, and other parameters were output for use in the EDT analysis. Lastly, the HEC-RAS model was run in unsteady mode for the Scenarios and time series shown in Table 3, and the water quality (water temperature) module within HEC-RAS was used to predict daily average water temperatures at cross sections. These water temperatures were used in both the EDT and NGD analyses.

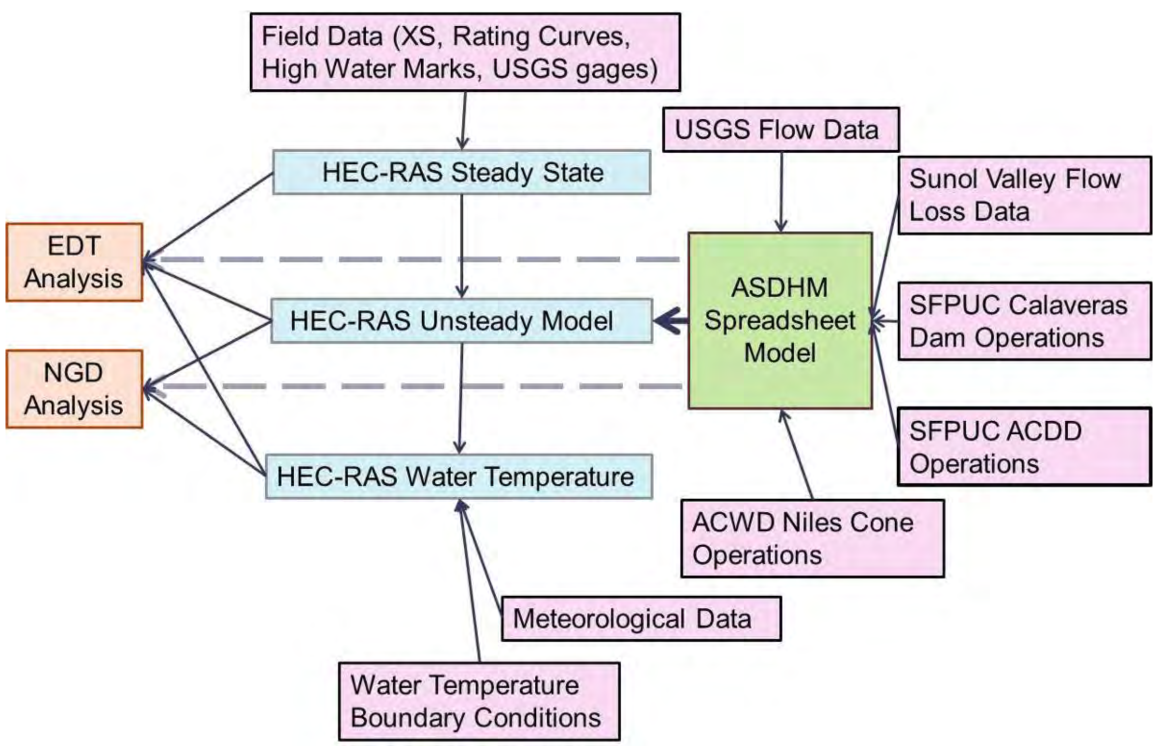

Figure 2. Components of Alameda Creek flow and temperature modeling effort.

2 HYDROLOGIC MODELING

Study Element #8 of the Alameda Creek Study Plan (M&T 2008) focused on developing a water budget model for the Alameda Creek watershed. The Hydrology Subgroup initiated this study element for the portion of Alameda Creek from ACDD to the San Francisco Bay, excluding Arroyo de la Laguna until a later date. The purpose of the "water budget model" evolved with the hydrology needs of EDT and NGD, and a variety of model approaches were explored to meet both the water budgeting need as well as the hydrology needs of the EDT and NGD models. HEC-HMS was initially investigated to evaluate whether it could provide the predictive accuracy needed for the EDT and NGD models. Validation testing with measured impaired hydrology indicated it performed reasonably well for higher flows, but its accuracy for predicting the low flows needed by the EDT and NGD models was insufficient. The ASDHM had improved predictive accuracy at low flows, and the Hydrology Subgroup chose to apply ASDHM rather than HEC-HMS for the needs in Study Element #8. The HEC-HMS model will continue to be used by ACWD in their operational predictions and management.

2.1 ASDHM model overview

ASDHM is a spread sheet model which was first developed in 2009 during the Calaveras Dam Replacement Project (CDRP) permitting process to examine the Alameda Creek future hydrology related to environmental instream flow releases from the new Calaveras Dam. At the time, the system wide Hetch Hetchy Local Simulation Model (HHLSM) with monthly time step was the only available tool to assess operations of SFPUC facilities. Because objectives of the instream flow schedules were to maintain and enhance fish habitats downstream of ACDD and Calaveras Dam, relatively finer resolution hydrology was warranted to evaluate environmental benefits of different instream flow schedules. Therefore, it was necessary to develop a daily model that mimicked the ideal operations of ACDD and Calaveras Dam to assess hydrologic conditions downstream of them. At the confluence of Alameda and Calaveras creeks, about 93% of the watershed consists of regulated watershed. Due to the geographic boundary related to objectives, the initial version of the model did not cover the entire Alameda Creek watershed. When Calaveras Reservoir instream flow releases were agreed upon among SFPUC, National Marine Fisheries Service (NMFS), and the California Department of Fish and Game (CDFG) in June 2010, the ASDHM had been completed up to Node 7, located upstream of Arroyo de la Laguna confluence in Alameda Creek. The model was subsequently extended to San Francisco Bay for EDT and NGD analytical purposes, and to include ACWD proposed flows.

Under the umbrella of ASDHM, three different spreadsheet models have been developed: (1) unimpaired model, (2) measured impaired model, and (3) future scenarios model. While unimpaired and measured impaired models are an "as is" condition computation for the time period considered, the future ASDHM model allows simulation of "what if" scenarios, as varieties of conditions and parameters used as variables in the model can easily be customized. Figure 3 depicts simplified computational procedure employed in ASDHM.

The unimpaired and future ASDHM models can generate daily flows in cfs at 12 locations in Alameda Creek from 10/1/1995 to 9/30/2009, whereas the measured impaired (Scenario 4) ASDHM is limited to the period from 10/1/1999 to 9/30/2009 due to quality of measured streamflow data and incomplete (or missing) historical operational information for upstream dams. For example, the "Confluence gage" immediately downstream of the Calaveras Creek confluence was operated as a low flow gage from HY1996-2006, and only the last few years of data were computed for flows above 200 cfs. In addition, the rating curves for the Confluence and Welch Creek gages frequently shift, adding additional variability in flows at the upper end of Sunol Valley. The future ASDHM provides an option of incorporating SFPUC's future instream flow from Calaveras Dam and ACDD, as well as ACWD proposed bypass flows.

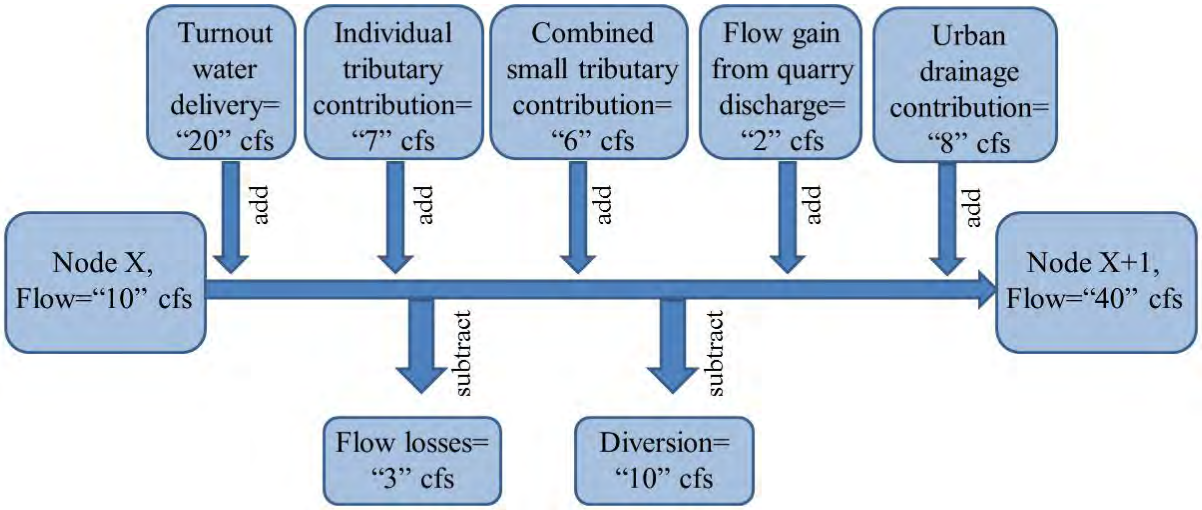

Figure 3. Simplified illustration of computational procedure incorporated in ASDHM.

The hydrologic outputs have currently been generated for six scenarios using ASDHM to facilitate EDT and NGD analyses (Table 3 and Table 4). Out of six scenarios outlined in Table 4, four (Scenarios 1, 3, 5, and 6) use the future ASDHM, in which different inputs or parameters are selected to generate output for different scenarios. Four of the six scenarios are being considered for EDT and NGD analyses, whereas other scenarios (such as Scenario 3 and Scenario 4) provide historical context of hydrologic discussions of Alameda Creek, and EDT or NGD may consider using them (such as Scenario 4) in the future. Table 4 provides a variety of assumptions incorporated at different locations broadly for scenarios considered. These include assumptions related to operations of ACDD and Calaveras Dam, Sunol Valley flow loss, computation of two regulated watersheds (San Antonio and Arroyo de la Laguna creeks), and ACWD operations. These assumptions will be discussed in subsequent sections as well and have also been elaborated in Appendix A on a node by node basis.

2.2 Unimpaired flow computations in Alameda Creek (Scenario 1 and 2)

Consistent with the ASDHM modeling approach, the unimpaired analysis on Alameda Creek was an additive model between computational nodes, which ignored flow routing, travel times, storage, and other hydrodynamic processes (Figure 3). Unimpaired computations for both upper Alameda Creek and Arroyo de la Laguna assume that the early 1900's data used to help generate unimpaired flow estimates reflected unimpaired land use, when in fact considerable changes had already occurred (e.g., draining of the lagoon on Arroyo de la Laguna). With these limitations in mind, the method used or simulated unimpaired flow at a variety of locations on a daily time step for the HY1996-2009 time series. With the exception of Node 1, all nodes had to estimate unimpaired flows for this time series due to lack of data and/or upstream flow regulation. Of the gaging stations listed in Table 2, only the above ACDD gage, Arroyo Hondo gage, Arroyo Mocho gage, and Dry Creek gage were assumed to reflect unimpaired hydrology; all other gages were below flow regulation structures. These unimpaired gages were used extensively to estimate unimpaired flows to the ungaged portions of the watershed between Nodes 1 and 12.

2.2.1 Computational methods

Using the additive method illustrated in Figure 3, the primary methods focus on how unimpaired flows were computed at each node (including contributions between nodes). Some of the gaging stations downstream of existing structures (e.g., Calaveras gage) had some periods of unimpaired flows, and we explored methods to extrapolate those older time series to reflect the HY1996-2009 time series. In all cases, there were too many assumptions required to apply them to the contemporary time series, and thus they primarily served to provide a qualitative comparison with computed unimpaired flows (e.g., are computed unimpaired late summer baseflows in wetter hydrologic years similar to those measured during the unimpaired record?). In most cases, we felt that expansion of HY1996-2009 data at the four unimpaired gages provided a better and more consistent method for estimating unimpaired flows. This expansion was done by a drainage area adjustment as follows (using Above ACDD gage as the example unimpaired gage):

> Drainage area at Above ACDD gage: 33 mi^2
> Drainage area at ungaged tributary: 1.5 mi^2
> Flow (unimpaired) at Above ACDD gage on day X: 10 cfs
> Computed unimpaired flow at ungaged tributary: 10 cfs * (1.5/33.3)=0.45 cfs

The unimpaired gage used to scale to the ungaged tributaries or watershed area between nodes was chosen to best reflect assumed orographic conditions for the ungaged tributary and/or watershed area (Table 5). Gages used to estimate unimpaired flows from tributaries and watershed areas downstream of dams were consistent between the unimpaired, impaired, and future ASDHM computations (i.e., accretion from unregulated watershed areas were computed consistently between the scenarios). Likewise, drainage areas were consistently used between the three ASDHM models, with the exception of unimpaired drainage area between Node 11 and Node 12, where the channel location (and drainage area) had changed when the flood control project was implemented (Figure 4).

Table 5. Summary of unimpaired computations at each node.

Computational node	Methods
Node 1 (Above ACDD gage)	Data obtained directly from USGS gage above ACDD
Node 2 (Calaveras gage)	Drainage area scaled from USGS gage on Arroyo Hondo
Node 3 (Confluence gage)	For period prior to Calaveras gage (10/95-10/99), Node 1 + Node 2 + drainage area scaling from USGS gage Above ACDD for watershed area between Node 1 and 3. Once Calaveras gage installed, backcalculated from Node 1 + (Confluence gage - impaired Calaveras gage - measured impaired Node 1)
Node 4 (Welch Creek gage)	Node 3 + drainage area scaled from USGS gage Above ACDD for watershed area between Node 3 and 4
Node 5 (above San Antonio Creek confluence)	Node 4 + drainage area scaled from USGS gage Above ACDD for watershed area between Node 4 and 5. Sunol Valley infiltration losses were assumed to be zero.
Node 6 (below San Antonio Creek confluence)	Node 5 + unimpaired contribution from San Antonio Creek (see Section 2.2.1.1)
Node 7 (above Arroyo de la Laguna confluence)	Node 6 + drainage area scaled from USGS gage Above ACDD for watershed area between Node 6 and 7. Gravel quarry pumping assumed zero since unimpaired predates quarry operations.
Node 8 (below Arroyo de la Laguna confluence)	Node 6 + unimpaired contribution from Arroyo de la Laguna, including Vallecitos Creek and Sinbad Creek (see Section 2.2.1.2).
Node 9 (Niles gage)	Node 8 + drainage area scaled from USGS gage on Dry Creek
Node 10 (below downstream-most rubber dam)	Node 9 + drainage area scaled from USGS gage on Dry Creek
Node 11 (Union City gage)	Node 10 + drainage area scaled from USGS gage on Dry Creek
Node 12 (Coyote Hills Regional Park)	Node 11 + drainage area scaled from USGS gage on Dry Creek. Drainage area computed for historic Alameda Creek channel location digitized from 1899 and 1906 USGS topographic maps (Figure 4).

Computations for each node are summarized in Table 5 and Appendix A. Computations at Node 6 and Node 8 required unimpaired flow estimates from San Antonio Creek and Arroyo de la Laguna, respectively. Computations of unimpaired flows from these tributaries were more complicated and are discussed in more detail in Sections 2.2.1.1 and 2.2.1.2, respectively. Unimpaired flows could be theoretically computed at Nodes 3 and 4 by simply subtracting measured flows between gages; however, due to variability in streamflow records for the various gages, there were large portions of time where computed unimpaired flows were below zero, which cannot occur. Therefore, rather than modifying the computations by zeroing out the negative values, we consistently applied the drainage area scaling approach, as it prevented negative flows from occurring and avoided the somewhat arbitrary zeroing of computed flows.

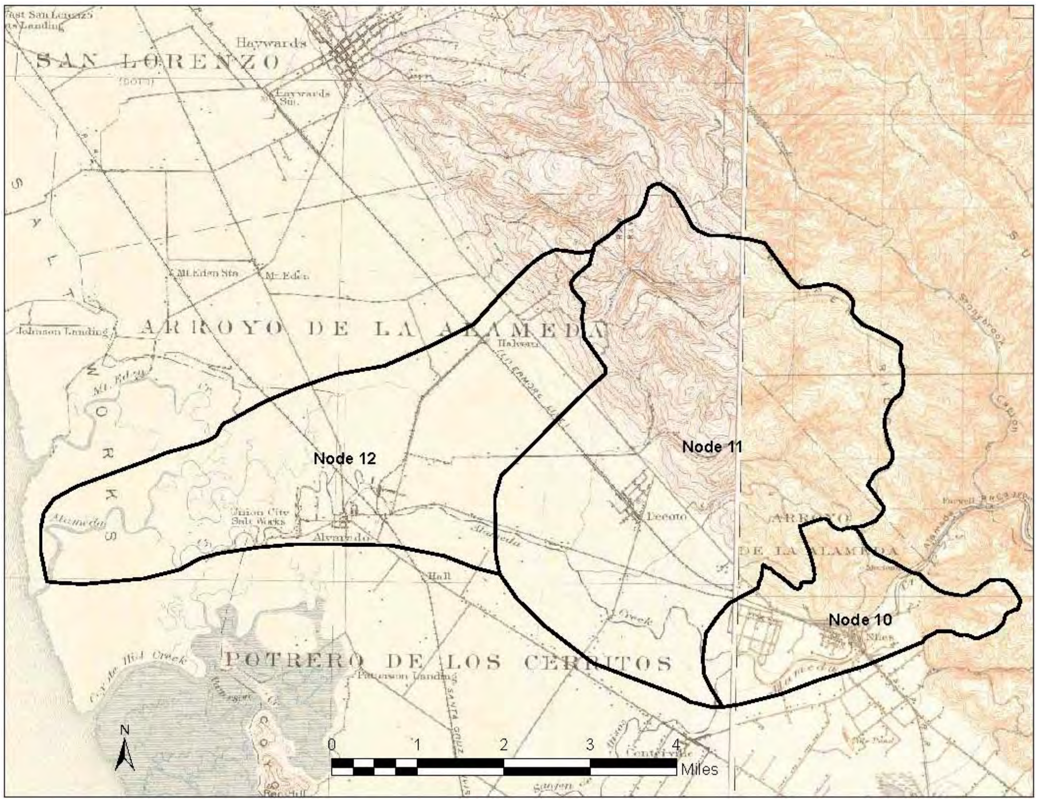

Figure 4. Example of drainage area boundary used in scaling unimpaired gages to ungaged tributaries and watershed areas, using the lower portion of Alameda Creek.

2.2.1.1 <u>San Antonio Creek unimpaired computations</u>

Review of the HY1912-1930 unimpaired flow data on San Antonio Creek and comparing with the unimpaired flow data on Alameda Creek near the Calaveras Creek confluence (Sunol gage in Table 2) showed that San Antonio Creek is much drier than Alameda Creek, and has zero flow much earlier than Alameda Creek. Therefore, a direct drainage area scaled from either the Arroyo Hondo or Above ACDD gage would over-estimate the unimpaired flow contribution from San Antonio Creek. After a number of exploratory approaches to use the various sources of data, we estimated unimpaired flows from San Antonio Creek as follows:

1. Estimate an unimpaired flow threshold at the Above ACDD gage where unimpaired flow (non-zero) would commence on San Antonio Creek.

a. Daily average flows at the Above ACDD gage for HY1912-1930 were computed by multiplying the measured unimpaired daily average flows at the Sunol gage by a drainage area adjustment (33.3 mi^2/37.5 mi^2).

b. Computed unimpaired daily average flows for the Above ACDD gage for HY1912-1930 were plotted against measured unimpaired daily average flows at San Antonio Creek for the same period to correlate when computed unimpaired flows at the Above ACDD gage translated into non-zero measured unimpaired flows at San Antonio Creek (a flow threshold at Above ACDD gage when unimpaired San Antonio Creek would begin to flow). These computations were aggregated by month and averaged, plotted, and a hand-drawn curve fit through the monthly averages to enable daily computations of when unimpaired San Antonio Creek would be non-zero (Figure 5).

2. Estimate the proportion of unimpaired flow volume on San Antonio Creek using the Above ACDD gage and SFPUC monthly inflow computations on San Antonio Reservoir.

   a. For October 1995 to September 2009, monthly inflow volumes (unimpaired) to San Antonio Reservoir were compared to monthly flows (unimpaired) at the Above ACDD gage. The resulting San Antonio Reservoir inflow volume is 42.5% of the Above ACDD flow volumes.

   b. For those dates where San Antonio Creek is estimated to be non-zero in Step 1b, compute unimpaired flows on San Antonio Creek by multiplying average daily flows at Above ACDD gage by 42.5%.

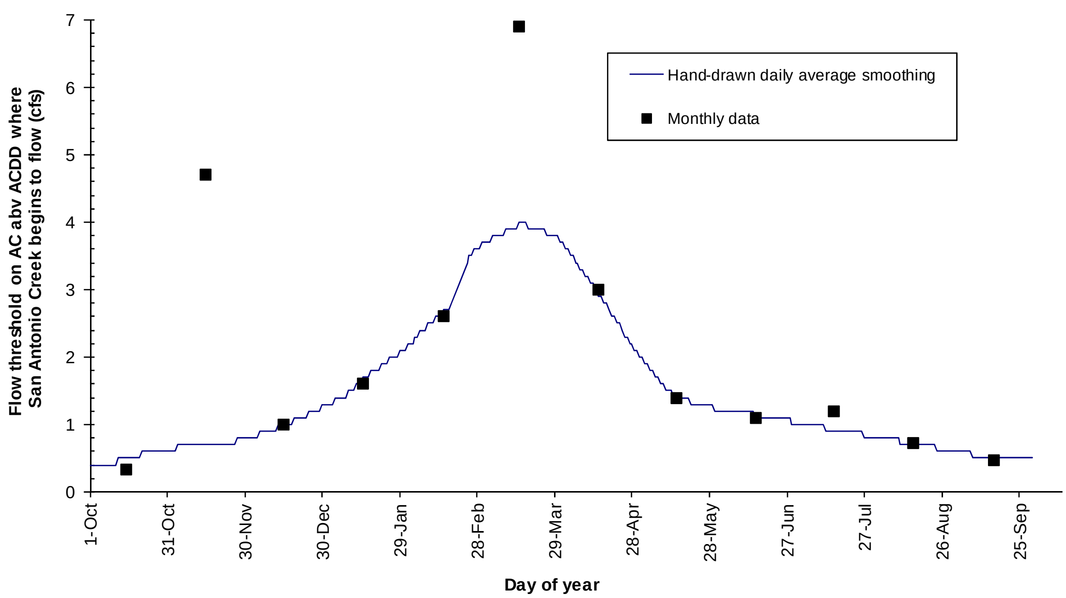

Figure 5. Comparison of average flows by month when computed unimpaired flows at Above ACDD gage translates to non-zero unimpaired flows on San Antonio Creek ("monthly data"), and hand-drawn curve to apply to HY1996-2009 Above ACDD daily average flows to estimate non-zero unimpaired flow thresholds on San Antonio Creek.

In summary, the method described above computes unimpaired flows on San Antonio Creek as zero flow up to a certain flow threshold at the Above ACDD gage, and 42.5% of the daily average flow at the Above ACDD gage thereafter. If the drainage area scaling approach was attempted, it would scale the Above ACDD gage by 111% (33 mi^2/37.5 mi^2), which would greatly overestimate the volume of unimpaired flow on San Antonio Creek. Scaling from Arroyo Mocho was also considered, but the Arroyo Mocho gage is further east than San Antonio Creek, and thus drier than San Antonio Creek. Having the monthly volumetric inflow data for San Antonio Reservoir allowed us to scale the daily average flow data from the Above ACDD gage such that a volumetric mass could be used rather than simply scaling the Above ACDD gage by drainage area.

2.2.1.2 Arroyo de la Laguna unimpaired computations

Estimating unimpaired flows in Arroyo de la Laguna was much more challenging given the degree of change in the watershed, complexity of runoff processes, and the lack of any unimpaired flow data during the HY1996-2009 time series (other than Arroyo Mocho for 10/1/1996-1/16/2002). After considerable investigation of various strategies and methods, the following strategy was used:

1. Estimate daily average flows for the November-May period (winter and spring higher flows) by conducting a drainage area adjustment from Arroyo Mocho.
2. Estimate daily average flows for the June-October period (summer and fall baseflows) based on monthly average flows measured at the Arroyo de la Laguna near Verona gaging station for the HY1912-1919 and HY1921-1930 "unimpaired" period.

For the November-May period, unimpaired daily average flow data from Arroyo Mocho were required. Because the unimpaired Arroyo Mocho gage was discontinued after 1/16/2002, the 1/17/2002 to 9/30/2009 data gap needed to be filled using unimpaired flows from the Above ACDD gage. Using overlapping daily average flow data at both gages from 10/1/1995 to 1/16/2002, the average proportion between the two gages for each month in the November-May period was computed (Figure 6). To estimate daily average flow on Arroyo Mocho during this November-May period, the daily average flow at Above ACDD gage was multiplied by the proportion appropriate for that month (e.g., 78% for February) for each day. The November period was in the transition between baseflows and the initiation of the high flow season, which is why the proportion is much lower than the subsequent months. We considered using the HY1912-1919 and HY1921-1930 "unimpaired" Arroyo de la Laguna flows to extend summer and fall baseflow computations into November, but this would have dampened any storm-generated runoff events (which typically begin in November). Therefore, we used the Arroyo Mocho scaling approach for November to incorporate fall freshets.

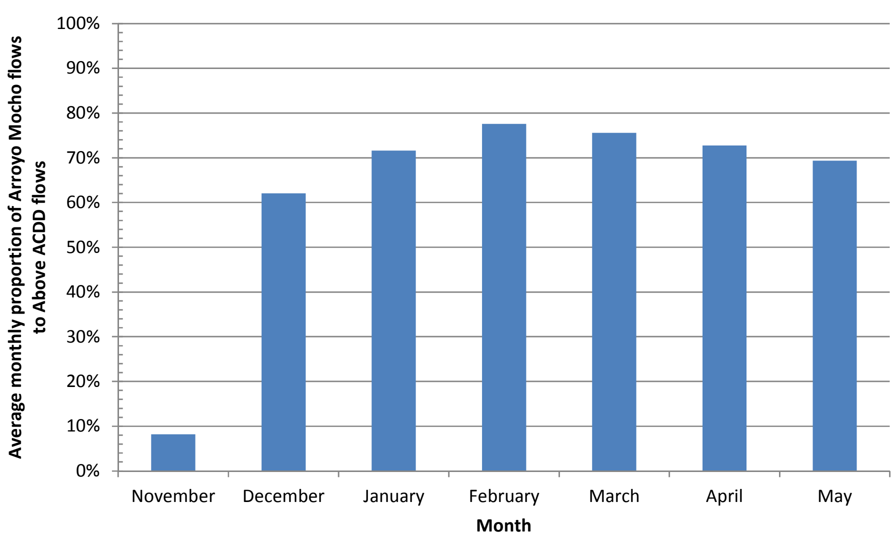

Figure 6. Average proportion of daily average flows between Arroyo Hondo and Above ACDD gages by month for the 10/1/1995 to 1/16/2002 overlapping record.

Once the 1/17/2002 to 9/30/2009 Arroyo Mocho flow record was backfilled with these computed flow values, the entire daily average record for HY1996-2009 for the months of November-May was computed at the Verona gage by drainage area adjustment from the Arroyo Mocho gage (Arroyo Mocho flow × (403 mi^2 /38.2 mi^2)). This drainage area scaling approach should be treated with caution. Unit runoff magnitude varies with drainage area (runoff/mi^2), with smaller watersheds having a higher unit runoff magnitude than larger ones due to flow routing, storage, peak flow attenuation, and differences in peak flow travel times within tributaries (Mann et al., 2004). The scaling up from a small watershed to a larger one by drainage area assumes a constant unit runoff magnitude, which may be reasonable when the two watersheds are similar drainage areas, but the difference in Arroyo Mocho (38.2 mi^2) compared to Arroyo de la Laguna at Verona (403 mi^2) is large. In addition, the effect of the lagoon under unimpaired conditions was likely very substantial in attenuating unimpaired flood peaks. Therefore, this drainage area scaling computation would tend to over-predict daily average flow magnitudes for unimpaired high flows at the Verona gage. Non-peak flow magnitudes during the November-May period may be more reasonably predicted by the drainage area computation because the flow routing errors described above are largely avoided.

For the June-October period, we initially attempted to correlate summer-fall baseflows on Arroyo Mocho to Arroyo de la Laguna at Verona; however, flows at Arroyo Mocho were often zero through the summer, so this approach was abandoned. Instead, we assumed that summer-fall baseflows as measured at the Verona gage between HY1912-1919 and HY1921-1930 represented unimpaired flows. To dampen daily variability in the historic record at Verona, daily average flows were averaged for each month during the June-October period, and then daily average flows for any given day were interpolated between these monthly values (Figure 7). Because the averaging was done over the entire HY1912-1919 and HY1921-1930 period, there is no distinction between different years; therefore, summer-fall baseflows were the same for every year during the HY1996-2009 time series. As with the November-May estimates, this method has several sources of uncertainty, primarily the assumption that the HY1912-1930 flows as measured at the Verona gage reflect unimpaired conditions. There were likely upstream diversions occurring, the base level of the lagoon had been lowered, the hydrologic buffering effect of the lagoon eliminated, and groundwater pumping was likely occurring. The overall effect is that the computed unimpaired summer-fall baseflows are likely substantially lower than truly unimpaired conditions.

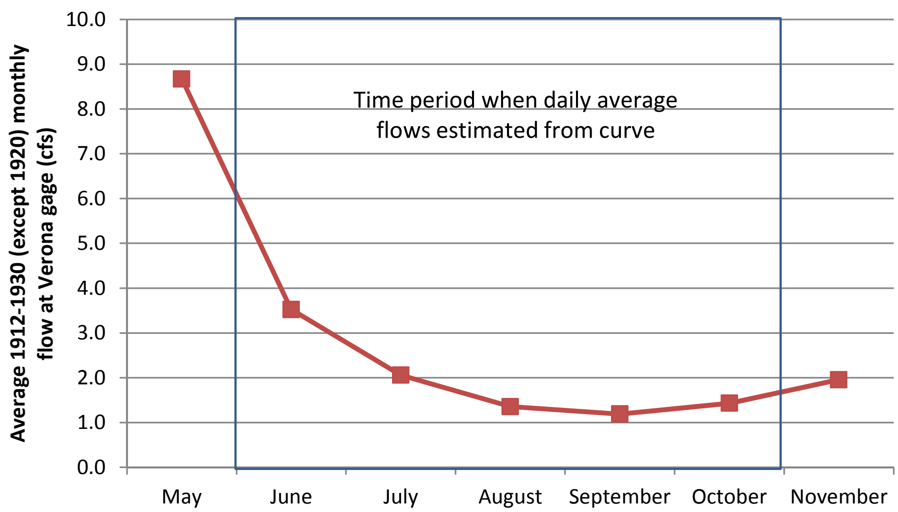

Figure 7. Monthly average flows at the Verona gaging station (USGS #11-176900) for the June-October months over the HY1912-1919 and HY1921-1930 "unimpaired" flow record at that gage. May and November values computed to allow early June and late October values to be computed via interpolation.

Once daily average flows were computed for the two seasonal periods, they were merged into a continuous daily average flow record for 10/1/1995 to 9/30/2009, representing input into the ASDHM model between Node 7 and Node 8. This method sometimes caused sharp transitions across the October-November boundary and May-June boundary.

2.2.2 Results and discussion

In contrast to the measured impaired condition (Scenario 4), the unimpaired flow record could not be validated with measured data, since there are no measured unimpaired data between Node 1 and Node 12 for the HY1996-2009 time series. Some visual evaluations were made between computed unimpaired flows during the late spring and early summer season of some hydrologic years to verify that the scaled drainage area approach was producing reasonable flow estimates.

Unimpaired flows downstream of Node 8 should be treated with substantially more caution, since the unimpaired flows were largely based on the HY1912-1930 record at Arroyo de la Laguna near Verona, which was certainly not truly unimpaired during that period. The lagoon had been drained and base level lowered, such that the buffering effect of the lagoon had long since been eliminated by 1912. In addition, there were likely numerous low flow diversions and wells for agricultural and municipal uses. Regardless, many of the expected hydrologic changes between unimpaired and impaired conditions resulting from the combination of upstream dams and urbanization can be explored in a comparative plot (Figure 8):

- Despite the upstream storage reservoirs on upper Alameda Creek and Arroyo del Valle, early season storms (November-December) are dampened under the unimpaired scenario compared the impaired scenario with extensive urban runoff and flood control system in Livermore Valley. This buffering of early season peaks, as well as mid-winter peaks, would have likely been even more pronounced under truly unimpaired conditions, with the upstream lagoon further buffering flood peaks.

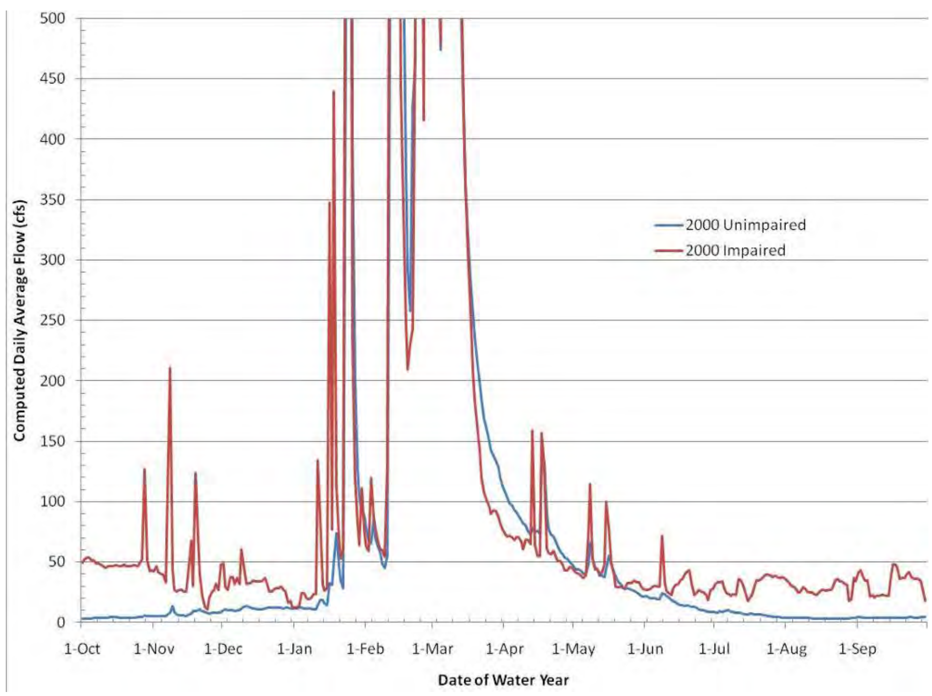

Figure 8. Comparison of 2000 computed unimpaired flows versus measured impaired flows at the Niles gage (USGS #11-179000), illustrating some of the hydrologic changes from upstream urbanization on streamflow hydrology through Niles Canyon.

- Summer baseflows between Node 8 and Node 9 are higher under impaired conditions due to imported Delta water from the (SBA). However, computed unimpaired flows are likely underestimated because the 1912-1930 “unimpaired” record at Verona: (a) reflected upstream diversions and wells were in place, and (b) did not document the likely buffering effect of the upstream lagoon and higher groundwater table. Both would have likely further elevated unimpaired summer baseflows higher than that shown in Figure 8. How much higher is unknown, and likely relegated to qualitative descriptions in historical surveys and narratives.
- The spring recession is much faster under impaired conditions, likely due to upstream storage reservoirs and diversions, faster routing of late spring storm runoffs, decreased groundwater table, and loss of the lagoon. Computed unimpaired flows also likely underestimate true unimpaired conditions, as the absence of upstream diversions and wells, combined with the buffering effect of the upstream lagoon and higher groundwater table, would have likely caused a more gradual spring runoff than that shown in Figure 8.

2.3 Measured impaired flow computations in Alameda Creek (Scenario 4)

The measured impaired flow model results in streamflow at 12 nodes incorporating actual operations of Calaveras and ACDD dams during the period from 10/1/1999 to 9/30/2009. In other words, the measured impaired flow model generates daily average streamflows at 12 nodes to supplement what stream gages (had there been any) at those nodes would have observed from 10/1/1999 to 9/30/2009.

2.3.1 Computational methods

The model begins with the use of streamflow data at three locations: (1) Above ACDD gage (USGS #11-172945; upstream of Node 1), (2) Calaveras gage (USGS #11-173500; Node 2), and (3) Confluence gage at the confluence of Alameda and Calaveras creeks (USGS #11-173510; Node 3) to compute streamflow below ACDD (Node 1). The missing high flows observations (discussed later) at Node 3 (USGS # 11-173510) were filled using observed streamflows at the Welch Creek gage (USGS #11-173575). Once the mass balance was accomplished at Node 3, the remaining downstream nodes were calculated based on drainage area adjustment, flow loss, flow gain, and urban drainage contribution, depending on the expected hydrologic processes between upstream and downstream nodes (see Figure 1). Because the temporal resolution of the model is daily, routing effect was omitted. Different assumptions incorporated in the model at each node have been documented in Appendix 1. The instantaneous behavior of Alameda Creek, which influenced contribution to Calaveras Reservoir through the ACDD tunnel, and types and periods of streamflow records from three primary gages, posed significant challenges in the model development. Those challenges and how they were tackled are briefly described below.

2.3.1.1 <u>Alameda Creek Diversion Dam tunnel capacity and divertible flow to Calaveras Reservoir</u>

ACDD is a non-storage purpose diversion structure which allows diversion of Alameda Creek flow into Calaveras Reservoir through the ACDD tunnel (ACDT). The 1931 engineering capacity of the ACDD tunnel is 650 cfs and under the ideal condition, it is assumed that the tunnel can divert up to 650 cfs to Calaveras Reservoir depending on streamflow in Alameda Creek (SFPUC 2011). Any flow greater than 650 cfs would instantaneously flow downstream of ACDD. Therefore, flow at Node 1 (i.e. below ACDD) depended on two factors: (1) whether the ACDD tunnel gates were opened or not, and (2) the instantaneous flow in Alameda Creek. When tunnel gates are closed, the flow at Node 1 is the same as the flow upstream of ACDD (as measured by the Above ACDD gage). When ACDD gates were opened, the flow below ACDD depended on the instantaneous flow above ACDD. Because Alameda Creek possesses an extremely instantaneous characteristic, observed daily average streamflows do not capture instantaneous dynamics of ACDD (Figure 9). Therefore, a "divertible flow" to Calaveras Reservoir from ACDD was estimated using 15-minute streamflow data. The "diverted flow" to Calaveras Reservoir was then cumulated to a daily average value depending on ACDD tunnel condition (opened or closed) to estimate the flow at Node 1.

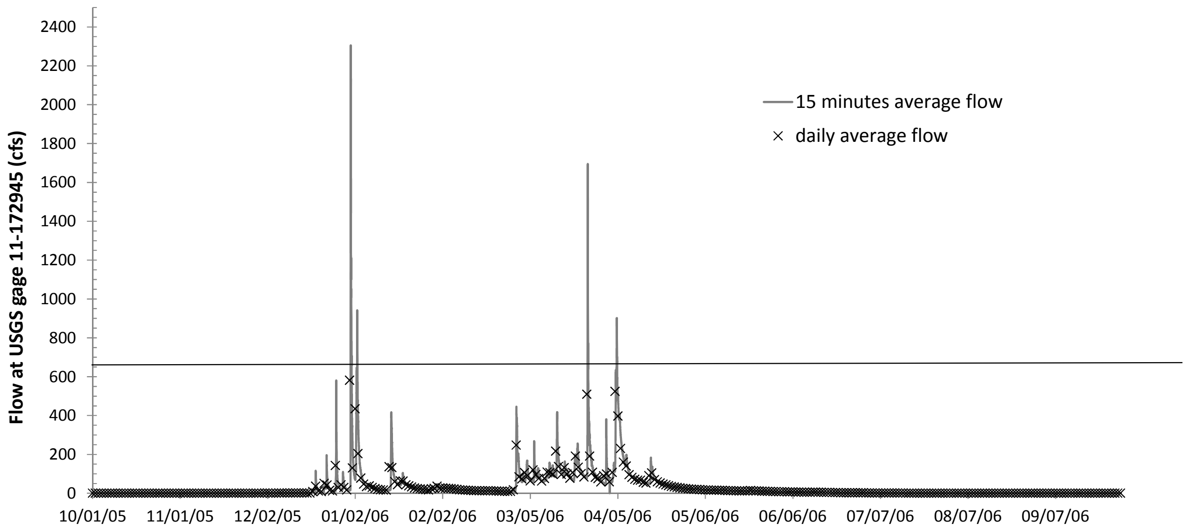

Figure 9. Average 15-minute and daily streamflows observed at the Above ACDD gage (USGS #11-172945) for HY2006, depicting effect of instantaneous flow on ACDD divertible flow to Calaveras Reservoir and flow at Node 1 (i.e., below ACDD).

2.3.1.2 Data availability from three primary gages and Calaveras Reservoir operation

While Alameda Creek is a relatively well-monitored Creek, the recording period and types of available data varied for three primary gages used in the model (Table 6). The streamflow data from the Calaveras gage (Node 2) were available only after 05/23/2002. Until HY2006 the Confluence gage (Node 3) was designated as a low flow gage and only low flow data were available (< 200 cfs). Therefore, streamflow data recorded at the Welch Creek gage (Node 4; about 4 miles downstream of the Confluence gage) were used to fill the missing higher flows at the Confluence gage (Node 3) employing the drainage area adjustment method. The daily average streamflow between gages at Node 3 and Node 4 (for the period when both gages recorded streamflow) was highly correlated (r^2 = 0.98) and missing higher flows could have been filled using the regression equation. The drainage area adjustment method was used instead because predicted missing values from the regression method and drainage area adjustment were similar, and the latter offered consistency in computational method employed in this model development.

Once the missing high flows were filled at the gage site of Node 3, varieties of computational approaches were employed to estimate flow at Node 1 and contribution from unregulated areas using a mass balance approach (Figure 3) for different computational periods. For example, computations after 5/23/2002 used the following procedure: (1) filled missing values at Node 3 using streamflow data from Node 4, (2) computed release or spill from the Calaveras Reservoir using Node 2 flow data, (3) computed ACDD diverted flow to Calaveras Reservoir based on ACDD operational information and observed streamflow above ACDD, (4) computed flow below ACDD based on ACDD operational information and observed streamflow above ACDD, (5) computed contribution from unregulated areas below ACDD in Alameda Creek, and (6) computed contribution from unregulated areas below Calaveras Dam. Everything remains the same for the period between 10/1/1999 and 5/22/2002, except that the flow at Node 2 (i.e., below Calaveras Reservoir) was calculated at the last step.

During the mass balance analysis, error from the gage data needed to be distributed to either the gage site or to the unregulated area. In the analysis, the error was primarily distributed to the unregulated area. However, there were instances when certain error needed to be distributed to a gage site as well. For example, there were some instances when the flow at the Calaveras gage below Calaveras Dam was higher than the flow at the confluence of Alameda and Calaveras Creeks. In such cases the error was distributed to the Calaveras gage. For this reason there could be instances when the modeled impaired flow at the Calaveras Creek gage (Node 2) could be different than the observed USGS streamflow for some days.

Table 6. Availability of data types and period from primary USGS gaging stations.

Period	Calaveras gage (USGS #11-173500; Node 2)	Above ACDD gage (USGS #11-172945; upstream of Node 1),	Confluence gage (USGS #11-173510; Node 3)	Welch Creek gage (USGS #11-173575; Node 4)
10/01/1999 – 5/22/2002	No	Yes	Yes (days with > 200 cfs not available)	Yes
05/23/2002 – 09/30/2009	Yes	Yes	Yes (days with > 200 cfs not available until HY2006)	Yes

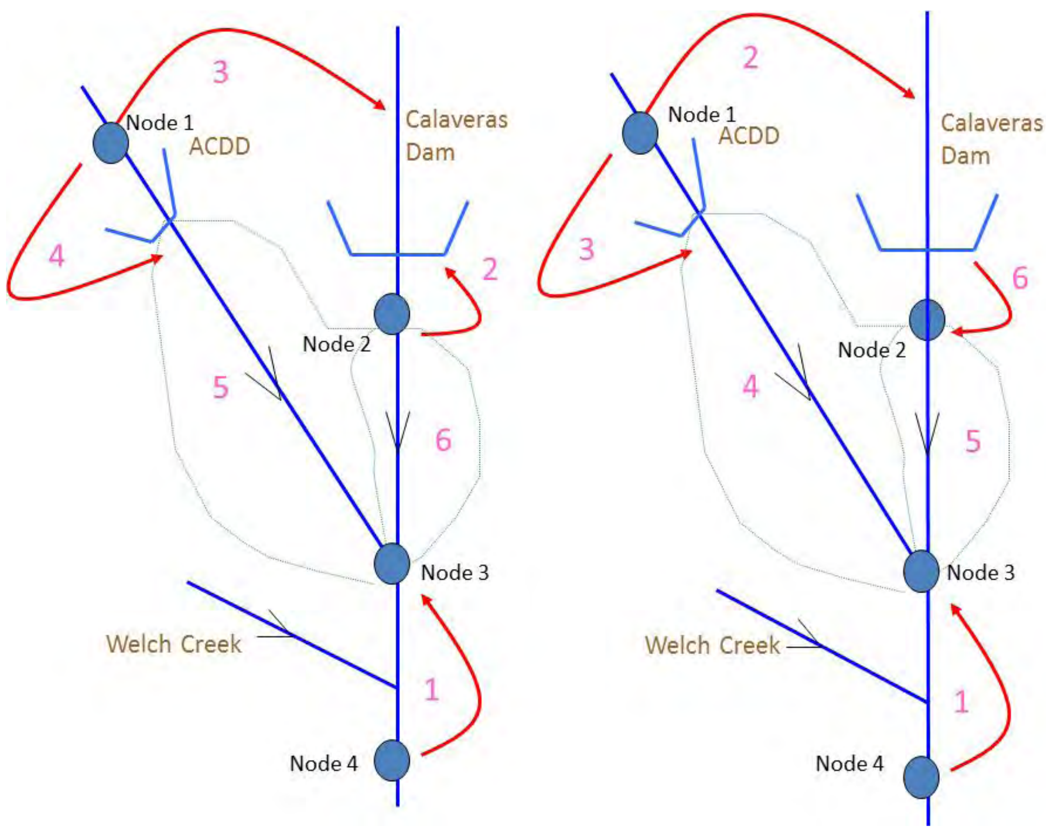

Figure 10. Schematic illustration of step-wise analytical mass balance procedure using three primary gages (Calaveras gage at Node 2, Above ACDD gage upstream of Node 1, and Confluence gage at Node 3), auxiliary information including ACDD tunnel operation and capacity, unregulated drainage areas (as shown by 5 and 6 in the figure), and streamflow data from the Welch Creek gage at Node 4 to fill the missing flow data at Node 3. Left figure shows analytical procedure for period after 05/23/2002, and the right figure shows analytical procedure for period between 10/1/1999 and 05/22/2002 when streamflow data for the Calaveras gage were unavailable.

Once the mass balance among Nodes 1, 2 and 3 were established, Node 4 to Node 12 were calculated based on drainage area adjustments, flow loss, flow gains, and urban drainage contribution. Urban drainage contribution occurs between Nodes 10 and 12. Flow losses occur between Node 4 and 5 and flow gain occurs between Node 5 and Node 6. The premise for flow loss and gain incorporated in the model is briefly described below.

2.3.1.3 Premise for Sunol Valley flow loss and gains incorporated in the model

Due to the highly porous and permeable nature of the Sunol Valley alluvium between Node 4 and Node 5 in Alameda Creek, the surface flow that enters the valley is lost to groundwater. It is expected that these losses happened in this reach historically. However, the aggregate mining operation in Sunol Valley has shifted Alameda Creek substantially and has probably altered the way flow losses occur in Sunol Valley compared to historical conditions.

The Natural Resources Division of the SFPUC has carried out an extensive monitoring program related to stream habitat conditions in Alameda Creek in the last 10 years (SFPUC, 2010). As part of monitoring activities, experimental instream flow releases occurred from Calaveras Reservoir from 4/17/2008 to 7/8/2008. Four different flows (≈24 cfs, ≈17 cfs, ≈10 cfs, and ≈6 cfs) were sequentially released from the reservoir for a week or two during the experimental release period. Following the flow stabilization of each flow category, extensive streamflow measurements were taken at numerous locations between the Calaveras gage and the confluence of Alameda Creek with Arroyo de la Laguna (Figure 11). The summary results indicate that for flow to be present at Node 5, the flow at Node 4 needs to be > 17 cfs. This conclusion is consistent with previous similar studies carried out by Trihey and Associates (2003) and Entrix (2004). Based on this information, a constant flow loss of 17 cfs was assumed between Node 4 and Node 5 in the measured impaired flow analysis.

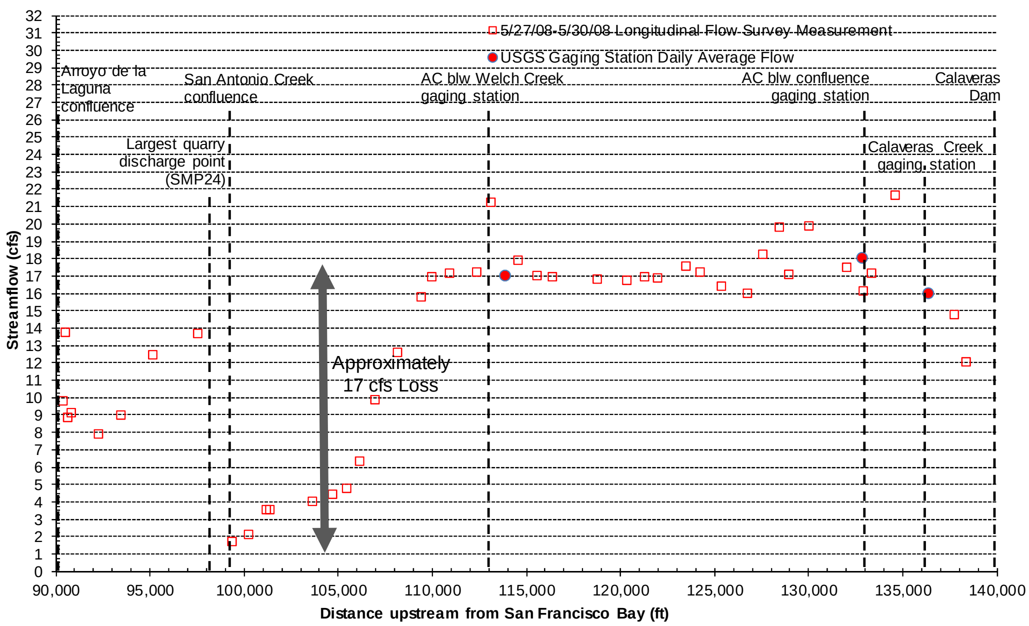

Figure 11. Instantaneous streamflow measured at different locations in Alameda Creek from Calaveras Creek gage (Node 2) location to the confluence with Arroyo de la Laguna (Node 7) during the experimental release from Calaveras Reservoir in the HY2008. The chart indicates that for flow to be present at the San Antonio Creek confluence (Node 5), the flow at the Welch Creek gage (Node 4) needs to be > 17 cfs.

A portion of surface water lost to Sunol Valley reaches to gravel pits of surface mining pit (SMP)-30, operated by the DeSilva Group, and SMP-24, operated by Hanson Aggregates (Figure 12). A portion of collected water in the pits is used for quarry operation purposes and a portion is discharged back into the stream. In general, quarry pit discharge into the stream occurs every year (and continuously except for a few summer months) from SMP-24 and occasionally from SMP-30. The discharge input to Alameda Creek from SMP-24 was available as a monthly average from April 1998 to October 2007 and as daily average values after October 2007. Discharge into the Creek from SMP-30 was not available for the model period. In the computation of measured impaired flow, the flow gain from SMP-24 is considered to occur at Node 6.

Therefore, in the measured impaired flow analysis (Scenario 4), a 17 cfs flow loss was assumed to occur between Node 4 and Node 5, and the flow gain from quarry pit (SMP-24) was assumed to occur between Node 5 and Node 6. Flow losses in Niles Cone between Node 9 and Node 10 were computed from the historic gaging record and ACWD diversions.

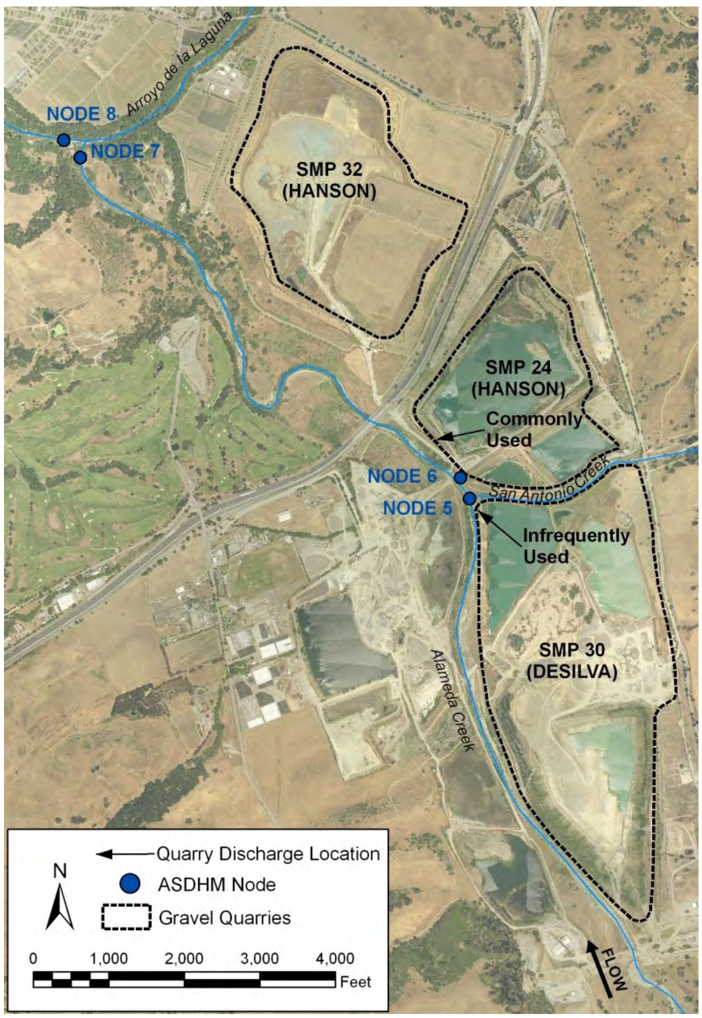

Figure 12. Gravel quarries in lower Sunol Valley and approximate discharge points. There is a cut-off wall on SMP-32, a partial cut-off wall on SMP-24, and no cut-off wall on SMP-30.

2.3.1.4 Contribution from San Antonio Creek

The San Antonio Creek gage (#11-174000) located just downstream of San Antonio Reservoir provides streamflow data related to spill and other releases from San Antonio Reservoir from 10/1/1999. Streamflows from the San Antonio Creek gage represent the contribution from San Antonio Creek to Node 5 and are needed to calculate flows at Node 6. The measured impaired flow model (Scenario 4) offers a provision of incorporating the contribution from watersheds below San Antonio Reservoir (discussed in the future scenarios model in Section 2.4.3.4) to Node 6 although such contribution was omitted in Scenario 4.

2.3.1.5 Urban drainage contribution

Once the flow at Node 6 was calculated, Nodes 7, 8, and 9 were calculated by incorporating accretion from additional watershed areas between two consecutive nodes. The impaired flow from Arroyo de la Laguna watershed was obtained from the Verona gage (#11-176900). The contribution from Arroyo de la Laguna includes Sinbad Creek, Vallecitos Creek (including flow diverted to Vallecitos Creek from the SBA for ACWD), and the watershed adjacent to Alameda Creek between the Verona gage and Alameda Creek confluence.

Nodes 10, 11, and 12 receive flow contribution from urban drainage, as well as from natural watersheds. ACWD diverts water from Alameda Creek for its operation between Nodes 9 and 10. Alameda County Flood Control District (ACFCD) and Alameda County Public Work Agency (ACPWA) provided information related to urban storm drainage, which helped delineate urban drainage between nodes to model contribution from urban areas at Nodes 10, 11, and 12 (Table 7).

Table 7. Natural watershed and urban drainage contribution at Nodes 10, 11, and 12.

From	To	Natural watershed (mi^2)	Urban drainage (mi^2)
Node 9	Node 10	1.66	1.20
Node 10	Node 11	1.59	3.59
Node 11	Node 11	2.27	7.69

To estimate flow contribution from urban drainage, we explored both rational as well as empirical methods. Streamflow data from similar urban streams were available at two locations in San Lorenzo Creek and one location in Castro Valley Creek, which were located at about 7 miles aerial distance from the study site (Table 8). The difference in average streamflow between upstream and downstream gaging sites in San Lorenzo Creek provided unique data to estimate unit urban drainage contribution because the area between these two gages was entirely urbanized. These data were available from 10/1/1997 to 9/30/2009. Similarly, most of the watershed above the Castro Valley gage is urbanized. The streamflow data from the Castro Valley Creek gage were available for the entire modeling period.

The use of observed urban streamflow to estimate urban contribution was found superior when compared to outcome from the rational method because it retained variability related to the timing of rainfall. Therefore, we used observed data to estimate urban drainage contributions to Nodes 10, 11, and 12. For the measured impaired flow model, we used streamflow observed at two San Lorenzo Creek gages to estimate the unit urban drainage contributions for the period between 10/1/1999 to 9/30/2009. The use of measured streamflow data to estimate the urban drainage contributions to Nodes 10, 11, and 12 assumed similar rainfall between the San Lorenzo Creek and lower Alameda Creek areas for the modeling period. Considering proximity of these two areas, in general, this assumption was considered realistic.

Table 8. Information on urban gaging locations in San Lorenzo and Castro Valley creeks.

Basin/location	USGS station number	Drainage Area	Data availability
San Lorenzo; downstream location	11-181040	44.6 mi^2	Entire model period (i.e., HY1996-2009)
San Lorenzo; upstream location	11-181000	37.5 mi^2	Since 10/1/1997
Castro Valley	11-181008	5.51 mi^2	Entire model period (i.e., HY1996-2009)

2.3.1.6 ACWD operations

For the computation of measured impaired flow at Node 10 (based on computed flow at Node 9), ACWD diversion data were necessary. To retain the integrity of observed flows, we computed measured impaired Node 11 flow from “computed measured impaired Node 9 flow” prior to computing “measured impaired Node 10 flow.” The measured impaired Node 11 flow was computed as “computed measured impaired Node 9 flow” + “(observed flow at the Union City gage [USGS #11-180700]” – “observed flow at the Niles gage [USGS #11-179000]).” Measured impaired Node 10 flow was then computed as “measured impaired Node 11 flow” – “observed USGS flow at upper Dry Creek” + “Old Alameda Creek diversion” + “contribution from natural watershed between Node 9 and Node 10” + “contribution from urban watershed area between Node 9 and Node 10.” When flow in the flood channel is >2,450 cfs, a bypass structure has the ability to bypass up to 40 cfs in the old Alameda Creek channel, and ASDHM incorporates this diversion occurring between Node 10 and Node 11 in the computation.

2.3.1.7 Validation of measured impaired flow model

The Niles gage (USGS #11-179000) is the only gage significantly downstream from the Confluence gage located at Node 3 (one of the three primary gages used for mass balance). ASDHM predicts flow at the Niles gage (Node 9), which is about 15 miles downstream from the Confluence gage at the confluence of Alameda and Calaveras creeks (Node 3). The observed and simulated streamflows at the Niles gage (USGS #11-179000) was used to evaluate the model.

We considered the potential influence of the operational period of USGS primary gages and operation of ACDD during the model evaluation, and evaluated the model for three different periods. As discussed in Section 2.3.1.2, the three primary USGS gages used in the model operated at different times. Similarly, due to DSOD restriction in Calaveras Reservoir, ACDD gates were closed during early the DSOD period from 10/24/2004 to 3/13/2007 (SFPUC 2011); all three primary gages were functioning at this time. The computational error in Node 1 during this period was expected to be very low (within the range of streamflow measurement error), as the simulated flow at Node 1 was same as the observed flow upstream of ACDD. Therefore, this period was considered the best period for model evaluation. Similarly, since streamflow data were available from all three primary gages between 5/23/2002 and 9/30/2009, the period from 5/23/2002 to 9/30/2009 was considered the second best period for model evaluation. Model evaluations were therefore performed for three different periods: (1) from 10/24/2004 to 3/13/2007, (2) from 5/23/2002 to 9/30/2009, and (3) from 10/1/1999 to 9/30/2009 (the entire modeling period). Because low flows were of primary importance, we evaluated the model for entire flow levels and as well as for flows < 100 cfs.

Streamflows representing three different time steps were chosen for evaluation purposes: (1) annual volume, (2) monthly average flow, and (3) daily average flow. Three statistical parameters were used: (1) coefficient of determination (r^2), (2) mean absolute error, and (3) percent bias. Mean absolute error (MAE) and percent bias (PB) were calculated from equation 1 and 2.

$$\text{MAE (\%)} = 1/n\sum_{i=1}^{n} abs[(Q_{obs} - Q_{sim})/Q_{obs}] \tag{1}$$

$$\text{PB (\%)} = 1/n\sum_{i=1}^{n}[(Q_{obs} - Q_{sim})/Q_{obs}] \quad (2)$$

Where, Q_{obs} and Q_{sim} are observed and simulated streamflows for respective time steps.

Considering the measurement error inherent in observed streamflow data (USGS reports this to be on average ± 10% for daily average flow), we anticipated MAE and PB in the range of ±15% and ±10%, respectively. Similarly, the coefficients of determination were expected to be > 0.95 for annual and monthly flows and > 0.85 for daily flows. Meeting these criteria (particularly for low flows) was considered to depict outstanding model performance.

Table 9, Table 10, and Table 11 summarize three statistical parameters for entire flows and flows <100 cfs for three different periods. For all three different periods, r^2, MAE, and PB values meet expected thresholds for daily average flows for flows <100 cfs. For periods between 10/24/2004 and 3/13/2007 and between 5/23/2002 and 9/30/2009, all threshold criteria are met for r^2, MAE, and PB for flows <100 cfs as well as for the entire range of flows. MAE and PB for daily average flows for the period between 10/1/1999 and 9/30/2009 when the entire flow ranges were considered are 17% and 11%, slightly higher than the expected thresholds, but not substantially higher. The coefficients of determination were found slightly lower for annual and monthly flows for the period between 10/1/1999 and 9/30/2009 for flows <100 cfs (Table 11) primarily due to the difference in annual flow volume in HY1999 and HY2000 and monthly average flow differences in January and February. HY1999 and HY2000 encompass the period when the Calaveras gage (USGS #11-173500) below Calaveras Dam did not exist. Because MAE and PB were 4% and -1%, respectively, the overall evaluation for the period 10/1/1999 and 9/30/2009 for annual and monthly evaluations for flows <100 cfs were considered reasonable. Importantly, daily average flow evaluation parameters for the period between 10/1/1999 and 9/30/2009 were within the evaluation thresholds for flows <100 cfs. The scatter plots between observed and simulated flows for different periods and flow ranges are shown in Figure 13 for visual summary. Similarly, Figure 14 and Figure 15 show time series comparisons of observed and simulated streamflows for different periods and flow ranges. These figures add to greater visual understanding between observed and simulated flows in depicting performance of the model for its intended applications.

Table 9. ASDHM validation matrices including r^2, MAE, and PB for flows <100 cfs and entire range of flows for the period between 10/23/2004 and 3/6/2007 during which ACDD gates were closed.

10/24/2004 - 3/13/2007 (flow < 100 cfs)			
Parameter	**r^2**	**MAE (%)**	**PB (%)**
Annual Volume	1.00	3%	3%
Monthly Volume	0.95	10%	3%
Daily Flow	0.87	11%	3%

10/24/2004 - 3/13/2007 (flow > 0 cfs)			
Parameter	**r^2**	**MAE (%)**	**PB (%)**
Annual Volume	1.00	11%	-10%
Monthly Volume	0.99	10%	-10%
Daily Flow	0.98	15%	-10%

Table 10. ASDHM validation matrices including r^2, MAE, and PB for flows <100 cfs and entire range of flows for the period between 5/23/2002 and 9/30/2009 during which steamflows from all four primary USGS gages were available.

05/23/2002 - 9/30/2009 (flow < 100 cfs)			
Parameter	**r^2**	**MAE (%)**	**PB (%)**
Annual Volume	0.99	2%	2%
Monthly Volume	0.95	4%	2%
Daily Flow	0.86	12%	2%

05/23/2002 - 9/30/2009 (flow > 0 cfs)			
Parameter	**r^2**	**MAE (%)**	**PB (%)**
Annual Volume	1.00	10%	-10%
Monthly Volume	0.98	8%	-10%
Daily Flow	0.97	15%	-10%

Table 11. ASDHM validation matrices including r^2, MAE, and PB for flows <100 cfs and entire range of flows for the modeling period.

10/01/1995 - 9/30/2009 (flow < 100 cfs)			
Parameter	**r^2**	**MAE (%)**	**PB (%)**
Annual Volume	0.84	4%	-1%
Monthly Volume	0.72	4%	-1%
Daily Flow	0.85	14%	-1%

10/01/1995 - 9/30/2009 (flow > 0 cfs)			
Parameter	**r^2**	**MAE (%)**	**PB (%)**
Annual Volume	1.00	12%	-11%
Monthly Volume	0.99	7%	-11%
Daily Flow	0.97	17%	-11%

2.4 Future and computed impaired flow computations in Alameda Creek (Scenario 5 and Scenario 6)

Once ASDHM was sufficiently validated in Scenario 4, we applied it to predict flows for Scenario 5 (future) and Scenario 6 (computed impaired). Future flow computations assume proposed future flow releases from the following three facilities: Calaveras Dam, ACDD, and ACWD surface water diversions. Proposed future flows from SFPUC facilities (Calaveras Dam and ACDD) were developed under the Calaveras Dam Replacement Project (CDRP), and proposed future flows from ACWD facilities were developed under an ACWD, NMFS, and DFG informal consultation process for fish passage projects between Node 9 and Node 10. Flows from Arroyo de la Laguna are assumed to be measured impaired, although because of the versatility of the ADSHM future scenario model, computation related to any proposed future scenarios from Arroyo de la Laguna or other portions of the watershed can be easily accommodated.

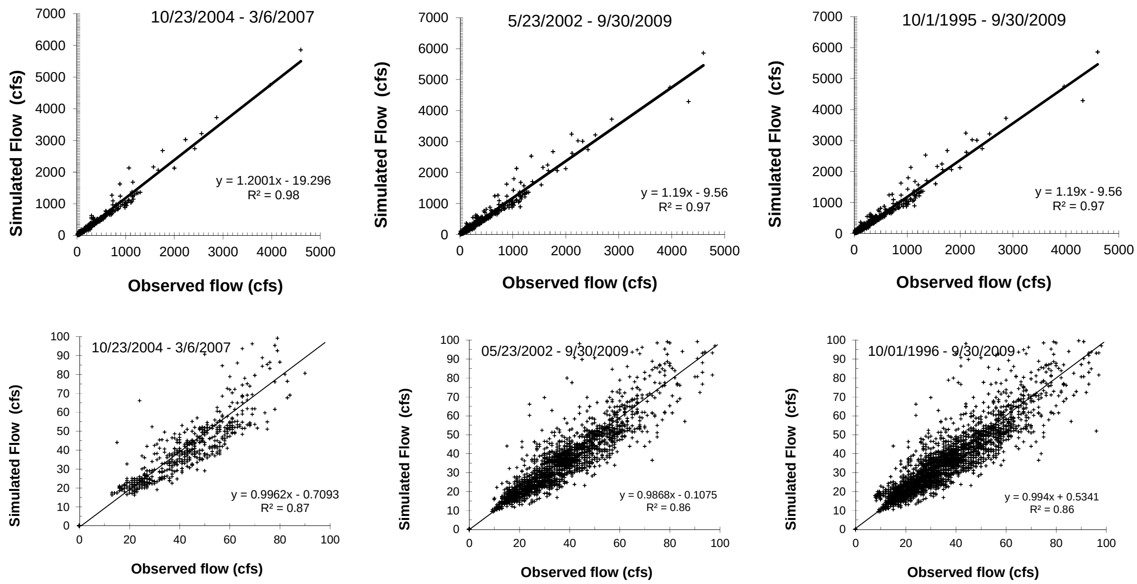

Figure 13. Correlation between observed and simulated daily average flows at Node 9 (Niles gage) for all flows (top) and for flows <100 cfs (bottom) during different periods.

2.4.1 Proposed future flows at ACDD and Calaveras Dam

The new SFPUC instream flows would be maintained at two compliance locations: (1) The USGS gage below the replacement Calaveras Dam, and (2) a new streamflow gage below ACDD. After completion of the CDRP, the SFPUC would provide releases from Calaveras Dam as described in Table 12and Table 13 (NMFS 2011). In order to develop instream flow schedules below Calaveras Dam that reflect watershed hydrologic conditions, a water-year classification was developed based upon monthly cumulative flows over 26 years of record at the Arroyo Hondo gage (USGS #11-173200), an unregulated tributary upstream of Calaveras Reservoir. Cumulative monthly streamflows at the Arroyo Hondo gage were ranked as exceedance probabilities, and then divided into two water-year types: "Normal/Wet" (0-60% exceedance probability), and "Dry" (>60% exceedance probability). Each hydrologic year begins on October 1 and ends on September 30. The use of monthly cumulative flow in the water-year type classification allows the instream flows to change from one water-year type to another within a hydrologic year depending on cumulative monthly runoff totals, as determined on December 29 and April 30 from the Arroyo Hondo gage. The cumulative runoff totals from October 1 to December 29 determine the instream flow schedule for January 1 to April 30. Similarly, cumulative runoff totals from October 1 to April 30 determine the instream flow schedule from May 1 to September 30. Using this classification, it is expected that any month would be classified as a Dry month four times out of every 10 years and Normal/Wet six times during the same 10 year period. Ramping schedules between the different periods are shown for a Dry year in Table 12 and for a Normal/Wet year in Table 13.

The SFPUC proposes to install screens at the ACDD tunnel, which will reduce the maximum diversion capacity of the ACDD tunnel from 650 cfs to 370 cfs (SFPUC 2011), and the following minimum bypasses and diversions would be implemented for ACDD compliance (NMFS 2011):

- No diversion from April 1 to November 30
- Diversion of up to 370 cfs from December 1 to March 31
- Minimum flow of 30 cfs immediately below ACDD during the diversion period from December 1 to March 31 when water is present in Alameda Creek above ACDD.

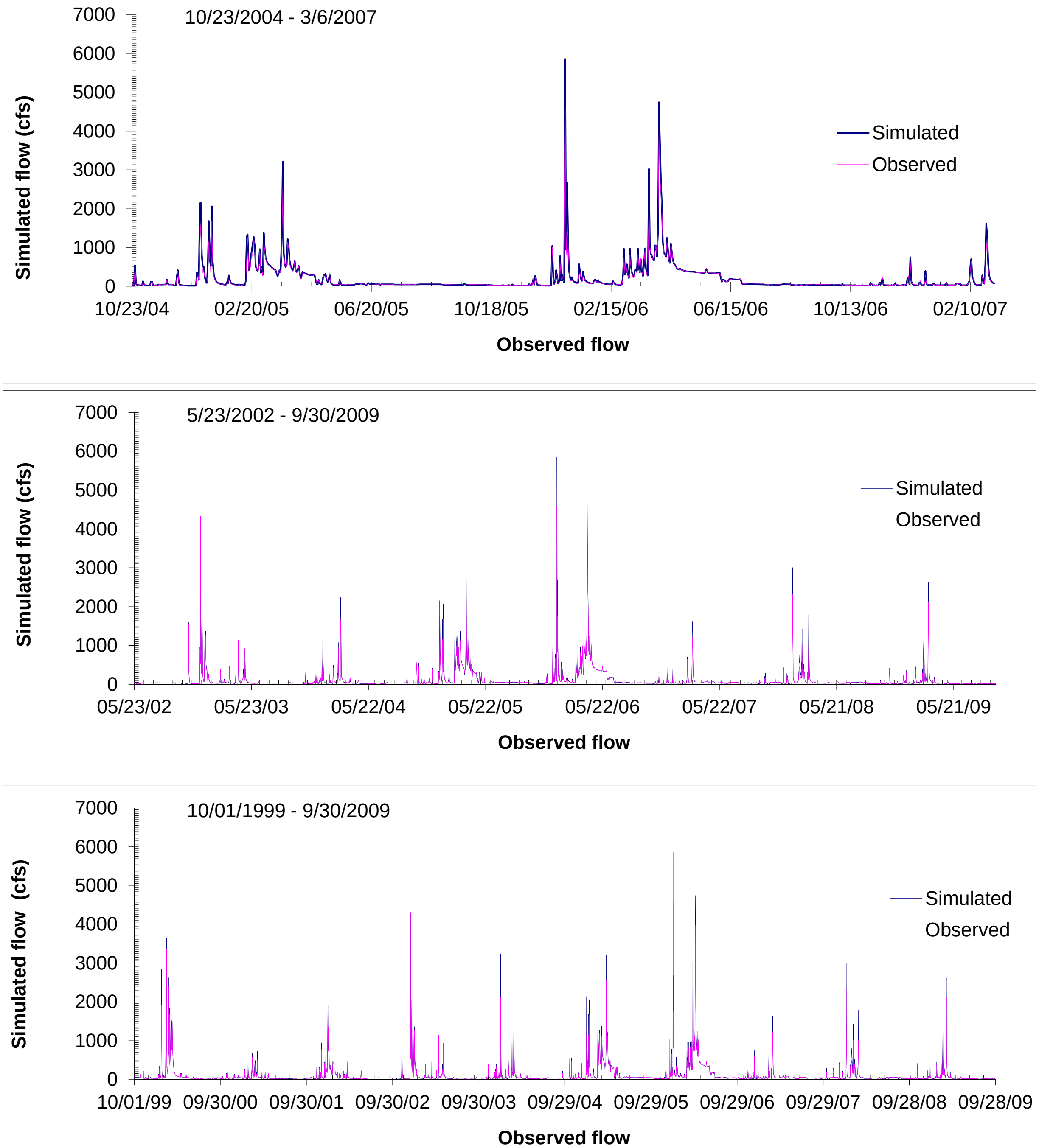

Figure 14. Time series comparison of observed and simulated daily average flows at Node 9 (Niles gage USGS #11-179000) for different periods.

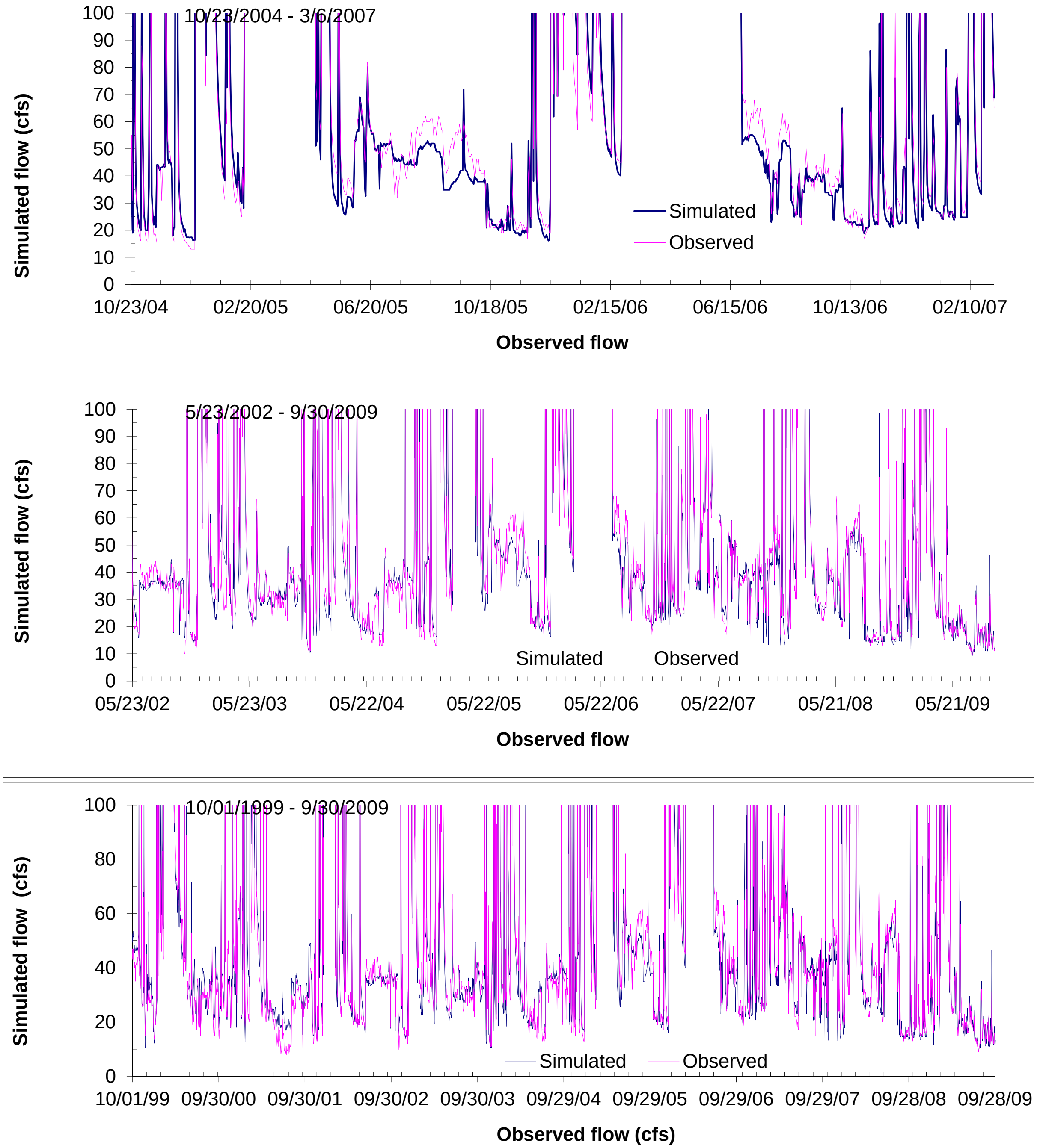

Figure 15. Time series comparison of observed and simulated daily average flows for flows <100 cfs at Node 9 (Niles gage USGS #11-179000) for different periods.

Table 12. Summary of proposed instream daily average flow and ramping schedules below Calaveras Dam for Normal/Wet hydrologic year (Schedule A).

Flow schedule decision date	Flow schedule application period	Cumulative Arroyo Hondo flow volumes for hydrologic year classification (MG)	Flow requirement (cfs)	Flow component
N/A	October 1-2	N/A	9	Downramp
N/A	October 3-31	N/A	7	Baseflow
N/A	Nov. 01 – Dec. 30	N/A	5	Baseflow
Dec. 29	December 30	N/A	7	Upramp
Dec. 29	December 31	N/A	10	Upramp
Dec. 29	Jan. 01 – Apr. 30	> 360	12	Baseflow
Apr. 30	May 01 – Sept. 30	> 7,246	12	Baseflow

Table 13. Summary of proposed instream daily average flow and ramping schedules below Calaveras Dam for Dry hydrologic year (Schedule B).

Flow schedule decision date	Flow schedule application period	Cumulative Arroyo Hondo flow volumes for hydrologic year classification (MG)	Flow requirement (cfs)	Flow component
N/A	October 1-31	N/A	7	Baseflow
N/A	Nov. 01 – Dec. 30	N/A	5	Baseflow
Dec. 29	December 31	N/A	7	Upramp
Dec. 29	Jan. 01 – Apr. 30	<= 360	10	Baseflow
Apr. 30	May 01 – Sept. 30	<= 7,246	7	Baseflow

2.4.2 Proposed future flows at ACWD diversion facilities

Future operations within ACWD's Ground Water Recharge Facilities (GWRF) will involve operating a series of fish ladders, rubber dams, and off-stream diversions to achieve identified bypass flow objectives for the Alameda Creek Flood Control Channel (ACFCC) downstream of ACWD's facilities. In order to meet these objectives, facilities will be operated in accordance with the bypass flow schedule identified in Table 14, which describes flow bypass thresholds and downstream flow targets designed to facilitate passage of adult and juvenile steelhead within the ACFCC. Table 14 identifies two distinct periods of time to define steelhead migration: (1) an in-migration season, which occurs from January 1 and continues until March 31; and (2) an outmigration season, which occurs from April 1 and continues until May 31 of each year. Table 14 identifies daily average downstream flow requirements based on daily average watershed derived inflow measured at the Niles gage (USGS #11-179000, Node 9) for both migration periods. Bypass flow targets are also required for the non-migration season, which occurs from June 1 to December 31 of each year. These non-migration period flows are required to keep a continually wetted corridor from ACWD's facilities out to San Francisco Bay.

Table 14. Proposed ACWD daily average instream bypass flow schedule. The net flows at the Niles gage (USGS #11-179000) do not include imported water from the SBA.

Season	Time period	Net daily averaged flow at Niles gage (cfs)	Proposed minimum bypass flows at BART Weir (cfs)
Diversion / In-migration season	Jan 1 - Mar 31	> 700	Rubber dams down, diversions closed, all flow at Niles gage (minus instream percolation) passes BART Weir
		> 400	Diversions closed, all flow at Niles gage (minus instream percolation) passes BART Weir
		100 - 400	25 cfs + SFPUC fisheries bypass/releases that arrive at Niles gage
		30 - 100	25 cfs [1]
		<30	20 cfs (minus instream percolation) [2]
Diversion / Out-migration season	April 1 - May 31 (Normal/Wet years) [3]	> 700	Rubber dams down, diversions closed, all flow at Niles gage (minus instream percolation) passes BART Weir
		> 400	Diversions closed, all flow at Niles gage (minus instream percolation) passes BART Weir[4]
		< 400	12 cfs + SFPUC fisheries bypass/releases that arrive at Niles gage
	April 1 - May 31 (Dry/Critical years) [3]	> 700	Rubber dams down, diversions closed, all flow at Niles gage (minus instream percolation) passes BART Weir
		> 400	Diversions closed, all flow at Niles gage (minus instream percolation) passes BART Weir
		>25	12 cfs + SFPUC fisheries bypass/releases that arrive at Niles gage[4]
		<25	5 cfs [5]
Non-diversion / Non-migration season	June 1 - Sep 30	> 700	Rubber dams down, all flow at Niles gage (minus instream percolation) passes BART Weir
		< 700	all flow at Niles gage (minus instream percolation) passed BART Weir
Diversion / Non-migration season	Oct 1 - Dec 31	> 700	Rubber dams down, all flow at Niles gage (minus instream percolation) passes BART Weir
		> 400	Diversions closed, all flow at Niles gage (minus instream percolation) passes BART Weir
		< 400	5 cfs [6]

[1] If less than 25 cfs arrives at the BART Weir, all of the flow arriving at the BART Weir shall be bypassed. No water will be released from storage to meet bypass flow requirements.

[2] If less than 20 cfs arrives at the BART Weir, all of the flow arriving at the BART Weir shall be bypassed. No water will be released from storage to meet bypass flow requirements.

[3] Normal/Wet conditions are years when water-year rainfall to date (as of April 1 at Fremont) is greater than the 60% annual exceedance value. Dry/Critical conditions are years when water-year rainfall to date (as of April 1 at Fremont) is less than the 60% annual exceedance value.

[4] If less than 12 cfs arrives at the BART Weir, all of the flow arriving at the BART Weir shall be bypassed. No water will be released from storage to meet bypass flow requirements.

[5] If flows are less than 25 cfs under Dry/Critical conditions, ACWD to provide minimum of 12 cfs + SFPUC fisheries bypass/releases for 7 consecutive days in April and 7 consecutive days in May (days to be specified by NMFS/CDFG). If ACWD off-stream diversions have been reduced to zero and less than 12 cfs arrives at the BART Weir, all of the flow arriving at the BART Weir shall be bypassed. No water will be released from storage to meet bypass flow requirements.

[6] If less than 5 cfs arrives at the BART Weir, all of the flow arriving at the BART Weir shall be bypassed. No water will be released from storage to meet bypass flow requirements.

2.4.3 Computational methods

The model simulates streamflow at 12 locations for varieties of operations for historic climatic conditions from 10/1/1995 to 9/30/2009. As mentioned previously, out of six scenarios currently considered, four use future scenarios ASDHM. This section illustrates different computational components of the future scenarios ASDHM with examples from Scenario 5 and Scenario 6 whenever necessary. Figure 16 schematically illustrates varieties of processes incorporated in the future scenarios ASDHM. Each of the significant components of the model is described subsequently.

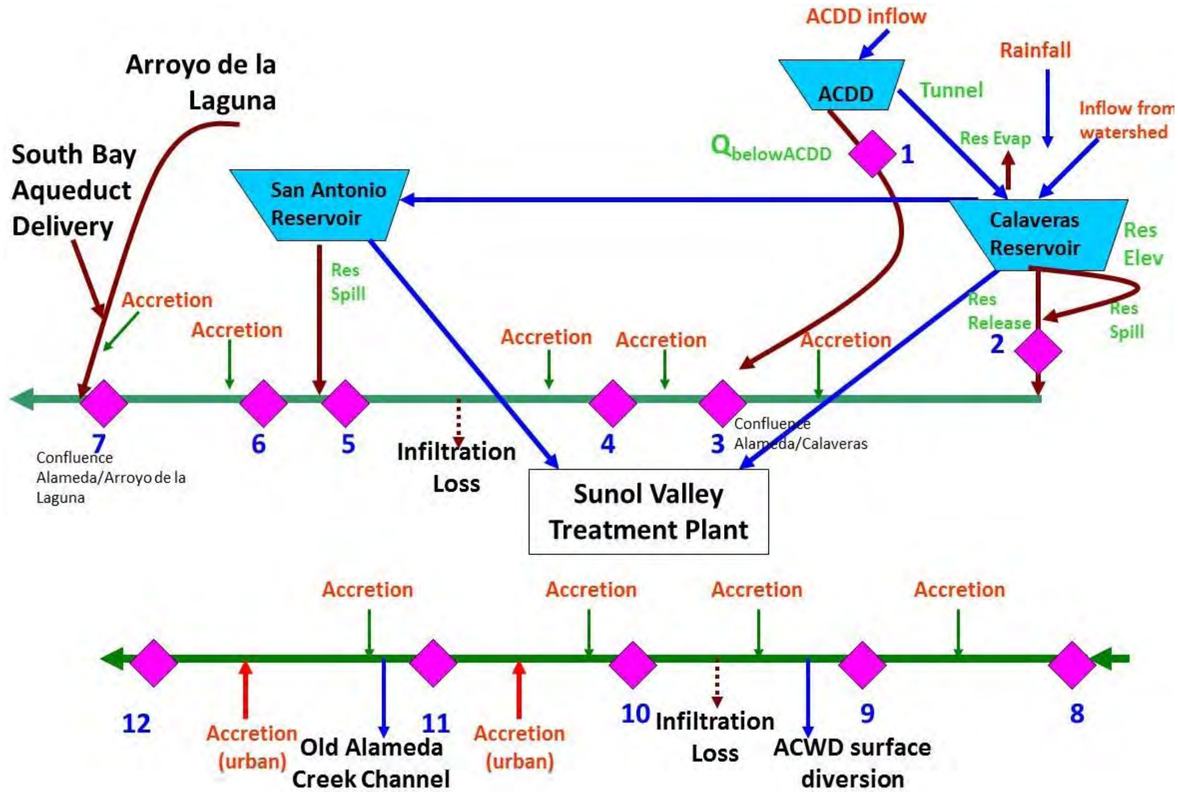

Figure 16. Schematic illustration of computational processes incorporated in the future scenarios ASDHM. Blue numbers signify ASDHM nodes.

2.4.3.1 ACDD operations

The future scenarios ASDHM can analyze a variety of operations at ACDD. For example, the new instream flow compliance from ACDD (as required in Scenario 5) requires different operation of ACDD than currently occurs. The installation of screens at the ACDD tunnel is expected reduce the maximum diversion capacity of the ACDD tunnel from 650 cfs to 370 cfs. In addition, there would be no diversion from April 1 to November 30. Diversion occurs (up to 370 cfs) December 1 to March 31. Minimum flow of 30 cfs is maintained immediately below ACDD during the diversion period from December 1 to March 31 when water is present in Alameda Creek above the diversion dam.

Depending upon modeling scenarios conditions, daily average divertible flow from ACDD to Calaveras Reservoir is computed using 15-minute measured streamflow at the Above ACDD gage (USGS #11-172945) for reasons explained in the previous section. Some of these conditions for Scenario 5 and Scenario 6 are depicted in Figure 17 for illustration. Whether or not the divertible flow could be diverted to Calaveras Reservoir depends on two factors: (1) condition of ACDD tunnel gates (opened or closed), and (2) condition of Calaveras Reservoir (full or not). For example in Scenario 6, divertible flows could be diverted only from December 1 to March 31, whereas in Scenario 5, no such restriction exists. If Calaveras Reservoir is full on any day, the divertible flow is routed downstream through ACDD. Flows Above ACDD + divertible flows result in flow at Node 1 (i.e., flow below ACDD).

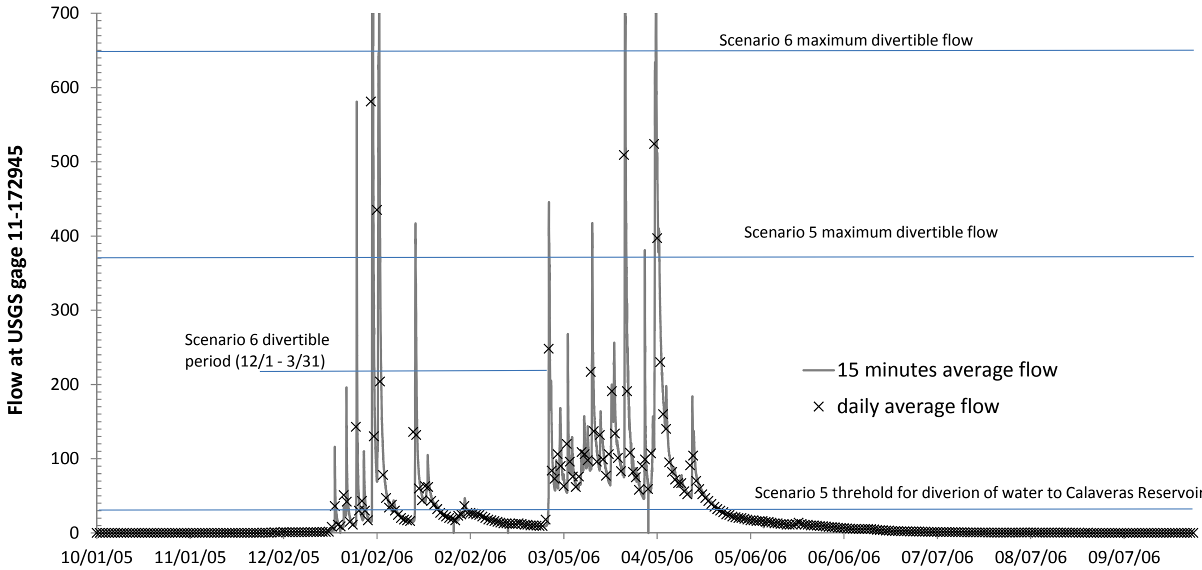

Figure 17. Average 15-minute and daily flows measured at the Above ACDD gage (USGS #11-172945) for HY2006, depicting effect of instantaneous flow on ACDD divertible flow to Calaveras Reservoir for Scenario 5 and Scenario 6.

2.4.3.2 Calaveras Dam operations

The model simulates Calaveras Reservoir volume and elevation based on total inflow and outflow from the reservoir. The reservoir was constructed to a capacity of 96,800 acre-feet (31.5 billion gallons) and is currently constrained by DSOD interim operating restrictions to an operating capacity of 37,800 acre-feet (12.4 billion gallons). The new reservoir will have the same full capacity of about 31.5 billion gallons. Calaveras Reservoir receives inflow from Arroyo Hondo, Calaveras Creek, small tributaries surrounding Calaveras Reservoir and bypassed Alameda Creek flow through the ACDT. The model begins with usage of observed streamflow from 10/1/1995 to 9/30/2009 from the Arroyo Hondo gage (USGS #11-173200) and Above ACDD gage (USGS #11-172945). Arroyo Hondo comprises about 80% of the watershed upstream of Calaveras Reservoir. The remaining 20% constitutes the Calaveras Creek and associated watersheds upstream of the reservoir. The observed Arroyo Hondo flow is therefore scaled to incorporate contribution from Calaveras Creek and surrounding watersheds.

Water from Calaveras Reservoir flows by gravity through the Calaveras Pipeline to the Sunol Valley Treatment Plant (SVTP), and then flows to the Alameda Siphons where it is combined with the Hetch Hetchy water supply. Water from Calaveras Reservoir can also be transferred to San Antonio Reservoir. In the current version of the model, the observed transfer values were used with the exception that transfers for HY2006 were replaced by transfers for the similar HY1996 (in terms of Arroyo Hondo Flow) because HY2006 transfers did not represent typical transfers for such years.

The evaporation from Calaveras Reservoir was simulated based on the same algorithm incorporated in the Hetch Hetchy Local Simulation Model (HHLSM), which was derived based on net evaporation values for Del Valle Reservoir (Steiner 2007). An existing physical relationship between a reservoir's storage and surface area is used to determine the surface area for computed reservoir storage on a daily basis. The computed reservoir surface area is then used by the model to estimate net evaporation for each day of the simulation. The volume of water directly contributed by rainfall on the water surface of the reservoir was simulated based on the daily rainfall observed close to the reservoir and reservoir water surface area for that particular day.

A variety of instream flow release schedules from Calaveras Reservoir can be selected in the future scenarios model. For example, Scenario 6 uses the CDRP instream flow release agreed among SFPUC, NMFS, and CDFG in June 2010. Calaveras Reservoir spills to Calaveras Creek when reservoir elevations exceed 756.20 ft. The current version of the model does not take into account operations of two existing cone valves to manage uncontrolled spill. The operation of cone valves is assumed to be limited to instream flow releases. Calaveras Reservoir releases in the form of instream flow or spill (at times) contribute to flow at Node 2. In the computation of flow at Node 2, the contribution from the small watershed area between the dam and Node 2 was omitted.

2.4.3.3 Flow loss and gains in Sunol Valley

Once Node 1 and Node 2 flows are computed, Node 3 flow is computed by incorporating the contribution from unregulated areas between Node 1 and Node 3 in Alameda Creek and Node 2 and Node 3 in Calaveras Creek. Node 4 flow is then computed taking into account the contribution from unregulated areas between Node 3 and Node 4. As in the impaired flow model, the downstream flow routing and storage effect was omitted except during the calculation of ACWD bypass flow, because the estimation of ACWD bypass flow depended on SFPUC releases (discussed later). As explained in Section 2.3.1.3, flow loss occurs between Node 4 and Node 5. Node 5 also receives accretion flow from unregulated areas between Node 4 and Node 5 during larger storm events. Continuous release of water from Calaveras Reservoir and the proposed cut-off wall along gravel pits in Sunol Valley add to the complexity in flow loss and gain assumptions in the future scenarios ASDHM.

Currently, four different options for surface water losses (17 cfs, 10 cfs, 5 cfs, and 0 cfs) in Sunol Valley can be incorporated in the future scenarios ASDHM. These options have been provided basically to acknowledge the complexity of future losses in Sunol Valley. The complexity related to dynamics of future losses is contributed by two factors: (1) with instream flow release, Alameda Creek below the confluence with Calaveras Creek will become perennial. Alameda Creek has never been perennial, even in the unimpaired condition. Therefore, owing to year round stream bed saturation, it is possible that dynamics of surface-subsurface interaction may change in the course of time; and (2) the proposed new cut-off walls are also expected to influence subsurface and surface flow interaction in the Sunol Valley. Once these cut-off walls (approximately 20-80 ft deep) are installed, depending on their efficiency, the path of infiltrated water may be limited to parallel to the stream. Quarry pits are expected to get no flows (or the least flows). Therefore, surface-subsurface flow dynamics may change in the future. The current version of the model provides options of including either historic quarry gains or no gains. Since future operations of the quarries are difficult to predict, we assume future gains from quarry pits to be equal to historic gains.

In summary, in future scenarios model runs, losses and gains in Sunol Valley can be gamed as desired. For example, in Scenario 5 and Scenario 6, we assume 17 cfs loss and no gain from the gravel quarries for consistency and comparative purposes, owing to uncertainty of future quarry operation and unavailability of historic data related to quarry pit discharge to Alameda Creek from HY1996 to HY1998.

2.4.3.4 Contribution from San Antonio Creek

Node 6 is located downstream of the confluence with San Antonio Creek in Alameda Creek. Therefore, uncontrolled spill or release from San Antonio Reservoir contributes to this node. The San Antonio gage (USGS #11-174000) located just downstream of San Antonio Reservoir provides data related to spill and other releases from San Antonio Reservoir from 10/1/1999. Therefore, the simulation period of earlier versions of the future scenarios ASDHM downstream of Node 5 was constrained to HY1999-HY2009. In order to include Wet year samples from HY1996 to HY1999 downstream of Node 5, a relationship between reservoir elevation and daily average spill was established between the observed streamflow data from 10/1/1999 to 9/30/2009 and the reservoir elevation (manually observed). San Antonio Reservoir spilled during this period for about 25 days (in HY2006) and the spill ranged from 19 cfs to 445 cfs. These samples were considered enough to generate spillway rating curve as spillway ratings based on the spillway engineering design were not available for San Antonio Dam. Once this relationship was established, using observed reservoir elevation data, spill days and average daily spill were estimated from 10/1/1995 to 9/30/2009. Other releases (such as from cone valves) from San Antonio Reservoir for the period 10/1/1995 to 9/30/2009 were not available. It was assumed that such releases occurred during very wet conditions for a short period and would affect the outcome only for a few wet days over the HY1996-2009 time series.

The contributions from the watershed area between San Antonio Dam and the San Antonio Creek gage (0.86 mi^2) and between the gage site and the confluence with Alameda Creek (0.44 mi^2) have been set as optional in the model; the user is able to either include or exclude them. The influence of stream morphology on flow losses and gains below San Antonio Dam has never been monitored. Therefore, phenomena of losses in this reach are not as clear as in Sunol Valley on Alameda Creek. Due to this reason, contribution from the watershed area below San Antonio Reservoir was omitted in Scenario 5 and Scenario 6, although the provision of incorporating losses in that reach, if desired, has been incorporated in the model.

2.4.3.5 Node 9 – Node 11 computations

As in the measured impaired flow analysis, once the flow at Node 6 is calculated, Nodes 7, 8, and 9 are computed employing accretion from additional watershed areas. Nodes 10, 11, and 12 receive contribution from urban drainage as well as from natural watersheds. The method of estimating urban contributions is already described for the measured impaired model in Section 2.3.1.5. The major difference in the future scenario ASDHM (Scenario 5) is that ACWD bypass flow needs to be taken into account between Node 9 and Node 10. ACWD has reached preliminary agreements with NMFS and CDFG for bypass flow requirements as described in Section 0, Table 12 and Table 13. The future scenario ASDHM is linked to a separate spreadsheet within the model to incorporate ACWD bypass flow. Node 10 serves as the compliance location for ACWD and the Node 10 flow depends on ACWD bypass flow requirements. Therefore, in the future scenarios ASDHM (Scenario 5), Nodes 9 to 11 were computed sequentially. Once Node 10 was computed based on ACWD bypass flow requirements, the future scenario Node 11 flow was computed as “computed future Scenario Node 10 flow” + “Dry Creek contribution” + “contribution from natural watershed between Node 10 and Node 11” + “contribution from urban watershed between Node 10 and Node 11” – “old Alameda Creek bypass flow.” Node 12 was then computed based on computed Node 11 flow and contributions from urban and natural watersheds. However, when the future scenarios ASDHM was used to model the computed impaired scenario (Scenario 6), which did not include ACWD bypass flow, the computation involved for Nodes 10 to 12 was same as that for Scenario 4 as described in Section 2.3.1.5.

2.4.3.6 ACWD operations

For Scenario 5, determination of future ACFCC flows were calculated based on existing ACFCC flow data, integrated with the future bypass flows described in Table 14. During periods of time when ACWD’s historic observed operations did not allow for the correct minimum flow required under the future flow scenario, historic GWRF operations were revised to allow for the correct bypass rate. In contrast, when historic observed operations provided flow additional to the minimum rates described within Table 14, the ASDHM analysis assumed the additional flows would be available to remain in the channel under the future condition.

Specific flow thresholds during the in-migration and out-migration seasons require passage around ACWD's facilities and accounting of SFPUC fisheries flow releases originating from Calaveras Dam and ACDD. Historical observations indicate that these flow releases may take up to 17 hours to travel the required distance before contributing to the Niles gage (USGS #11-179000), necessitating a time lag when computing SFPUC additions to Node 9. To account for this delay, the future scenarios ASDHM assumes a 1-day lag from ACDD and Calaveras Reservoir releases to contribute to Node 9, due to the 1-day computational timescale for the ASDHM model.

2.5 Hydrologic modeling results

This section presents results of the ASDHM hydrologic analysis. The daily average streamflows from all six scenarios for all 12 nodes for 14 years have been provided on a CD in Appendix A. Since it is difficult, if not impossible, to present all hydrographs representing six scenarios, 14 years, and 12 nodes, we have illustrated representative hydrographs from selected hydrologic years. First, results are presented from three scenarios: (1) unimpaired (Scenario 2), (2) future (Scenario 5), and (3) computed impaired (Scenario 6). Both NGD and EDT use these three scenarios. Scenario 1, which is the base scenario for EDT analysis, has not been included because Scenario 1 and Scenario 2 are identical from Node 1 to Node 7 (unimpaired condition), and downstream of Node 7, the scenario portrays hypothetical combinations of unimpaired and impaired watershed conditions.

Results are presented from five hydrologic years representing ranges of exceedance probabilities from 1% to 81% (Figure 18). Hydrographs from four nodes, Nodes 4, 5, 9, and 10, are presented below. Node 4 was included because it is downstream of SFPUC's compliance location and is the most upstream node of Sunol Valley. Node 5 was selected because differences in hydrographs between Node 4 and Node 5 depict the influence of loss in Sunol Valley. Node 9 and Node 10 represent nodes upstream and downstream of ACWD bypass flow, respectively.

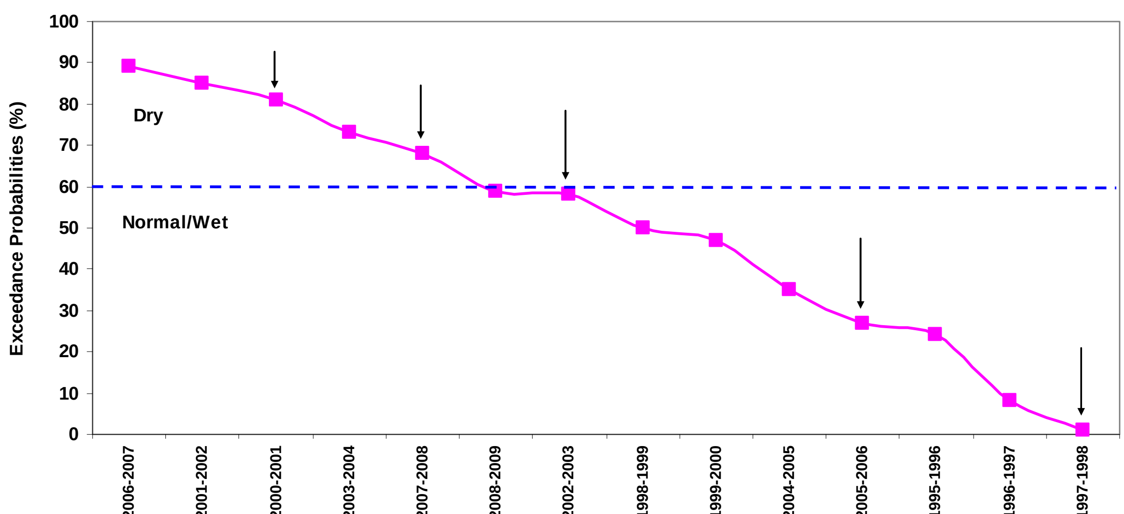

Figure 18. Streamflow exceedance probabilities for different years based on hydrologic year cumulated Arroyo Hondo flow. Arrows represent years selected for results presentations.

Figure 19 and Figure 20 depict hydrographs at Node 4 from October to March and from April to September, respectively. The hydrographs are plotted top to bottom for HY2001, HY2008, HY2003, HY2006, and HY1998, representing exceedance probabilities of 81%, 68%, 58%, 27%, and 1%, respectively. In general, at Node 4, future flows were always higher than computed impaired flows. However, there were instances during which Calaveras Reservoir was full in Scenario 6, resulting in spill, whereas the reservoir did not spill in Scenario 5 due to continuous release of instream flows. In Dry years, such as HY2001 and HY2008, future flows at Node 4 were higher than unimpaired flows almost from May to November (six months) due to instream flow releases from Calaveras Reservoir. During Wet years, such as HY2006, future flows were higher than unimpaired flows from July to November. Even in the wettest year, HY1998, during which rainstorm events were observed even in late May, future streamflows at Node 4 were higher than unimpaired flows from August to mid-November. During mid-winter, peak flows were higher in the unimpaired scenario but several >100 cfs peaks were observed in the future scenario even in the driest HY2001. These peaks, in general, resulted due to reduction in ACDD tunnel capacity to 370 cfs from 650 cfs. The flashy nature of Alameda Creek contributes to several higher peaks downstream of ACDD even in the driest year. Because ACDD in the future scenario is operated only from December 1 to March 31, larger streamflow peaks were observed in the future scenario compared to the computed impaired scenario, when rainstorm events occurred in November, December, April, and May.

Figure 21 and Figure 22 depict hydrographs at Node 5 from October to March and from April to September, respectively. The pattern of flows at Node 5 is similar to Node 4 for higher flows. Because the future scenario (Scenario 5) assumed present day streamflow loss in Sunol Valley and no gains from quarry pits to Alameda Creek as a conservative representation of surface water in the stream, the same scenario with “no loss in Sunol Valley” has also been presented for comparative purposes in Figure 21 and Figure 22. Depending on assumptions related to losses in Sunol Valley, Node 5 may or may not have flows from May to November. A complex interaction between perennial flow in the stream and the extent of cut-off walls to influence loss in the Sunol Valley may determine actual flow at Node 5, particularly between May and November.

Figure 23 and Figure 24 depict hydrographs for Node 9, and Figure 25 and Figure 26 depict hydrographs for Node 10. Modeled hydrographs at Node 9 during the fall and winter months for the computed impaired (Scenario 6) and future scenario (Scenario 5) reflect the flashy runoff characteristics associated with runoff from the Arroyo de la Laguna watershed for all presented exceedance probabilities. During the fall periods both the computed impaired (Scenario 6) and future conditions (Scenario 5) tend to have higher baseflow periods between storms when compared to the unimpaired scenario (Scenario 2). This is primarily due to developed land use characteristics of the Arroyo de la Laguna watershed, and intermittent contributions of imported water released to this reach for groundwater recharge use downstream by ACWD. This pattern of higher baseflows within this reach is also exhibited during the late spring and summer months as a result of the same two functions.

Flows at Node 10 reflect the timing and magnitude of discharges from ACWD’s facilities. These flows travel from Node 10 unimpeded downstream through a flood control channel, and out to San Francisco Bay. Inspection of the hydrographs indicates the during the fall and winter months, unimpaired peak flows tend to be higher than both the future and computed impaired scenarios. Base flows and lower flow rates are also noticeably different between all three scenarios for all exceedance probabilities, and reflect the modeled hydrologic conditions associated with ACWD’s historic and proposed future flow bypass schedule described in Table 14. These differences can be seen during both the fall/winter timeframe as well as the spring/summer periods.

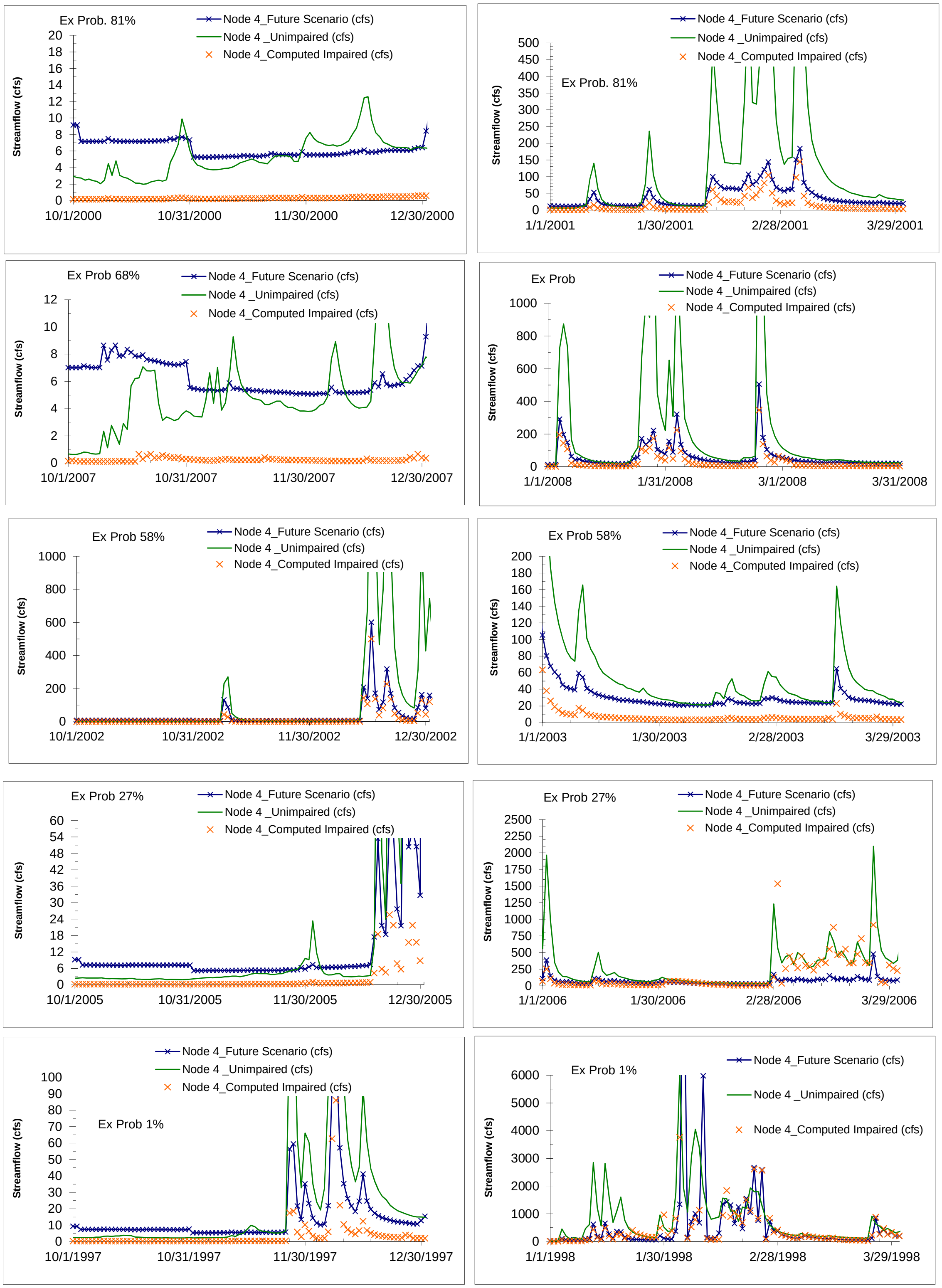

Figure 19. Flows at Node 4 for Scenario 2 (unimpaired), Scenario 5 (future), and Scenario 6 (computed impaired) from October to March for two Dry hydrologic years (2001, 2008), one hydrologic year on the Dry-Normal/Wet boundary (2003), and two Normal/Wet hydrologic years (2006, 1998).

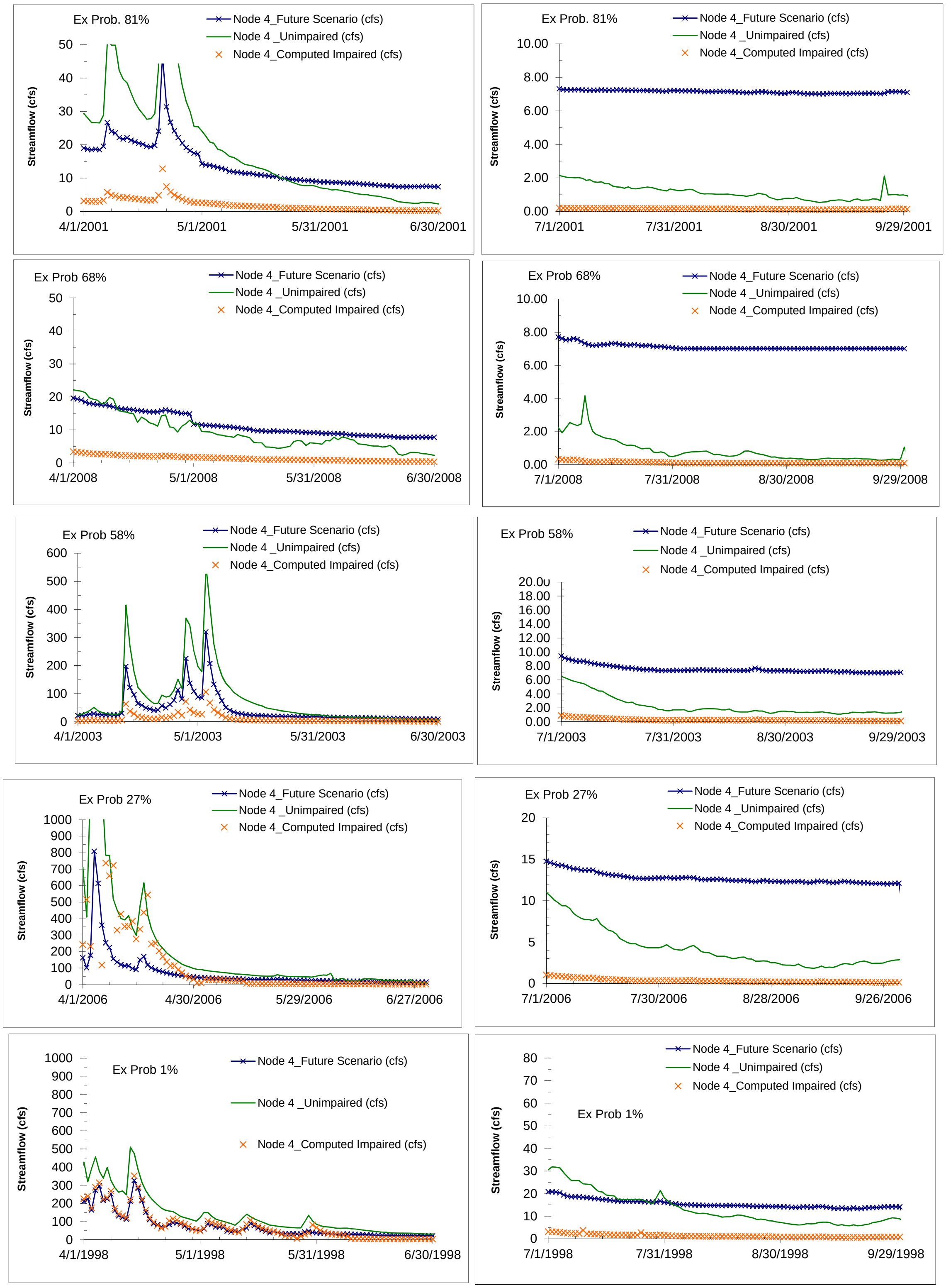

Figure 20. Flows at Node 4 for Scenario 2 (unimpaired), Scenario 5 (future), and Scenario 6 (computed impaired) from April to September for two Dry hydrologic years (2001, 2008), one hydrologic year on the Dry-Normal/Wet boundary (2003), and two Normal/Wet hydrologic years (2006, 1998).

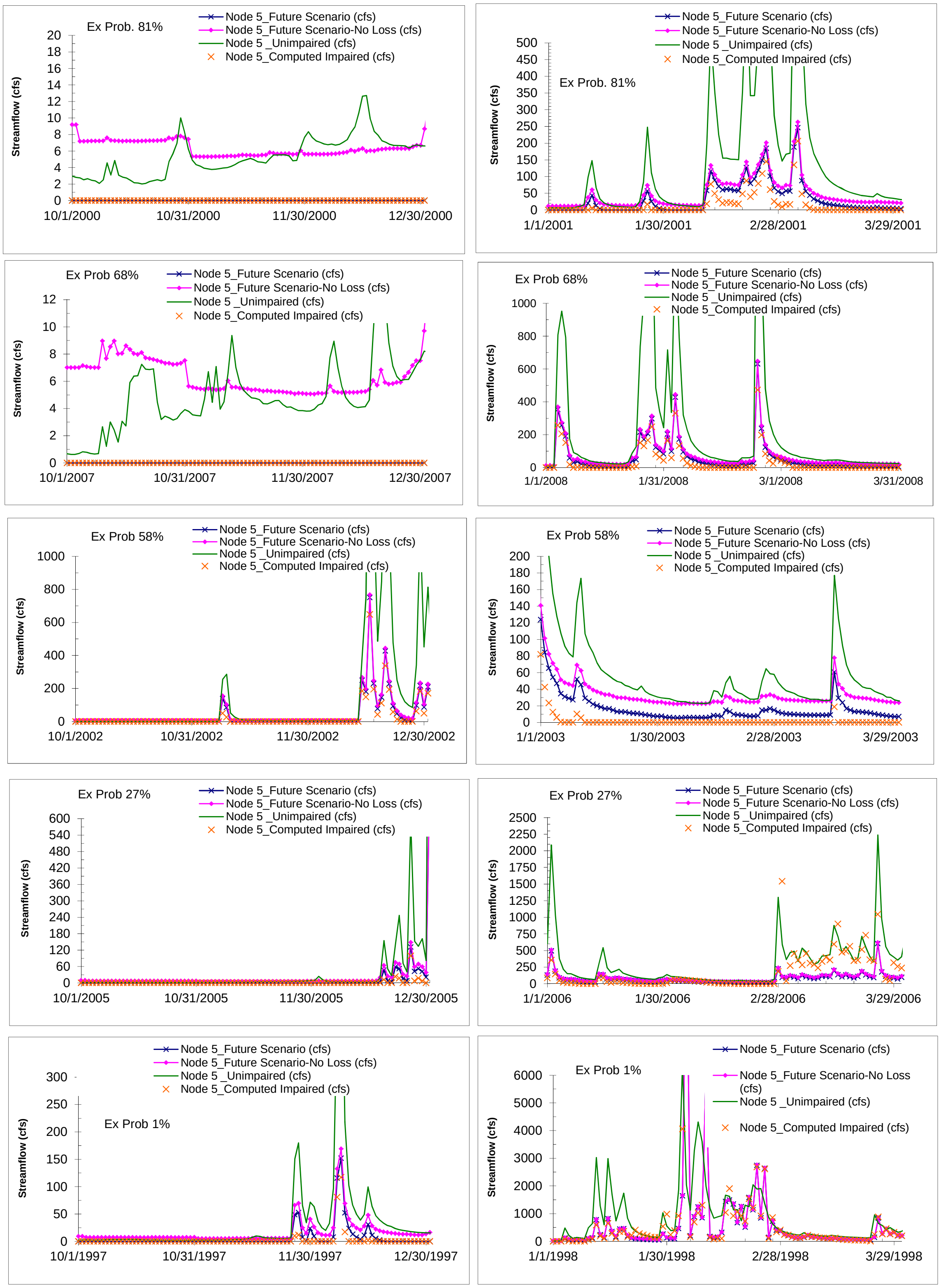

Figure 21. Flows at Node 5 for Scenario 2 (unimpaired), Scenario 5 (future), and Scenario 6 (computed impaired) from October to March for two Dry hydrologic years (2001, 2008), one hydrologic year on the Dry-Normal/Wet boundary (2003), and two Normal/Wet hydrologic years (2006, 1998).

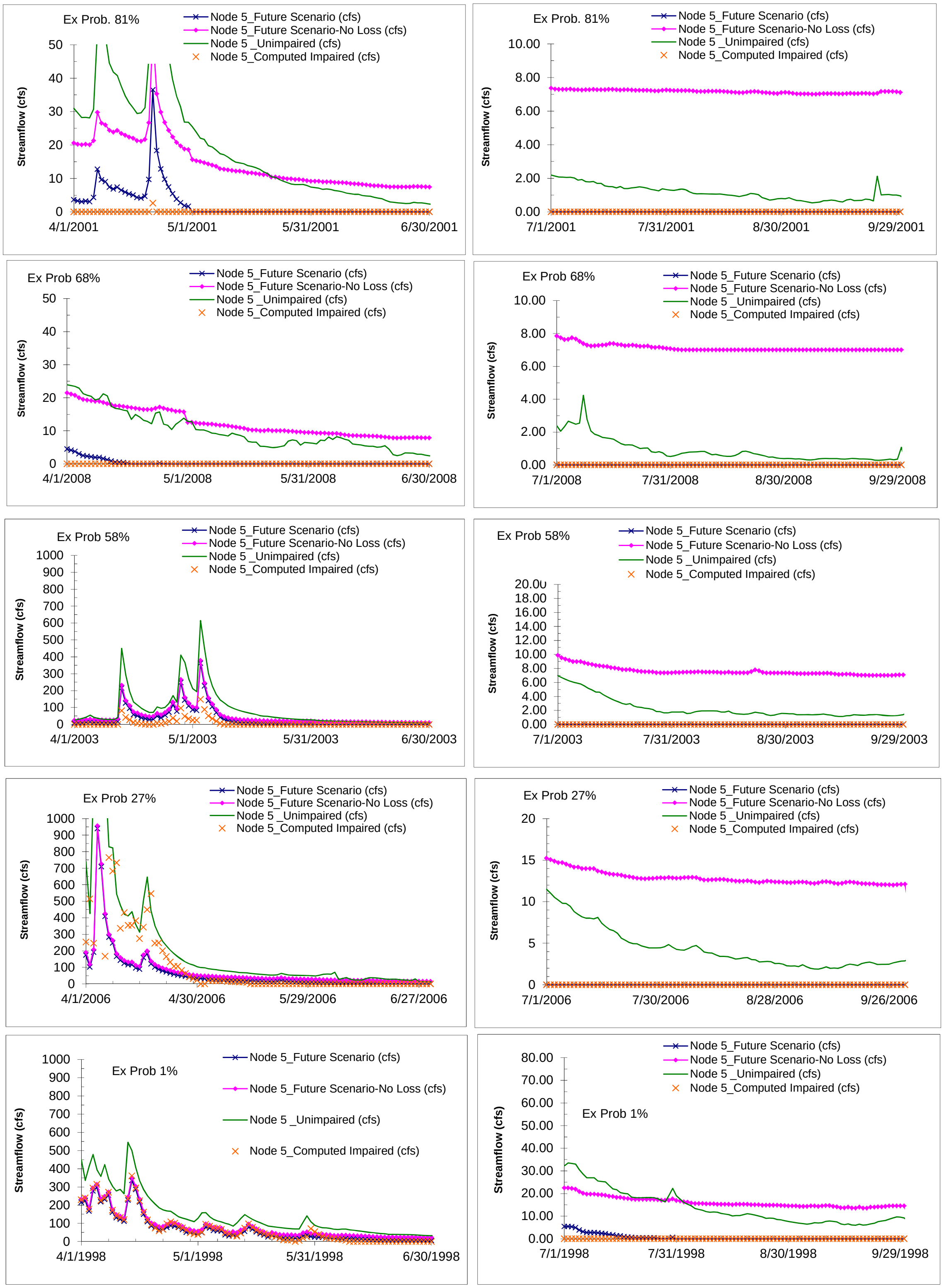

Figure 22. Flows at Node 5 for Scenario 2 (unimpaired), Scenario 5 (future), and Scenario 6 (computed impaired) from April to September for two Dry hydrologic years (2001, 2008), one hydrologic year on the Dry-Normal/Wet boundary (2003), and two Normal/Wet hydrologic years (2006, 1998).

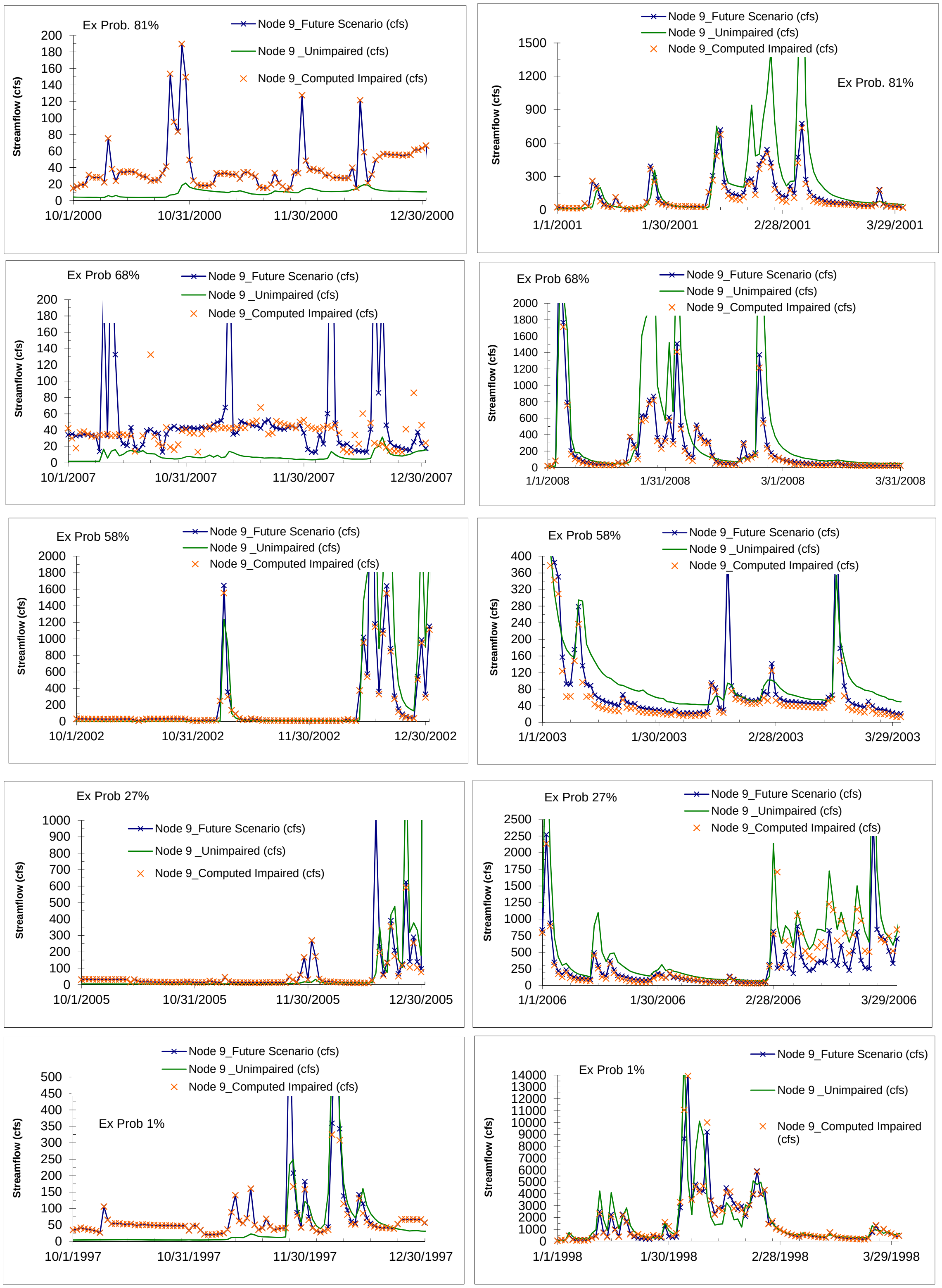

Figure 23. Flows at Node 9 for Scenario 2 (unimpaired), Scenario 5 (future), and Scenario 6 (computed impaired) from October to March for two Dry hydrologic years (2001, 2008), one hydrologic year on the Dry-Normal/Wet boundary (2003), and two Normal/Wet hydrologic years (2006, 1998).

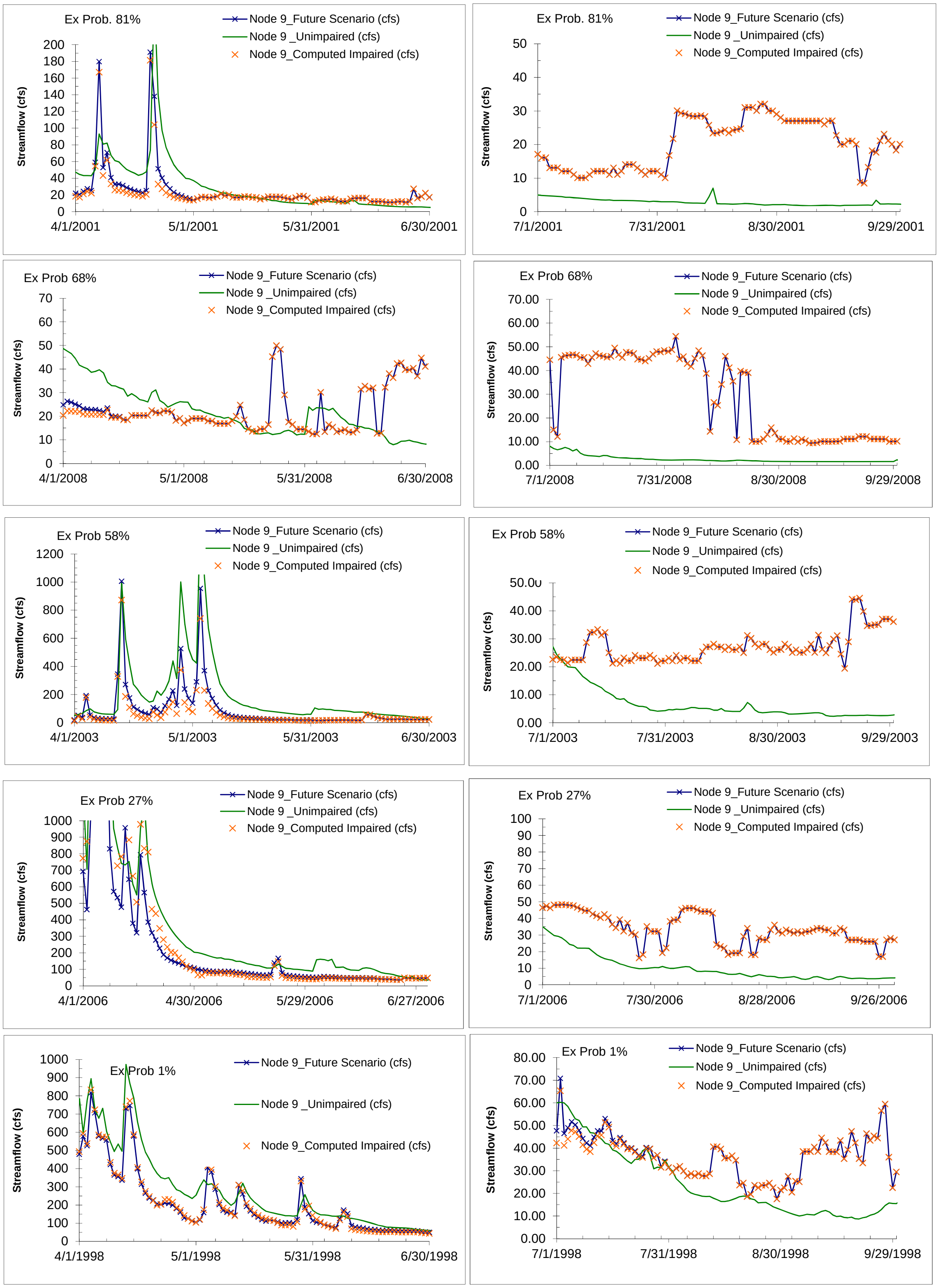

Figure 24. Flows at Node 9 for Scenario 2 (unimpaired), Scenario 5 (future), and Scenario 6 (computed impaired) from April to September for two Dry hydrologic years (2001, 2008), one hydrologic year on the Dry-Normal/Wet boundary (2003), and two Normal/Wet hydrologic years (2006, 1998).

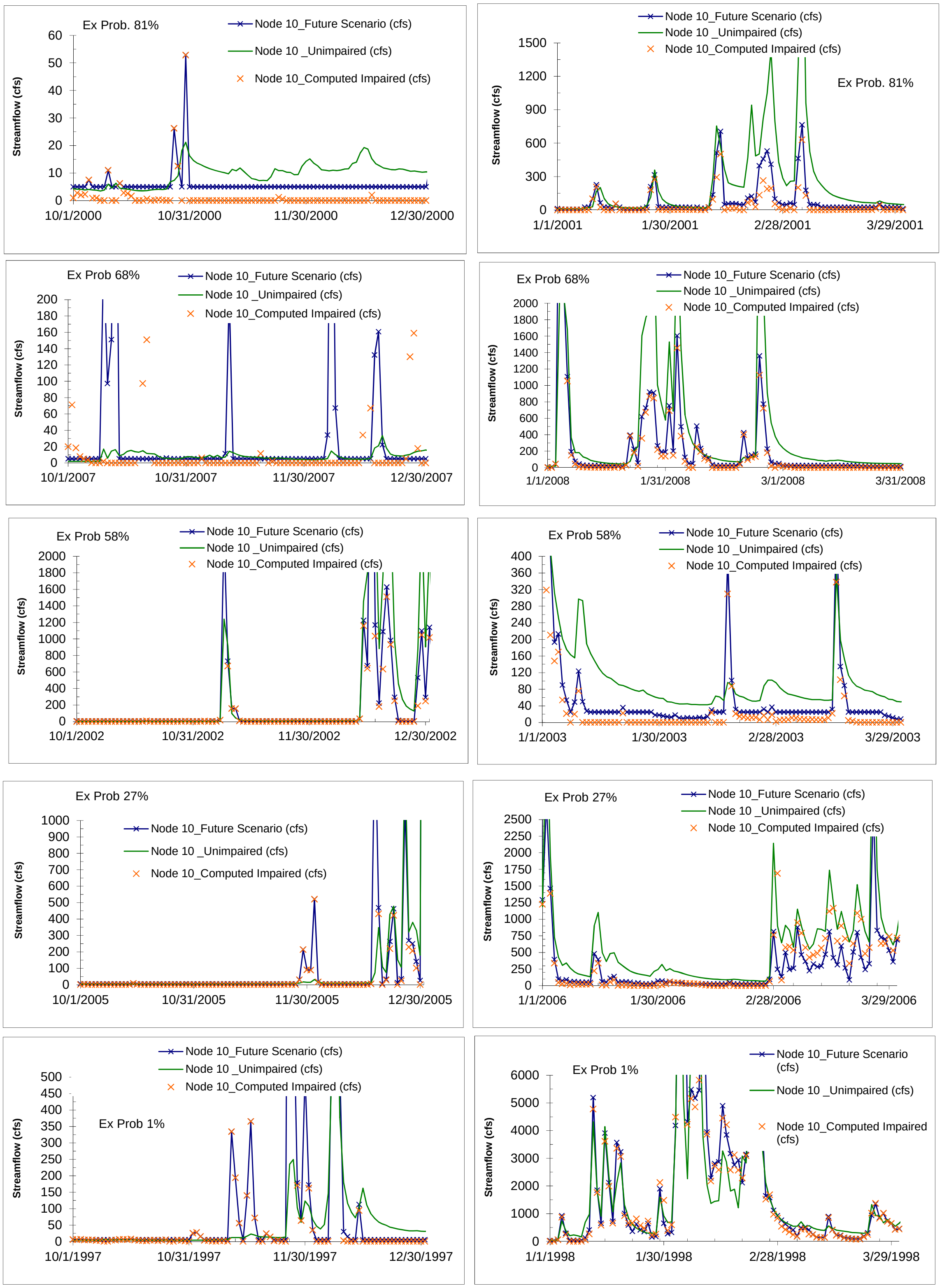

Figure 25. Flows at Node 10 for Scenario 2 (unimpaired), Scenario 5 (future), and Scenario 6 (computed impaired) from October to March for two Dry hydrologic years (2001, 2008), one hydrologic year on the Dry-Normal/Wet boundary (2003), and two Normal/Wet hydrologic years (2006, 1998).

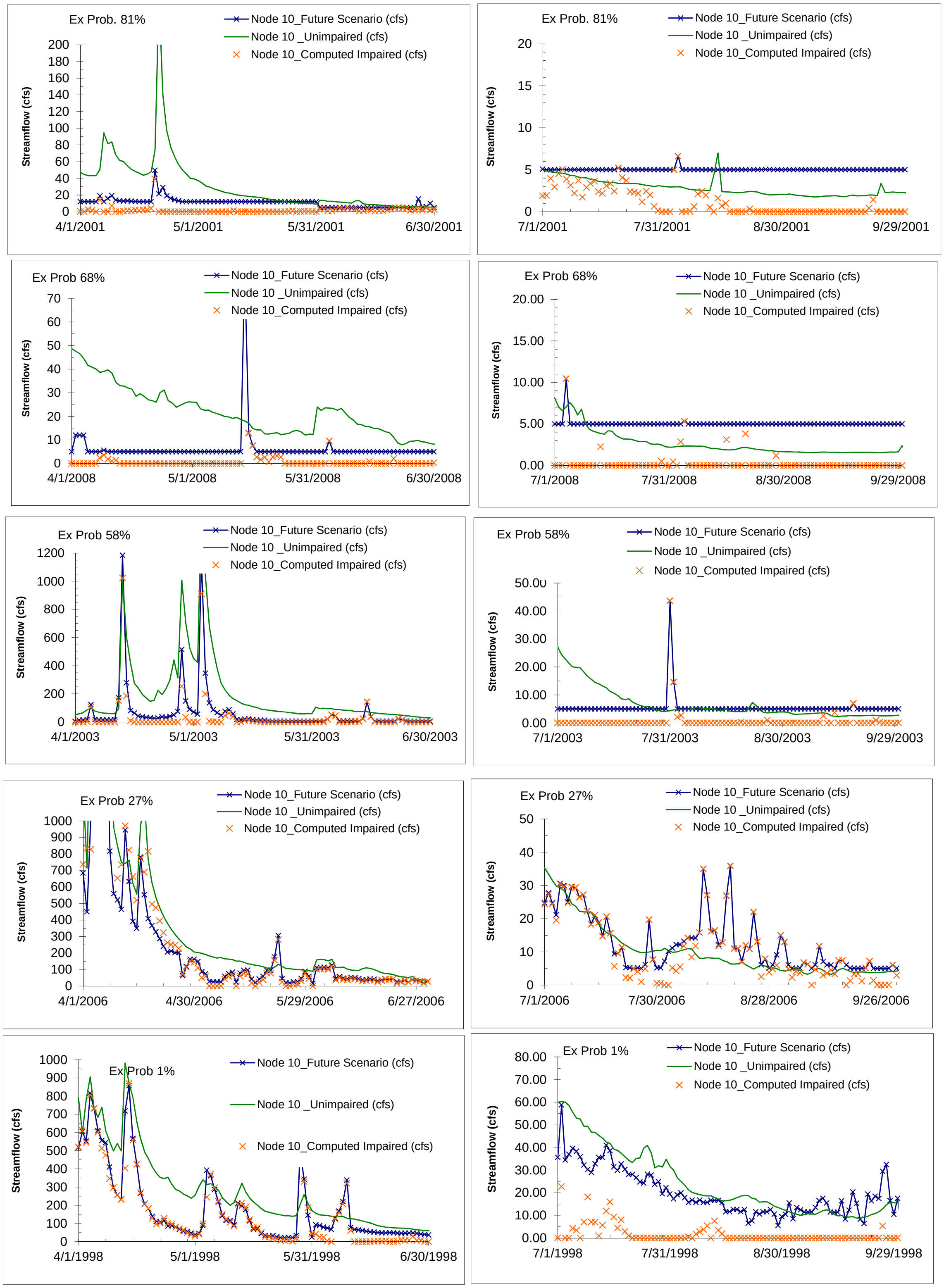

Figure 26. Flows at Node 10 for Scenario 2 (unimpaired), Scenario 5 (future), and Scenario 6 (computed impaired) from April to September for two Dry hydrologic years (2001, 2008), one hydrologic year on the Dry-Normal/Wet boundary (2003), and two Normal/Wet hydrologic years (2006, 1998).

3 HYDRAULIC AND WATER TEMPERATURE MODELING

3.1 HEC-RAS model overview

To quantify needed hydraulic and water quality characteristics required by both the EDT and NGD analyses, a one dimensional hydraulic model was developed. Model selection of the United States Army Corps of Engineers, Hydrologic Engineering Centers River Analysis Software 4.1.0 (HEC-RAS) was pursued mainly due to its public domain status and proven successful applications within a diverse array of river systems across the United States (ACOE 2008). Specifically, HEC-RAS was developed to identify cross-sectional top width and averaged depth as a function of flow, as well as to perform water temperature predictions to serve as inputs to the NGD and EDT analyses. To achieve these goals, steady, unsteady, and water quality models were created within the HEC-RAS framework, and populated with various data types including flow data from the ASDHM outputs.

3.2 HEC-RAS steady-state hydraulic modeling

3.2.1 Methods

To quantify cross-sectional averaged width and depth as a function of flow, a steady-state application of HEC-RAS was developed and run for various steady-state discharges ranging from 1 cfs to 18,000 cfs, as identified in Table 15. For each specific flow identified in the table, hydraulic characteristics (width, depth, area, etc.) were calculated and compiled for use in the EDT analysis. Because the EDT model computes physical fish habitat parameters using monthly average flows from ASDHM, the EDT model simply needed average widths and depths for all cross sections in an EDT model segment at a particular flow. Therefore, the HEC-RAS steady-state model output was used rather than output from the unsteady HEC-RAS model runs.

Table 15. Summary of flows used in steady-state HEC-RAS model runs.

Steady-state flows (cfs)								
1	55	110	165	240	350	460	3,000	14,000
5	60	115	170	250	360	470	4,000	15,000
10	65	120	175	260	370	480	5,000	16,000
15	70	125	180	270	380	490	6,000	17,000
20	75	130	185	280	390	500	7,000	18,000
25	80	135	190	290	400	600	8,000	
30	85	140	195	300	410	700	9,000	
35	90	145	200	310	420	800	10,000	
40	95	150	210	320	430	900	11,000	
45	100	155	220	330	440	1,000	12,000	
50	105	160	230	340	450	2,000	13,000	

Development of the steady-state model required compilation of various topographic and cross sectional survey data sets. Specifically, a ground survey was carried out measuring 114 cross sections from the ACDD (Node 1) to the Niles gage (Node 9) over a two week period in order to develop the needed cross section survey data set. Additional cross section survey data were obtained for the ACFCC from the Alameda County Public Works Department, as well as numerous other cross sections throughout the study area that were collected for previous projects. The model was populated with a total of 229 cross sections from Node 1 (just below the ACDD) to Node 12 (at the mouth of San Francisco Bay.) During this time, photos were taken for the majority of the surveyed cross sections, as well as relevant notes about general river morphologic characteristics, to help develop a qualitative data set used to assist steady-state model calibration and validation. Example locations of these cross sections are displayed in Figure 27.

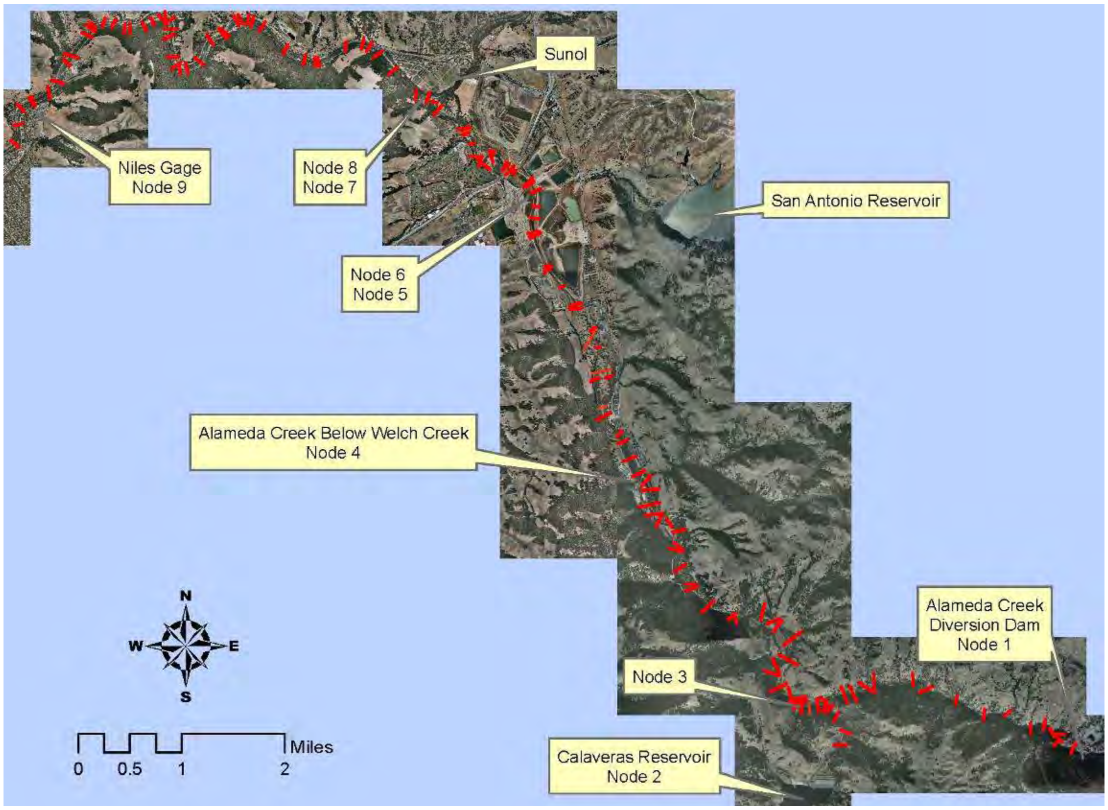

Figure 27. Cross sections used for steady-state and unsteady HEC-RAS model.

To optimize field survey resources, the field-surveyed cross sections were limited to the extent of the active creek channel, and did not include any floodplain or overbank features. To characterize overbank and floodplain scale features, these field-surveyed in-channel cross sections were combined with terrestrial LiDAR survey data of the out-of-channel areas collected for the County of Alameda in 2006. Using geospatial analysis tools to "stitch" these two datasets together, cross sections were generated that included the field-surveyed detail of the low flow channel and the accurate overbank and floodplain topography provided by the terrestrial LiDAR survey. These cross sections were then input into the HEC-RAS model for use in both steady-state and unsteady model runs. The results of an application of the cross section stitching routine are presented in Figure 28.

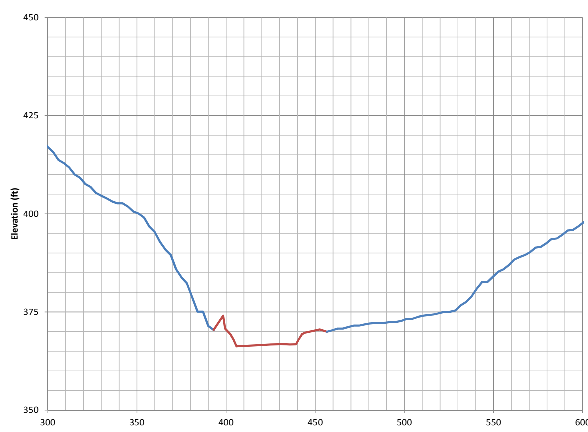

Figure 28. Example integration of field-based cross section surveys (red) with LiDAR based topography (blue) to generate final cross sections for the HEC-RAS model.

Determination of channel stationing and calculation of cross section positioning was performed using standard geospatial analysis tools within ArcMap. HEC-RAS steady-state model development required both main stem and overbank flow path distances between each cross section in order to adequately characterize hydraulic outputs. These values were calculated by overlaying surveyed cross sections with available aerial photos, and manually digitizing stream and overbank flow path distances, then inputting these distances into HEC-RAS as model input parameters.

Additional data were required for input to the HEC-RAS steady-state model before performing calibration and validation analyses. Additional data included initial estimates of Manning's *n* values to estimate channel and floodplain roughness characteristics at each cross section, available stream flow gaging stage-discharge rating curves that exist within the study area, and available surveyed high water marks.

3.2.2 Calibration and validation (2008-2009)

Calibration of the HEC-RAS steady-state model was carried out by comparing model outputs of water surface elevations with observed water surface elevations of the same discharge, at locations where measured data existed. Estimates of continuous water surface elevations are recorded for numerous flow events by the Niles gage (USGS #11-179000), Welch Creek gage (USGS #11-173575), Confluence gage (USGS #11-173510), and the Calaveras Creek gage (USGS #11-173500). The relative stage values reported by the USGS were converted into an elevation above mean sea level for inclusion into the steady-state model. The model was then allowed to run for the specified steady-state discharges identified in Table 15, and a modeled stage-discharge relationship was compared to the measured stage-discharge relationship developed by the USGS. If a noticeable deviation occurred between the modeled and measured stage-discharge relationship, the cross sectional roughness values were varied to obtain a better comparison between the two data sets. The process of model run, comparison, and roughness value adjustment was then repeated until a desirable fit between the two data sets was attained. Figure 29 demonstrates differing modeled stage-discharge relationships given differing cross-sectional averaged roughness values for the Welch Creek gage (USGS #11-173575).

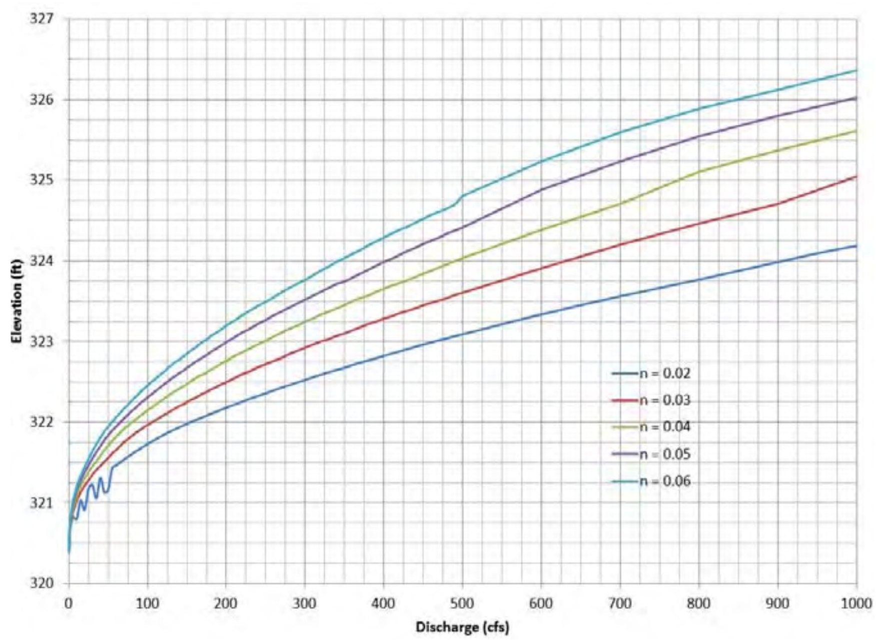

Figure 29. Modeled stage-discharge relationships with varying Manning's n *values using flows from the Welch Creek gage (USGS #11-173575).*

Once modeled and observed stage-discharge relationships were in agreement, the derived cross sectional roughness value was distributed to neighboring cross sections demonstrating similar roughness characteristics. These distributed roughness values were then validated with the qualitative data collected during the field surveys. Validation of the distributed roughness values resulted in minor revisions to cross section roughness predictions in the Lower Sunol Valley between Node 6 and Node 7, as this location had minimal observed stage-discharge data. Additional validation was performed for the steady-state model by comparing measured high water marks for sections of the study area to the steady-state model results. Figure 30, Figure 31, and Figure 32 show the steady-state calibration and validation model output results compared to measured streamflow data.

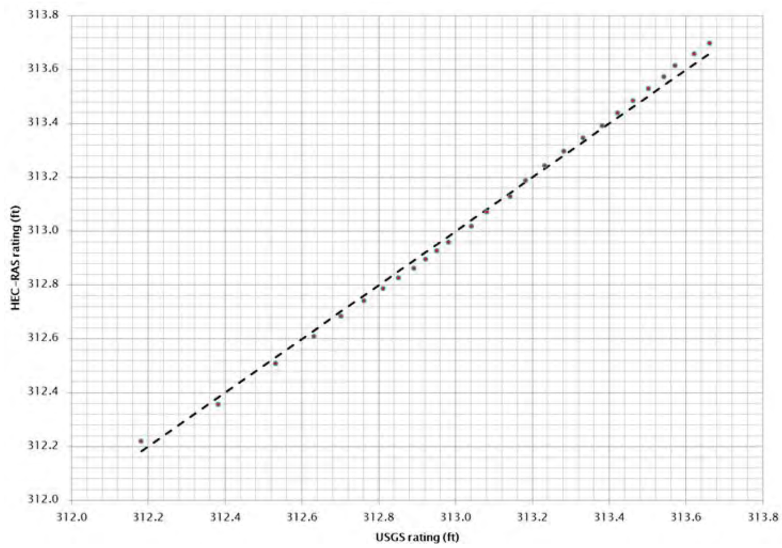

Figure 30. Observed vs. predicted stage-discharge relationships for the Welch Creek gage (USGS #11-173575, Node 4) for steady-state discharges ranging from 1 cfs to 300 cfs. Dashed line represents perfect agreement.

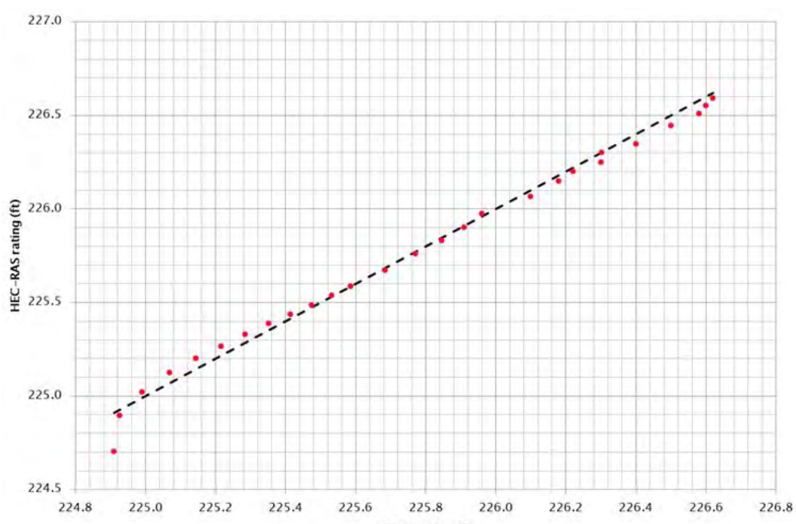

Figure 31. Observed vs. predicted stage-discharge relationships for the SFPUC gaging station at the Water Temple, immediately upstream of the Arroyo de la Laguna confluence (Node 7) for steady-state discharges ranging from 1 cfs to 300 cfs. Dashed line represents perfect agreement.

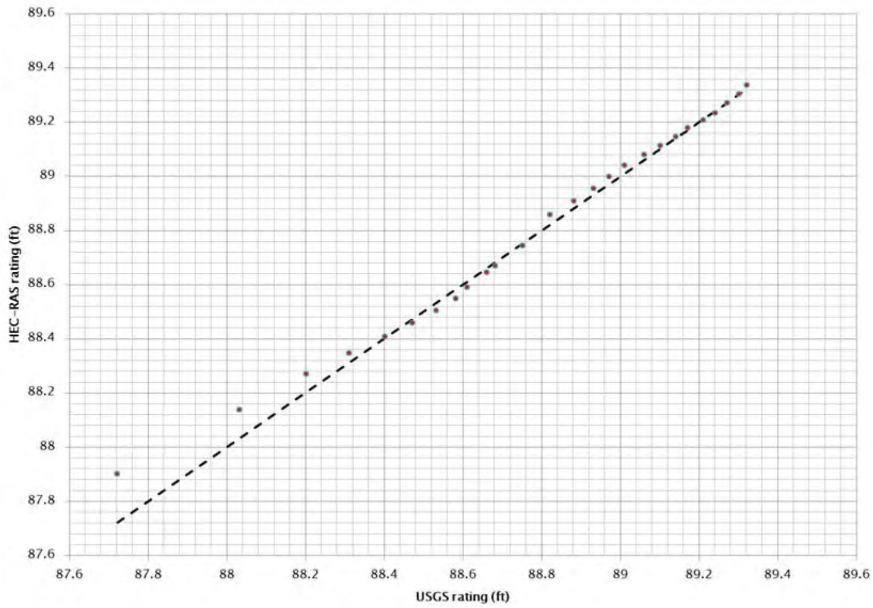

Figure 32. Observed vs. predicted stage-discharge relationships for the Niles gage (USGS #11-179000, Node 9) for steady-state discharges ranging from 1 cfs to 300 cfs. Dashed line represents perfect agreement.

3.2.3 Results

Results utilized from the HEC-RAS steady-state analysis include cross sectional averaged depth and wetted width as a function of steady-state flow at each of the 229 cross sections. These output data were then exported as a table for use in the EDT analysis. Examples of the results for individual cross sections located at the 12 node locations are provided in Figure 33 and Figure 34.

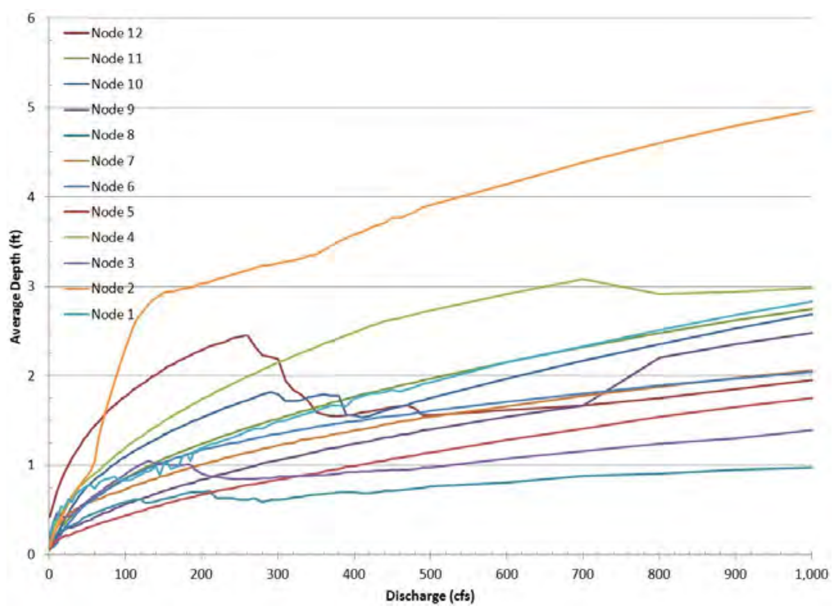

Figure 33. Average depth within individual cross sections located at each computational node as a function of flow from the steady-state HEC-RAS model.

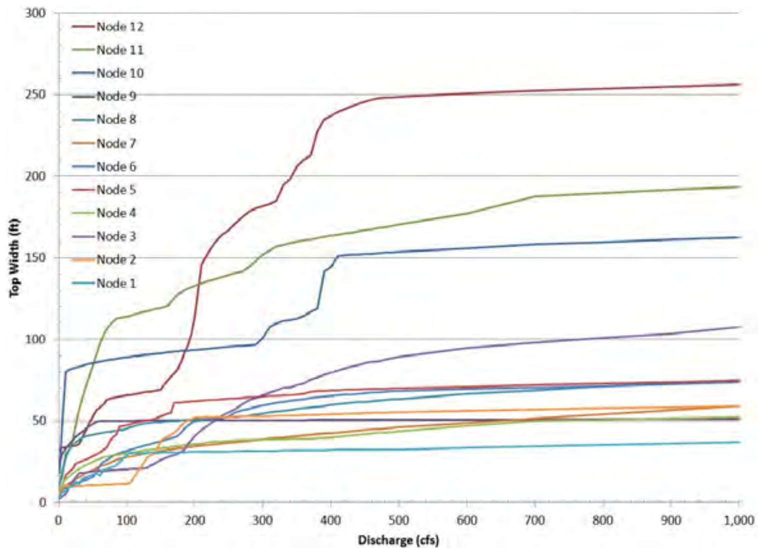

Figure 34. Total channel wetted top width as a function of local flow at each of the 12 nodes.

3.3 HEC-RAS unsteady water temperature modeling

Before initiating a water temperature analysis within HEC-RAS, an unsteady flow model must be developed. To develop the HEC-RAS unsteady flow model, inputs from the RAS steady-state model and time series inputs from the ASDHM model are required. Once these data sets have been incorporated into the HEC-RAS unsteady-state model, the model is calibrated and run with all available existing data. Then, the unsteady flow results can be used for water temperature model development and performing additional water temperature analyses.

3.3.1 Methods

HEC-RAS unsteady modeling differs from steady-state modeling by including time as an additional parameter. When modeling steady-state conditions, a single constant flow value is assumed over the entire study area, and hydraulic characteristics unique to that steady-state flow are developed. In contrast, when modeling unsteady-state flow, a time series of flow is routed through the study area. Routing flows in this manner results in hydraulic characteristics at each cross section which are a function of both flow and time. Unsteady flow hydraulic characteristics are required to adequately describe changes in water temperature over time and serve as an input to the water quality module HEC-RAS uses to perform water temperature analyses.

3.3.1.1 HEC-RAS unsteady hydraulic modeling

Development of the HEC-RAS unsteady hydraulic model required additional data inputs from various sources, as well as subdividing the analysis area so unsteady computations could occur on smaller reaches. To initiate development, geometric data utilized for the steady-state model were incorporated into the unsteady analysis. Due to the length of the study area and file size, the unsteady model could not be analyzed continuously from Node 1 to Node 12. Instead, the cross section data for the study area compiled for the steady-state model had to be characterized by a series of subreaches, which were then analyzed individually. Subdividing the unsteady flow computations in this manner served two functions: (1) it increased computational stability, and (2) it decreased the effects of model predictive error on downstream reaches. Reaches for the unsteady model were developed between each of the ASDHM computational nodes to allow streamlined integration with the RAS unsteady model boundary conditions and the ASDHM results. A total of six different subreaches were ultimately identified to characterize the study area between Node 1 and Node 12 (Table 16).

Table 16. Unsteady HEC-RAS model subreaches between Node 1 and Node 12.

Stream	Upstream boundary	Downstream boundary
Alameda Creek	ACDD (Node 1)	Node 3
Calaveras Creek	Calaveras Dam	Node 3
Alameda Creek	Node 3	Node 5
Alameda Creek	Node 5	Node 7
Alameda Creek	Node 7	Node 9
Alameda Creek	Node 9	Node12

Hydrology boundary condition data for each of the HEC-RAS unsteady model subreaches were provided from the outputs of the ASDHM model analysis. For example, the HEC-RAS reach encompassing cross sections between ASDHM Node 3 and Node 4 required a daily averaged flow input at the upstream boundary (Node 3) and at the downstream boundary (Node 4) before being able to perform computations. The model also required lateral inflow boundary conditions at a specific cross section or over a specified area, if there were any quantifiable flow accumulations over the length of the reach. This was an important component of identifying contributions from tributaries, such as Welch Creek and Stonybrook Creek. Similarly, if a computational reach was identified in ASDHM as a losing reach, flow could be removed from the system before starting the computations for the next reach downstream. By structuring the unsteady flow model in this manner, we could minimize any computational error that the model generated in the upper reaches from being transferred to a lower reach. For example, if the model had variable accuracy between Node 3 and Node 5, that error would not be transferred to the computations from Node 5 to Node 7 because the input boundary conditions for the subreach from Node 4 to Node 7 are based on ASDHM outputs for Node 4, and not the Node 4 results from HEC-RAS. Figure 35 illustrates this boundary condition assumption for the unsteady model computations, and additional detail on the water temperature boundary conditions are provided in Section 3.3.1.2.

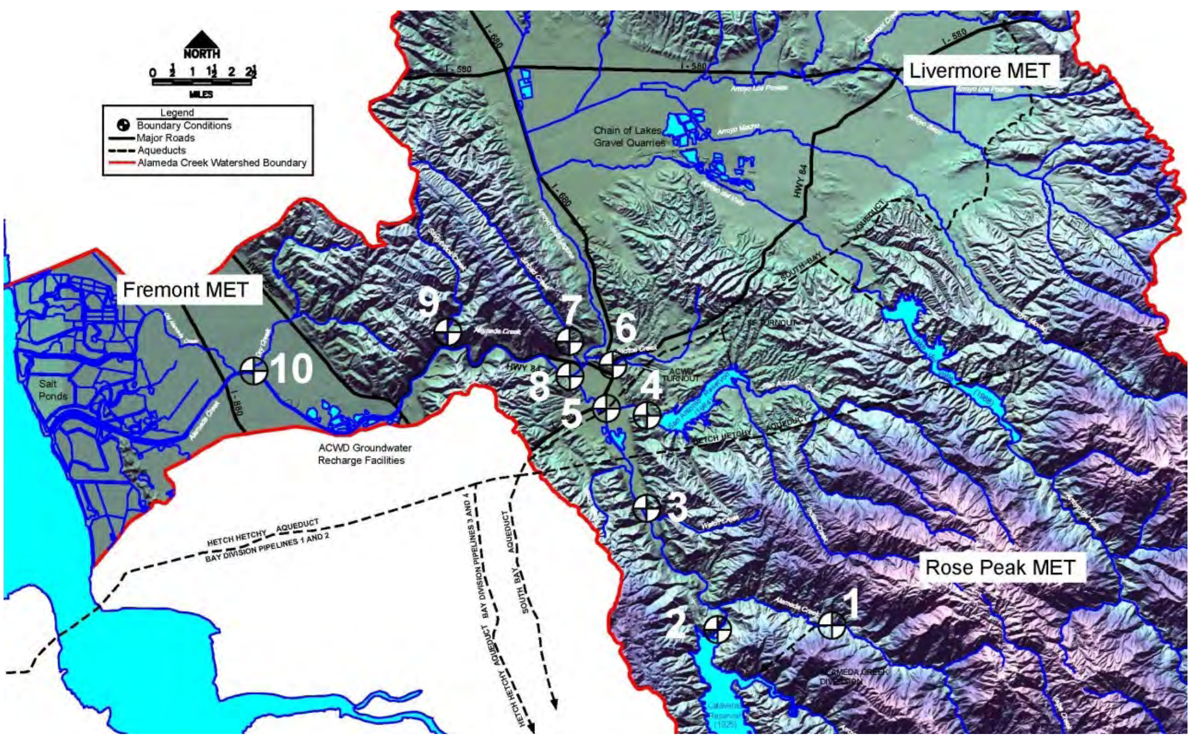

Figure 35. Hydrology and water temperature boundary condition locations for the unsteady HEC-RAS water temperature model, and meteorological stations (MET) used for the water temperature model.

HEC-RAS unsteady modeling also required a user input computational time step used to subdivide daily averaged input boundary condition flow data into acceptable computational durations. This subdivision served to enhance model predictive accuracy and computational stability. The computational time step identified as providing the best model stability and best unsteady flow prediction accuracy was 30 minutes. After the unsteady model computations were complete, the HEC-RAS program recalculated a daily averaged flow from the individual 30-minute computations to output a final daily averaged flow rate. This daily averaged flow rate was compared to the calculated ASDHM flows to validate the HEC-RAS model's final unsteady flow predictions. Deviations from the HEC-RAS predictions and the ASDHM predictions likely arose as a result of input parameters to the HEC-RAS model. Assumptions made for cross-sectional averaged roughness, cross section density, and computational time step all have impacts on the accuracy of the predictions. These parameters were evaluated to provide the best fit between the HEC-RAS predictions and the ASDHM predictions. Comparisons of the HEC-RAS unsteady flow and the ASDHM flow rates for two example computational nodes are provided in Figure 36 and Figure 37.

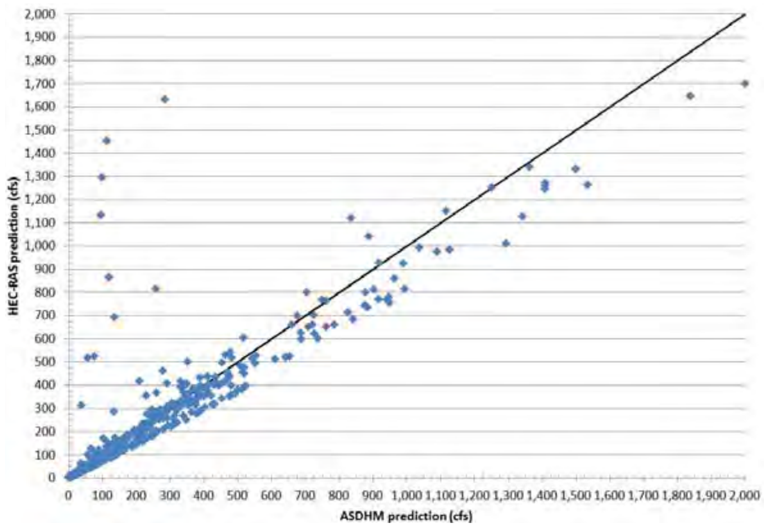

Figure 36. Comparison of HEC-RAS computed flows at Node 4 compared to ASDHM computed flows. Line represents perfect agreement.

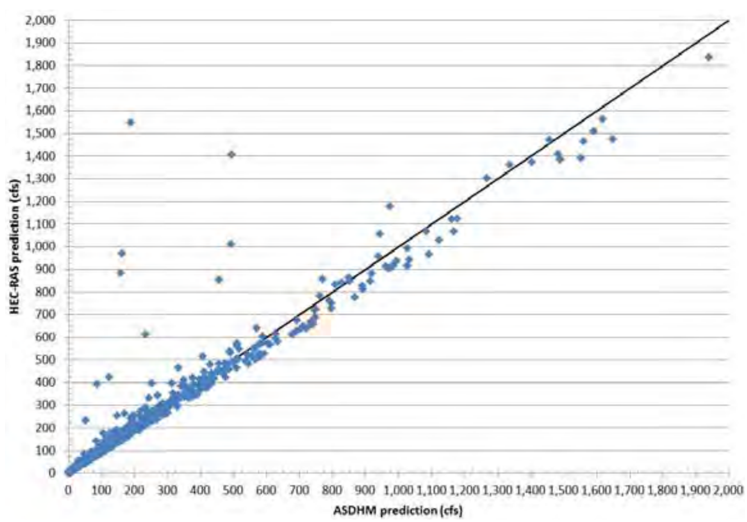

Figure 37. Comparison of HEC-RAS computed flows at Node 7 compared to ASDHM computed flows. Line represents perfect agreement.

After validation of the RAS unsteady flow computations, the unsteady model was run for each of the six subreaches with all the identified computational scenarios, resulting in a time series of hydraulic characteristics at each of the 229 cross sections. These data were then used as an input to the HEC-RAS water temperature module to perform the calibration, validation, and final model runs to generate estimates of water temperature data over the entire study area.

3.3.1.2 HEC-RAS water temperature model development

Water temperature predictions within HEC-RAS are performed using the water quality module. To run this module and generate reasonable water temperature predictions, many different types of input data are required. These data types include unsteady hydraulic data (generated by the unsteady HEC-RAS model), meteorological data measured close to or within the study area, and estimations of various coefficients used during the water temperature model calibration. Similar to the unsteady flow calculations, the water temperature model also requires a time series of water temperature data at the various model boundaries to serve as boundary condition inputs. Ideally, these boundary conditions would be generated from observed water temperatures measured for the entire duration of the analysis. Lack of water temperature data for these locations in the Alameda Creek system necessitated developing an alternate approach to estimate these required inputs. Along with these input data sets and boundary condition estimations, observed water temperature readings are needed throughout the study area to help calibrate the water temperature model, and to validate the final outputs.

To compute temperatures in mainstem Alameda Creek, the HEC-RAS model requires temperature boundary conditions from contributing tributaries. Temperature boundary conditions are daily average temperatures which are used to calculate the impact of tributary accretion (thermal loading) on water temperature in mainstem Alameda Creek. Some tributaries, such as Calaveras and San Antonio creeks, are regulated and so temperature boundary conditions will vary with each ASDHM scenario depending on facility operations. Boundary conditions for unregulated tributaries will not vary between ASDHM scenarios. Water temperature boundary conditions were computed for the following locations (Figure 35):

1. Alameda Creek above ACDD
2. Base of Calaveras Dam
3. Welch Creek
4. San Antonio Creek
5. Gravel Quarry discharge
6. Vallecitos Creek
7. Sinbad Creek
8. Arroyo de la Laguna
9. Stonybrook Creek
10. Dry Creek

Other smaller tributaries were omitted, as they are usually dry.

Boundary conditions were developed from existing water temperature data, when available within the HY1996-2010 time series. Most existing water temperature data are from 2007 to 2010, although some seasonal data are available back to HY2001. For periods when water temperature data are not available, a seasonal water temperature regression model can be developed to predict daily average water temperatures based on local meteorological conditions (Erickson et al. 2000, Morrill et al. 2005, Webb et al. 2003). To build the regression model, existing daily average water temperature were regressed with various durations of running average daily average air temperature for each season. Air temperature data was compiled from the most applicable meteorological (MET) station, which was usually the closest to the water temperature prediction location. Three MET stations were used: Rose Peak, Livermore, and Fremont (Figure 35). Various durations of running average daily average air temperatures were regressed with measured water temperatures, and assessed based on r^2 values of the regression and minimizing bias (Figure 38 and Figure 39). The best relationships were achieved using a three-day running average of daily average air temperature, which buffered the impact of sharp changes in air temperature on water temperature. Because air-water temperature relationships likely vary with different seasons and photoperiods, various seasonal regressions were also assessed based on r^2 values and the life history periodicities of salmonids. After review of the regression analyses, the following seasons were chosen:

- December 1 through January 31
- February 1 through May 31
- June 1 through August 31
- September 1 through November 30

Under Scenario 5 and Scenario 6, two of the boundary condition locations (San Antonio Creek and Calaveras Creek) reflect dam outlet works releases from the hypolimnion. Flow releases from Calaveras Dam will be the primary driver of management-induced changes to water temperature in Alameda Creek, particularly between Node 2 and Node 7. Therefore, an empirical temperature model of Calaveras Dam releases was completed to estimate water temperature boundary conditions in Calaveras Creek (Calaveras Dam Release Water Temperature Model).

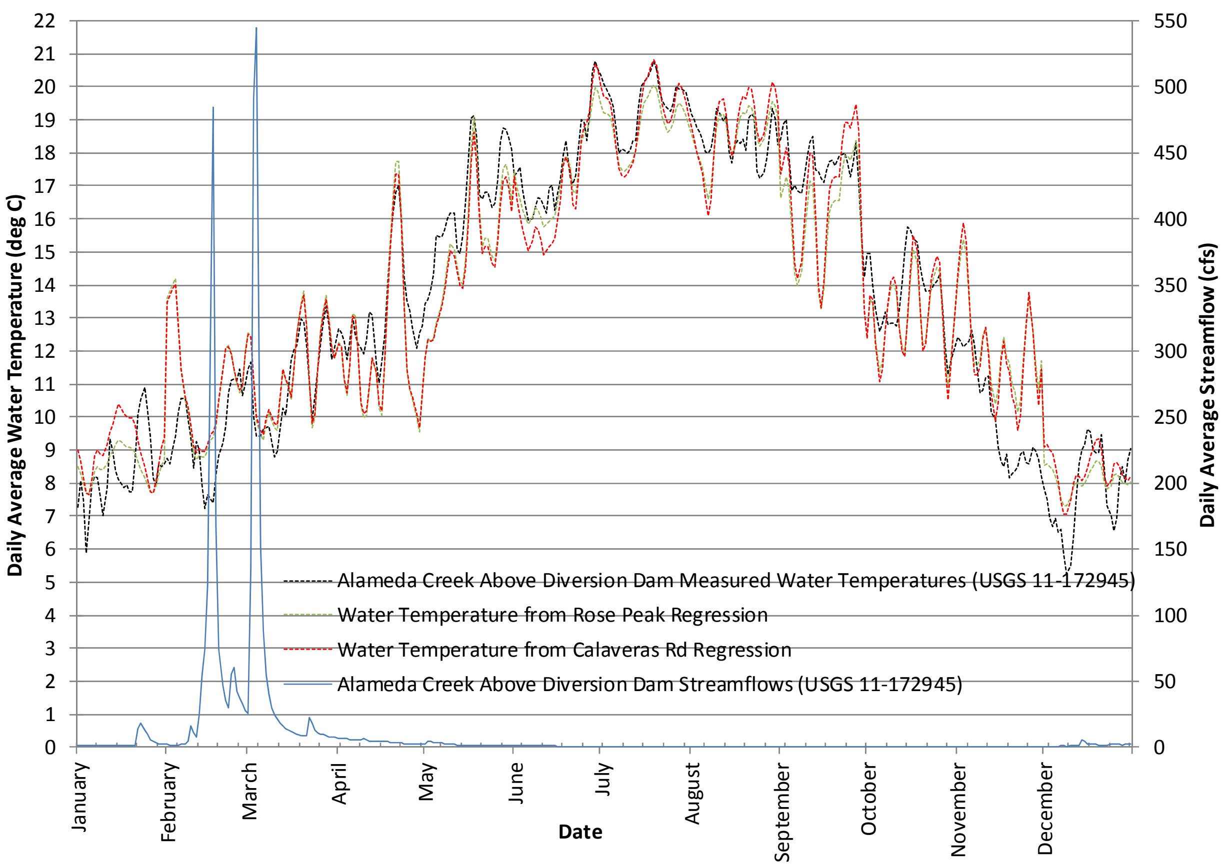

Figure 38. Example comparison of predicted daily average water temperature in 2009 at the Above ACDD gage (USGS #11-172945) using the 3-day average air temperature from two different meteorological stations.

The SFPUC has conducted limnology studies on Calaveras Reservoir between HY2000-2009 (e.g., SFPUC 2005) that document reservoir water temperature profiles over the entire year. Samples typically occurred every two to four weeks, so over the 10 years of data, empirical relationships could be developed between water temperature and depth from the surface of the reservoir. This period of record was divided into 24 bins to develop separate relationships for each ½ month of the year. Then, knowing a date of interest, the water surface elevation on that date, the depth-temperature relationship on that date, and the elevation of the outlet works (664 ft, 1929 NGVD), the release temperature could be predicted by the Calaveras Dam Release Water Temperature Model. Because there was variability between the various measurements in each bin, the average value was used for the boundary condition; however, the maximum and minimum values are also computed (Figure 40). The ASDHM model computes reservoir elevation for Scenario 4 for HY2000-2009, and for Scenario 5 and Scenario 6 for the HY1996-2009 analysis period, so the Calaveras Dam Release Water Temperature Model could predict daily average water temperatures on a daily basis for the respective analysis period. For unimpaired Scenario 1 and Scenario 2, a meteorological regression equation was used (Table 17 and Table 18).

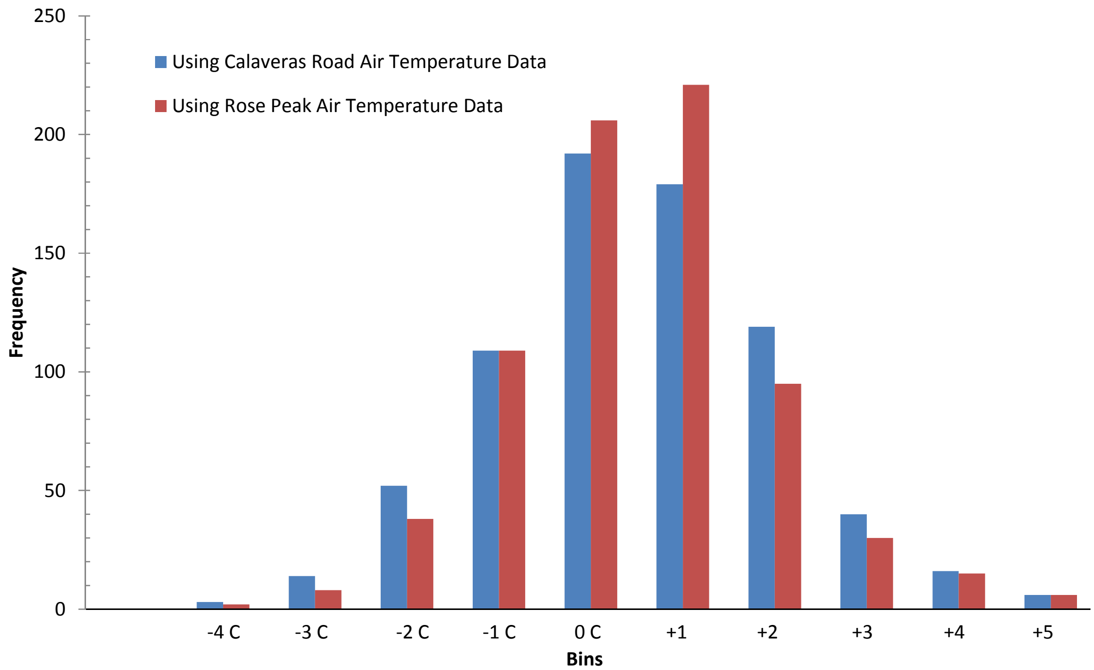

Figure 39. Example evaluation of bias between the two different meteorological stations considered for predicting water temperature boundary conditions at the Above ACDD gage location (USGS #11-173945, Node 1). In this example, the Calaveras Road meteorological station was chosen over the Rose Peak station.

Scenario 5 and Scenario 6 assume measured impaired releases from San Antonio Dam. When available, measured water temperatures were used as the boundary condition for these two scenarios; otherwise, the computed water temperatures from the MET regression analysis were used. We considered creating an empirical temperature model for San Antonio Reservoir in a similar manner as done at Calaveras Reservoir, but because impaired flows below San Antonio Dam are typically zero (seepage) and the infrequent high flow releases (spills) from San Antonio Dam are typically very short, we did not feel that it was worth creating a release temperature model for those small number of days where spills would occur. However, if needed, this model could be constructed and integrated into the HEC-RAS unsteady model in the future. Any tributary runoff downstream of San Antonio or Calaveras dams was estimated using the MET regression analysis.

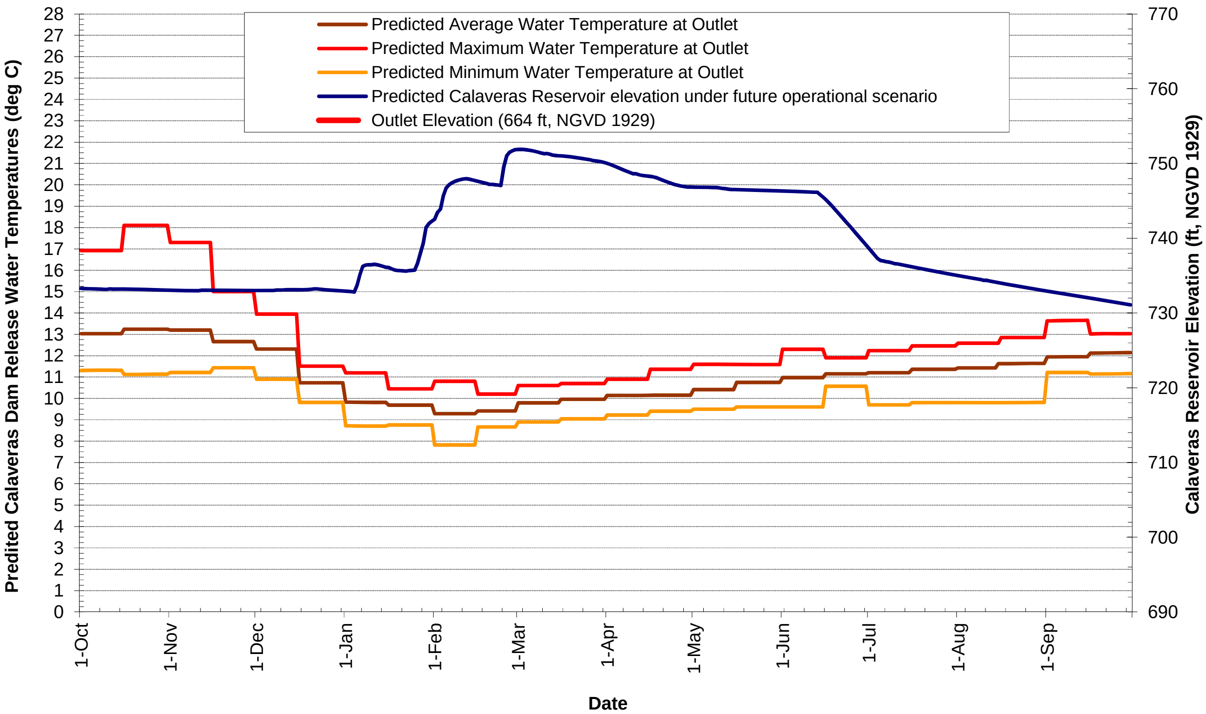

Figure 40. Example year of Calaveras Dam release temperature boundary conditions (2008, a Dry hydrologic year) from the Calaveras Dam Release Water Temperature Model. Predicted average values were used in the water temperature model.

The gravel quarry boundary conditions represent return flow pumped back into Alameda Creek from quarry operations in the lower Sunol Valley. Return flow temperature was not monitored directly; however, the SFPUC water temperature sensor W-10 documents water temperature of mainstem Alameda Creek immediately downstream of the quarry discharge point. A good estimation of return flow temperature was derived by isolating days when there was no streamflow upstream of W-10. For days when upstream flow was 0, W-10 was reporting temperature and flow exclusively from the quarry pumping. These data were regressed with Livermore air temperatures to develop seasonal equations for predicting return flow temperature.

For all other tributaries, seasonal regression equations (water temperature vs. air temperature) were computed for each year of the HY1996-2009 time series. The regression equations were used to estimate water temperature during periods when no existing water temperature data were available. Table 17, Table 18, Table 19, and 0 show the periods of available data, modeled data and the source of MET and hydrology data for the regression models for each tributary under ASDHM flow Scenario 1, Scenario 2, Scenario 5, and Scenario 6. Using the existing and modeled data for each scenario, daily average water temperature was computed for the HY1996-2009 time series at each tributary. These data were then available as input for the HEC-RAS unsteady water quality model.

Table 17. Water temperature boundary condition assumptions for ASDHM Scenario 1: Computed unimpaired Alameda Creek and measured impaired Arroyo De La Laguna.

Boundary condition location	Measured temperatures	Modeled temperatures	MET data
1. Alameda Creek Diversion Dam	Partial: Summer 2003-2007 Continuous: November 2007-present (*T-13)	1996-2002, fill gaps from 2003-2007 (*T-13)	Rose Peak
2. Base of Calaveras Dam	Use Arroyo Hondo (*T-17) Partial: Summer 2003-2006 Continuous: April 2007-present	1996-2002, fill gaps from 2003-2006 (*T-17)	Rose Peak
3. Welch Creek	Summer 2003	1996-present using ACDD regression	Livermore
4. San Antonio Creek	None	1996-present using ACDD regression	Livermore
6. Vallecitos Creek (SBA)	August 1996-present	N/A	N/A
6. Vallecitos Creek (Natural runoff)	May-Sept 2003	1996-2003, 2003-present	Livermore
7. Sinbad Creek	None	1996-present using Stonybrook regression	Livermore
8. Arroyo de la Laguna at Verona gage	Continuous: USGS gaging station Nov 2003-present	1996-2003	Livermore
9. Stonybrook Creek	Partial: 1999, 2000, 2003, 2004	1996-1999, 2001, 2002, 2005-present, fill gaps	Fremont
10. Dry Creek	None	1996-present using Stonybrook regression	Fremont

* The T-13 and W-10 gages represent existing SFPUC water temperature monitoring locations. All other water temperature data were based on USGS gages.

Table 18. Water temperature boundary condition assumptions for ASDHM Scenario 2: Computed unimpaired Alameda Creek and computed unimpaired Arroyo De La Laguna.

Boundary condition location	Measured temperatures	Modeled temperatures	MET data
1. Alameda Creek Diversion Dam	Partial: Summer 2003-2007 Continuous: November 2007-present (*T-13)	1996-2002, fill gaps from 2003-2007 *(T-13)	Rose Peak
2. Base of Calaveras Dam	Use Arroyo Hondo (*T-17) Partial: Summer 2003-2006 Continuous: April 2007-present	1996-2002, fill gaps from 2003-2006 (*T-17)	Rose Peak
3. Welch Creek	Summer 2003	1996-present using ACDD regression	Livermore
4. San Antonio Creek	None	1996-present using ACDD regression	Livermore
8. Arroyo de la Laguna confluence	None	1996-2009	Livermore
9. Stonybrook Creek	Partial: 1999, 2000, 2003, 2004	1996-1999, 2001, 2002, 2005-present, fill gaps	Fremont
10. Dry Creek	None	1996-present using Stonybrook regression	Fremont

* The T-13 and W-10 gages represent existing SFPUC water temperature monitoring locations. All other water temperature data were based on USGS gages.

Table 19. Water temperature boundary condition assumptions for ASDHM Scenario 5: Proposed future Alameda Creek and measured impaired Arroyo de la Laguna.

Boundary condition location	Measured temperatures	Modeled temperatures	MET data
1. Alameda Creek Diversion Dam	Partial: Summer 2003-2007 Continuous: November 2007-present (*T-13)	1996-2002, fill gaps from 2003-2007 (*T-13)	Rose Peak
2. Base of Calaveras Dam	None	Calaveras Dam Release Water Temperature Model	N/A
3. Welch Creek	Summer 2003	1996-present using ACDD regression	Livermore
4. San Antonio Creek	October 2008-present	1996-September 2008	Livermore
5. Gravel Quarry	None	1996-2009 (*W-10)	Livermore
6. Vallecitos Creek (SBA)	August 1996-present	N/A	N/A
6. Vallecitos Creek (Natural runoff)	May-Sept 2003	1996-2003, 2003-present	Livermore
7. Sinbad Creek	None	1996-present using Stonybrook regression	Livermore
8. Arroyo de la Laguna at Verona gage	Continuous: USGS gaging station Nov 2003-present	1996-2003	Livermore
9. Stonybrook Creek	Partial: 1999, 2000, 2003, 2004	1996-1999, 2001, 2002, 2005-present, fill gaps	Fremont
10. Dry Creek	None	1996-present using Stonybrook regression	Fremont

* The T-13 and W-10 gages represent existing SFPUC water temperature monitoring locations. All other water temperature data were based on USGS gages.

Table 20. Water temperature boundary condition assumptions for ASDHM Scenario 6: Computed impaired Alameda Creek and measured impaired Arroyo de la Laguna.

Boundary condition location	Measured temperatures	Modeled temperatures	MET data
1. Alameda Creek Diversion Dam	Partial: Summer 2003-2007 Continuous: November 2007-present (*T-13)	1996-2002, fill gaps from 2003-2007 (*T-13)	Rose Peak
2. Base of Calaveras Dam	None	Calaveras Dam Release Water Temperature Model	N/A
3. Welch Creek	Summer 2003	1996-present using ACDD regression	Livermore
4. San Antonio Creek	October 2008-present	1996-September 2008	Livermore
5. Gravel Quarry	None	1996-2009 (*W-10)	Livermore
6. Vallecitos Creek (SBA)	August 1996-present	N/A	N/A
6. Vallecitos Creek (Natural runoff)	May-Sept 2003	1996-2003, 2003-present	Livermore
7. Sinbad Creek	None	1996-present using Stonybrook regression	Livermore
8. Arroyo de la Laguna at Verona gage	Continuous: USGS gaging station Nov 2003-present	1996-2003	Livermore
9. Stonybrook Creek	Partial: 1999, 2000, 2003, 2004	1996-1999, 2001, 2002, 2005-present, fill gaps	Fremont
10. Dry Creek	None	1996-present using Stonybrook regression	Fremont

* The T-13 and W-10 gages represent existing SFPUC water temperature monitoring locations. All other water temperature data were based on USGS gages.

3.3.1.3 Model runs

Steps required to perform a water quality simulation within HEC-RAS mimic those discussed in the subreach computation procedure outlined in Section 3.3.1.1. The six subreaches identified in Table 16 were used for the water temperature calculation subreaches. To apply the water temperature calculations to this subreach framework required inputting water temperature boundary conditions at the upstream end of each reach, as well as boundary conditions for any lateral inflow identified during the unsteady flow analysis (Table 21, Figure 41). For reaches which include boundary condition data from the calculations described in Section 3.3.1.2, the calculated time series of water temperatures were used for the input data. For reaches having boundary conditions associated with water temperature predictions from an upstream reach, HEC-RAS predictions were used. For example, the upstream water temperature boundary condition for the computational reach between Node 4 and Node 5 would use the HEC-RAS computed water temperature output from the upstream subreach between Node 3 and Node 4.

Water temperature calculations within HEC-RAS occur at specific water quality "cells." These cells are usually defined by the area between two neighboring cross sections, but in some cases may span multiple cross sections in areas where cross sections are located in close proximity to each other. A minimum water quality cell length was specified to be 300 ft in order to coincide with the average measured cross section density. With a minimum water quality cell length of 300 ft, calculations of water temperature occur between two neighboring cross sections or on a 300 ft interval, if two neighboring cross sections are closer than 300 ft together. Water temperatures calculated for each water quality cell are transferred to the neighboring downstream cell along with computed cross-sectional hydraulic characteristics developed by the unsteady flow model. HEC-RAS uses these parameters to calculate water temperature at each downstream water quality cell until reaching the lowermost end of the subreach. An example of the location of water quality computational cells is presented in Figure 42. Water temperature outputs at a specific cross section are reported as the water temperature for the water quality cell directly upstream of the cross section of interest.

Table 21. Types of boundary condition used at each location in the HEC-RAS model.

Boundary condition location	Boundary condition type
Below Alameda Creek Diversion Dam	Point source input
Between Alameda Creek Diversion Dam and Calaveras Creek	Lateral inflow over subreach
Calaveras Creek	Point source input
Between Calaveras Creek and Indian Joe Creek	Lateral inflow over subreach
Indian Joe Creek	Point source input
Between Indian Joe Creek and Welch Creek	Lateral inflow over subreach
Welch Creek	Point source input
Between Welch Creek and Pirate Creek	Lateral inflow over subreach
Pirate Creek	Point source input
Between Pirate Creek and San Antonio Creek	Lateral inflow over subreach
San Antonio Creek	Point source input
Between San Antonio Creek and Arroyo de la Laguna	Lateral inflow over subreach
Arroyo de la Laguna	Point source input
Between Arroyo de la Laguna and Stonybrook Creek	Lateral inflow over subreach
Stonybrook Creek	Point source input
Between Stonybrook Creek and Niles Gage	Lateral inflow over subreach
Between Niles Gage and Dry Creek	Lateral inflow over subreach
Dry Creek	Point source input
Between Dry Creek and San Francisco Bay	Lateral inflow over subreach

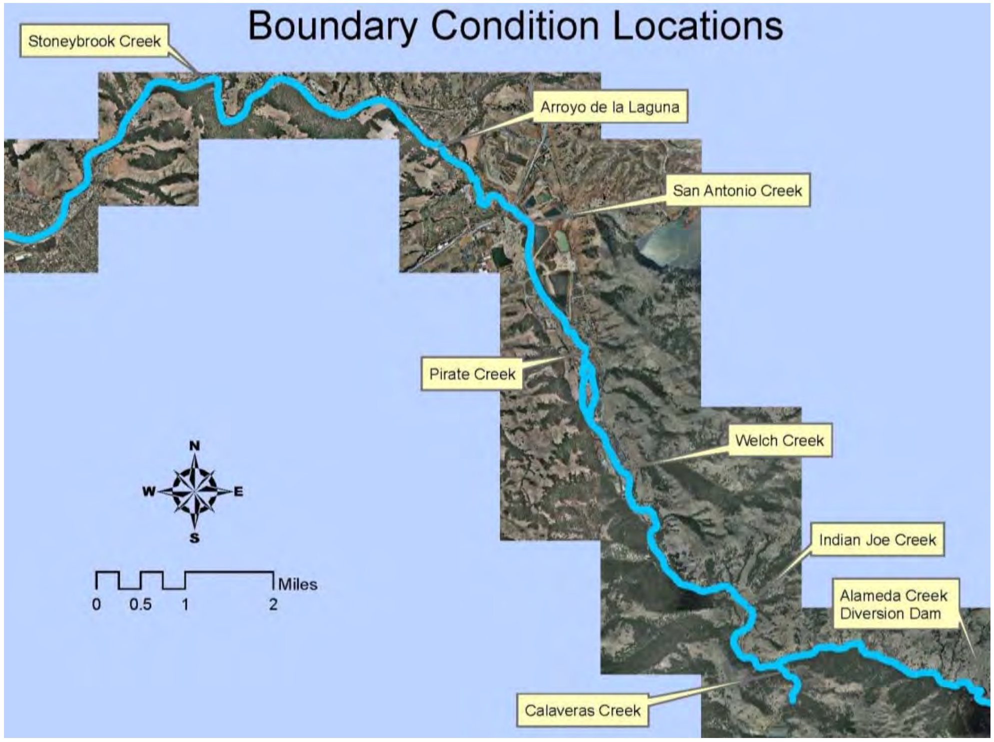

Figure 41. Example boundary condition locations for water temperature inputs.

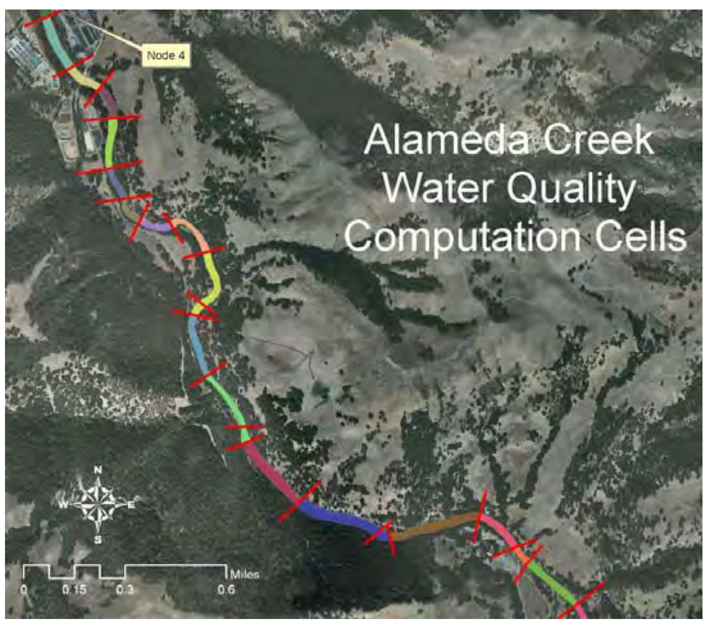

Figure 42. HEC-RAS water temperature model computational cells upstream of Node 4.

After all input data described in Section 3.3.1.2 were gathered and input to the water quality module, an initial water quality analysis was performed. Similar to the unsteady flow simulations, a computational time step was identified which differed from the boundary condition input time step. A computational time step of 1 hour was selected, as it provided the best model calculation stability, while optimizing model run time for all reaches. After hourly calculations were performed, HEC-RAS recalculated the output to report a daily average temperature value for each water temperature cell over the entire analysis period.

3.3.2 Water temperature model calibration and validation (2008-2009)

Once the input data required to run the water temperature model were included in the HEC-RAS program, the process of water temperature model calibration and results validation occurred. During the process of model calibration, observed water temperature data were used from eight locations spread throughout the analysis domain to facilitate the calibration process. Observed daily averaged water temperature data existed for numerous locations within the study reach starting in HY2008 and continuing through HY2009. This period of observed data allowed for a straightforward selection of HY2008 as the calibration period, while using daily averaged water temperature data from HY2009 to validate the predicted results.

Three meteorological data sets were available to use for water temperature model development. These three data sets consisted of meteorological data from the Rose Peak, Livermore, and Fremont locations. Other meteorological data within the study area existed but was of insufficient duration or poor data quality for use in the HEC-RAS model. Different subreaches of the water temperature model were assigned to different meteorological data sets, with Node 1 through Node 4 being assigned to Rose Peak data, Node 4 through Node 8 being assigned to Livermore data, and Node 9 through Node 12 being assigned to Fremont data. Assigning these data sets to specific areas of the water temperature model served to enhance the model's predictive ability for the individual regions. Furthermore, the three respective meteorological data sets were re-assigned to specific locations within a reach. This approach was applied to allow greater flexibility during model calibration within reaches with heterogeneous morphologic and vegetative characteristics. These characteristics can exhibit an influence on specific components of the energy budget calculations used to create local water temperature predictions, and structuring the application of meteorological data in this manner can allow for more accuracy when applying limited meteorological data to larger study areas.

Calibration of the water temperature model within HEC-RAS occurred by entering estimates of three meteorological coefficient parameters identified as the a, b, and c coefficients to the wind function. These coefficients serve to adjust the effect of measured wind speed on the energy calculations used by HEC-RAS theoretical formulas to provide a better estimate of site-specific conditions for each meteorological data set. Therefore, for locations where the same meteorological data set was applied to two different locations within a single subreach, the ability to develop two sets of calibration parameters existed. Initially these coefficients were estimated, and the model was allowed to run. Model results were then compared with observed data to determine the validity of the predictions (as well as the selected calibration coefficients). If the resultant water temperature predictions were not accurate, new coefficients were estimated and the model was re-run. This process continued until all subreaches of the water temperature model provided reasonable predictions of water temperature for the calibration period. Measured versus HEC-RAS predictions for Node 9 are displayed in Figure 43 to demonstrate the final model's predictive accuracy for the calibration period during HY2008.

After wind coefficients were developed for the respective meteorological data sets for the calibration period, the model was allowed to run for the validation period (HY2009). Validation analyses were carried out to ensure that coefficient selection remained valid outside of the calibration time frame of HY2008. Ideally the calibration and validation time periods would extend longer than a single year, but lack of continuous water temperature data for the Alameda Creek system before the calibration period precluded extending these analyses to additional time periods. The results of the validation analysis are presented in Figure 44.

3.3.1 Water temperature model results

HEC-RAS water temperature predictions for Node 4, 5, 9, and 10 for Scenario 2, Scenario 5, and Scenario 6 are presented below in Figure 45 through Figure 52. General water temperature trends are observed to be consistent throughout the scenarios presented for all nodes in the watershed. Water temperature within reaches of Alameda Creek which are upstream from the confluence of Arroyo de la Laguna are more sensitive to changes in flow regimes when compared to reaches below the confluence. This is likely due to the influence of water from the Arroyo de la Laguna boundary condition dominating the thermal and hydrologic regimes starting at Node 8.

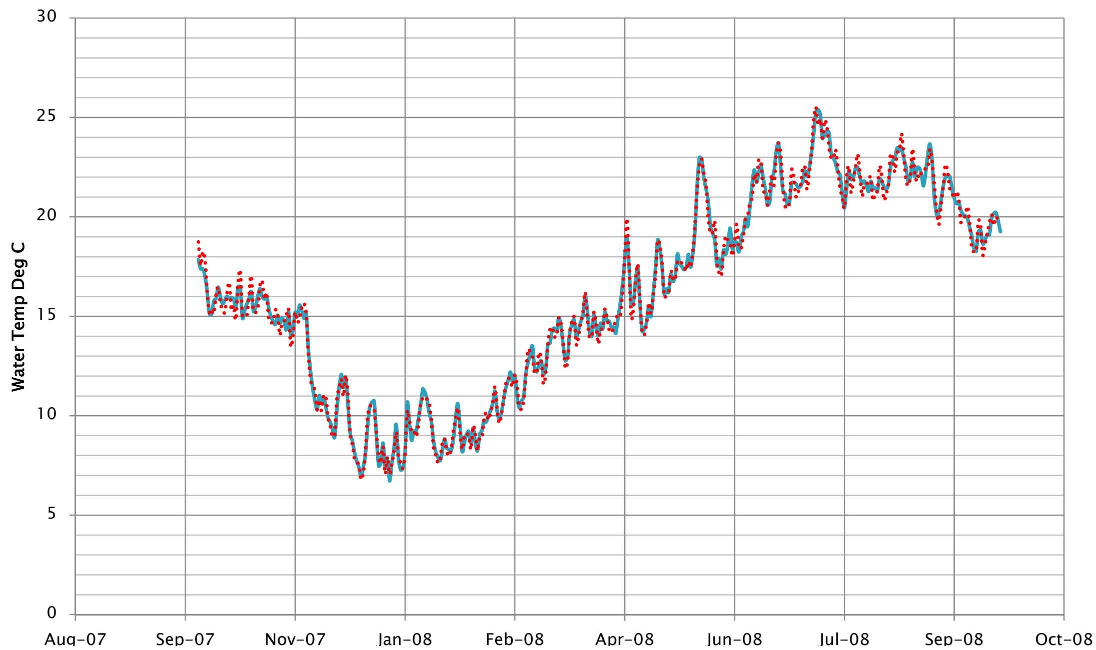

Figure 43. HY2008 model vs. observed water temperature at Niles gage (USGS #11-179000). Blue=observed, red dashed=predicted by HEC-RAS unsteady model.

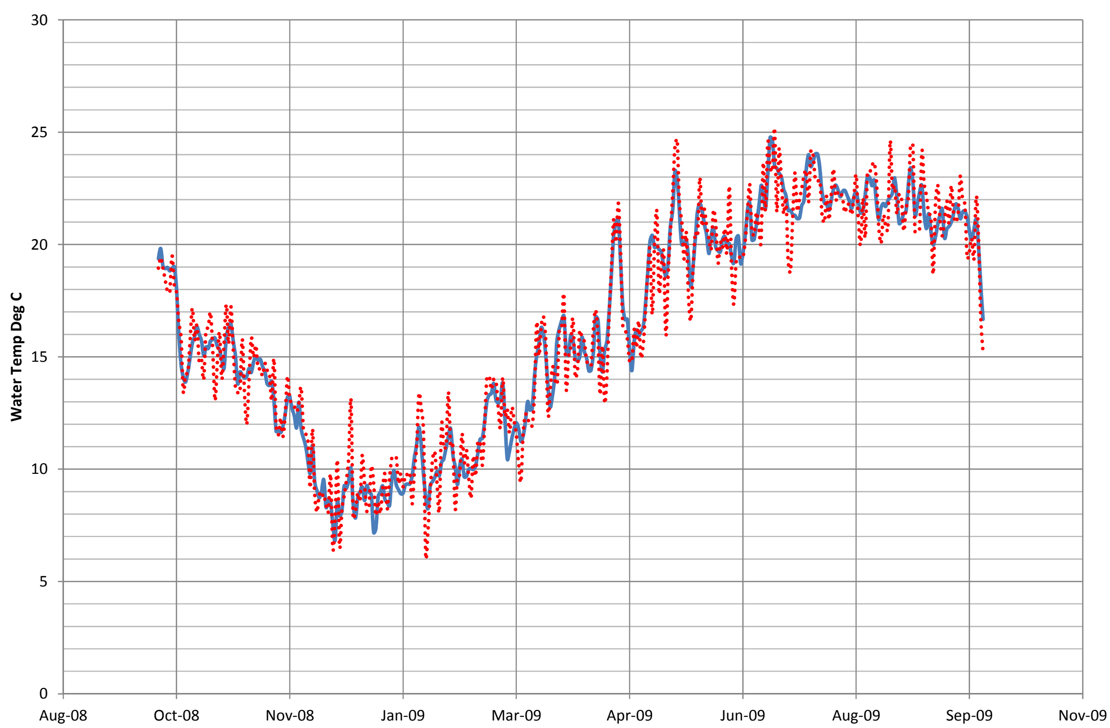

Figure 44. HY2009 model vs. observed water temperature at Niles gage (USGS #11-179000). Blue=observed, red dashed=predicted by HEC-RAS unsteady model.

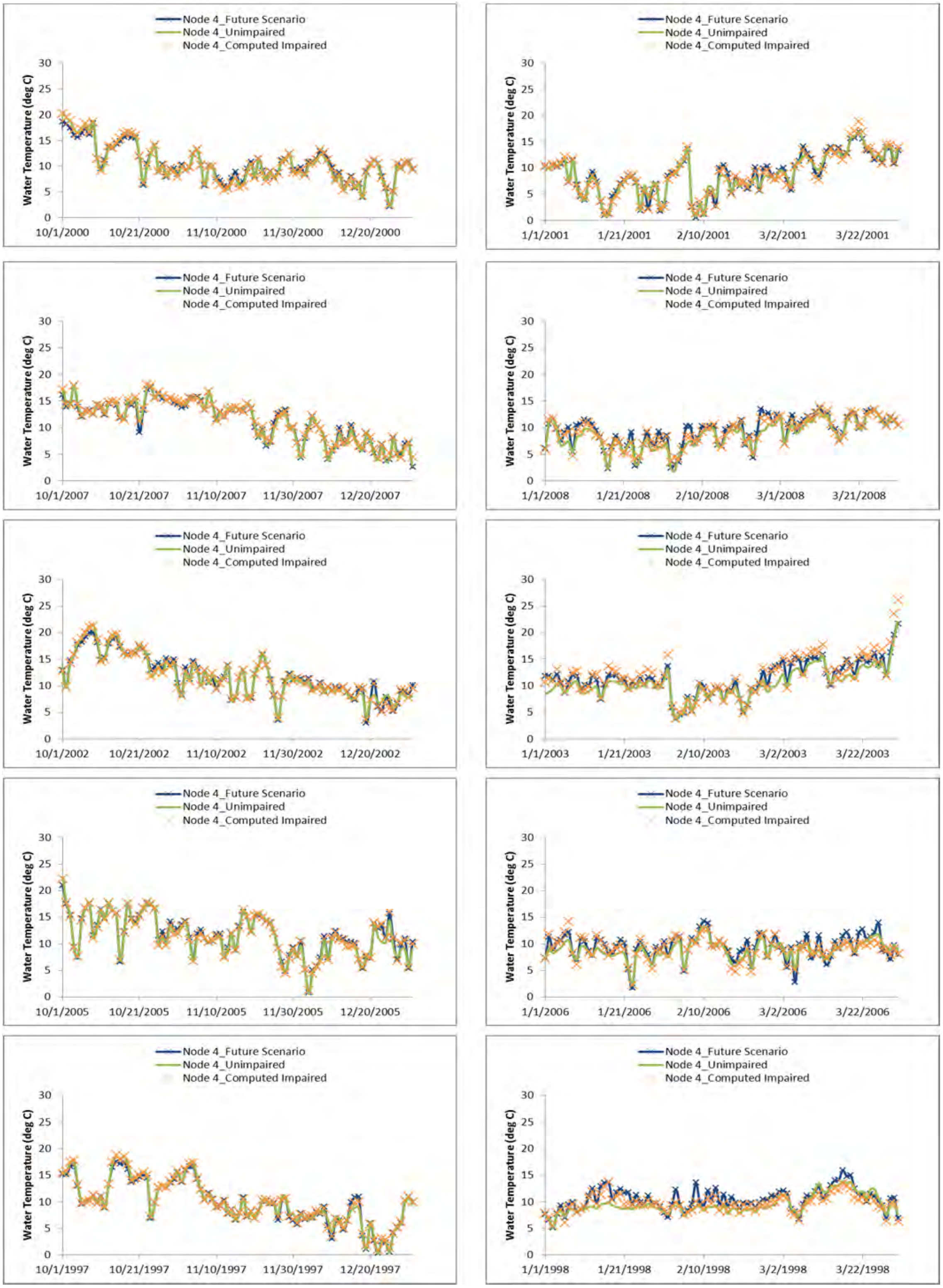

Figure 45. Water temperature at Node 4 for Scenario 2 (unimpaired), Scenario 5 (future), and Scenario 6 (computed impaired) from October to March for two Dry hydrologic years (2001, 2008), one hydrologic year on the Dry-Normal/Wet boundary (2003), and two Normal/Wet hydrologic years (2006, 1998).

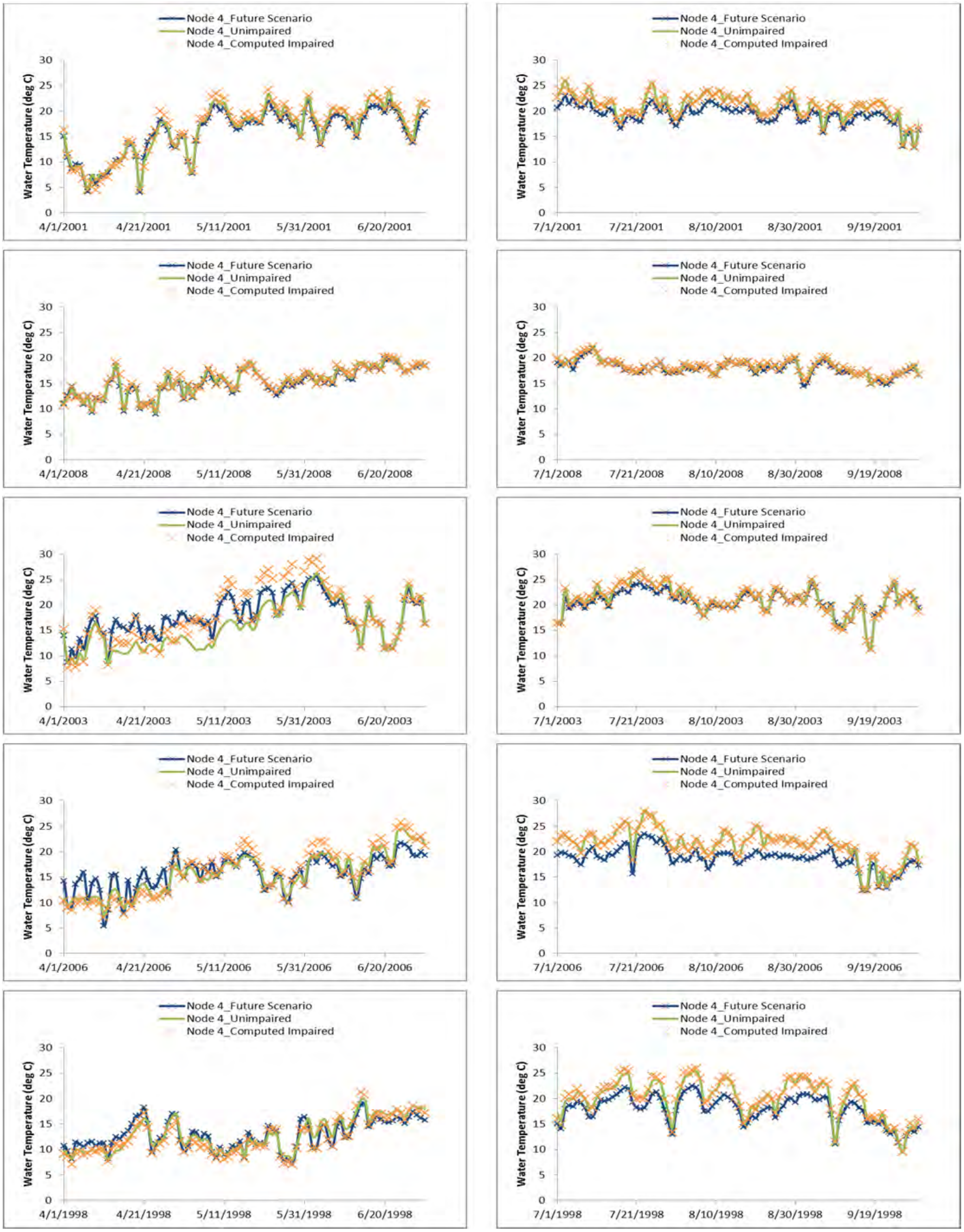

Figure 46. Water temperature at Node 4 for Scenario 2 (unimpaired), Scenario 5 (future), and Scenario 6 (computed impaired) from April to September for two Dry hydrologic years (2001, 2008), one hydrologic year on the Dry-Normal/Wet boundary (2003), and two Normal/Wet hydrologic years (2006, 1998).

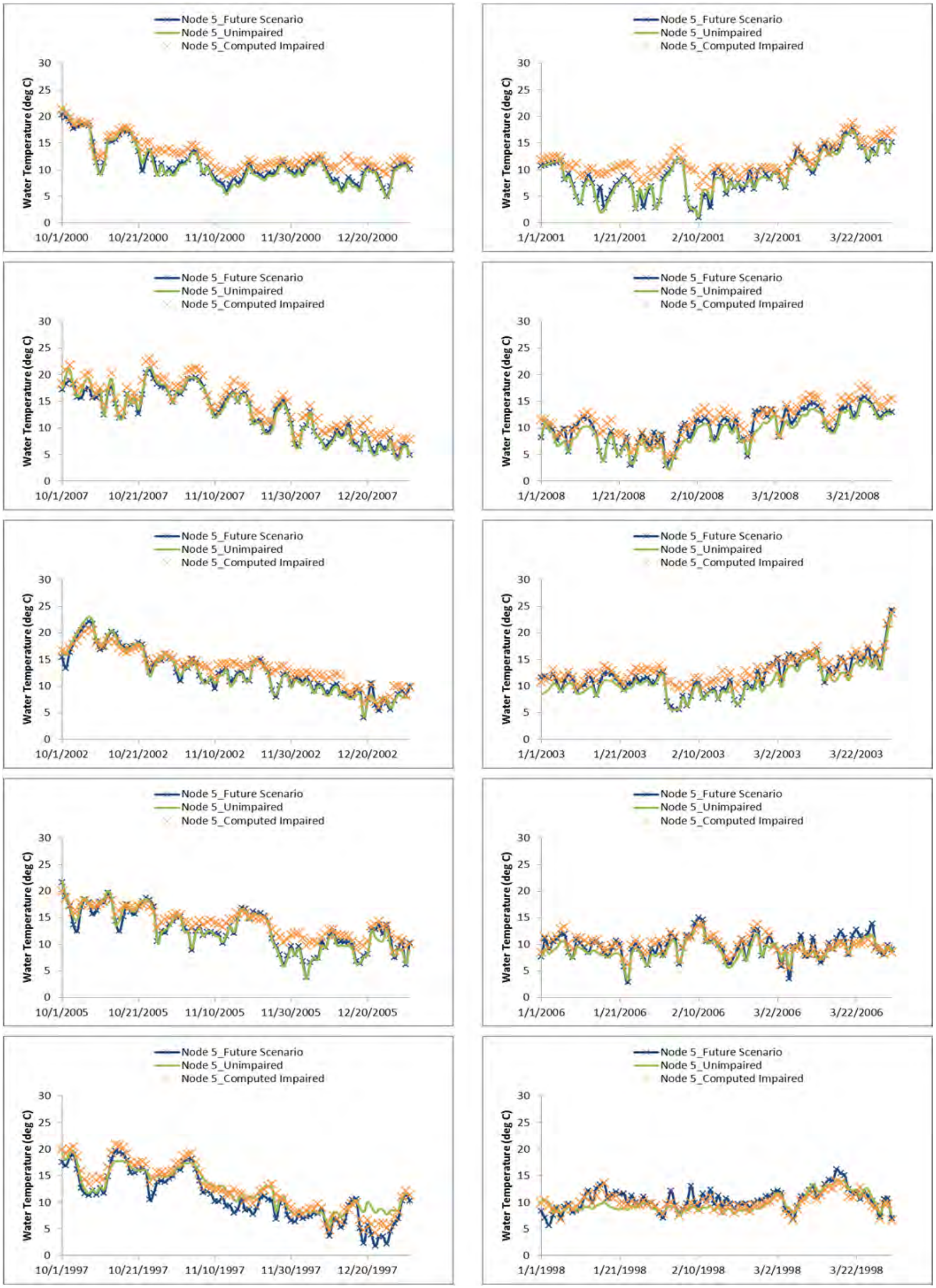

Figure 47. Water temperature at Node 5 for Scenario 2 (unimpaired), Scenario 5 (future), and Scenario 6 (computed impaired) from October to March for two Dry hydrologic years (2001, 2008), one hydrologic year on the Dry-Normal/Wet boundary (2003), and two Normal/Wet hydrologic years (2006, 1998).

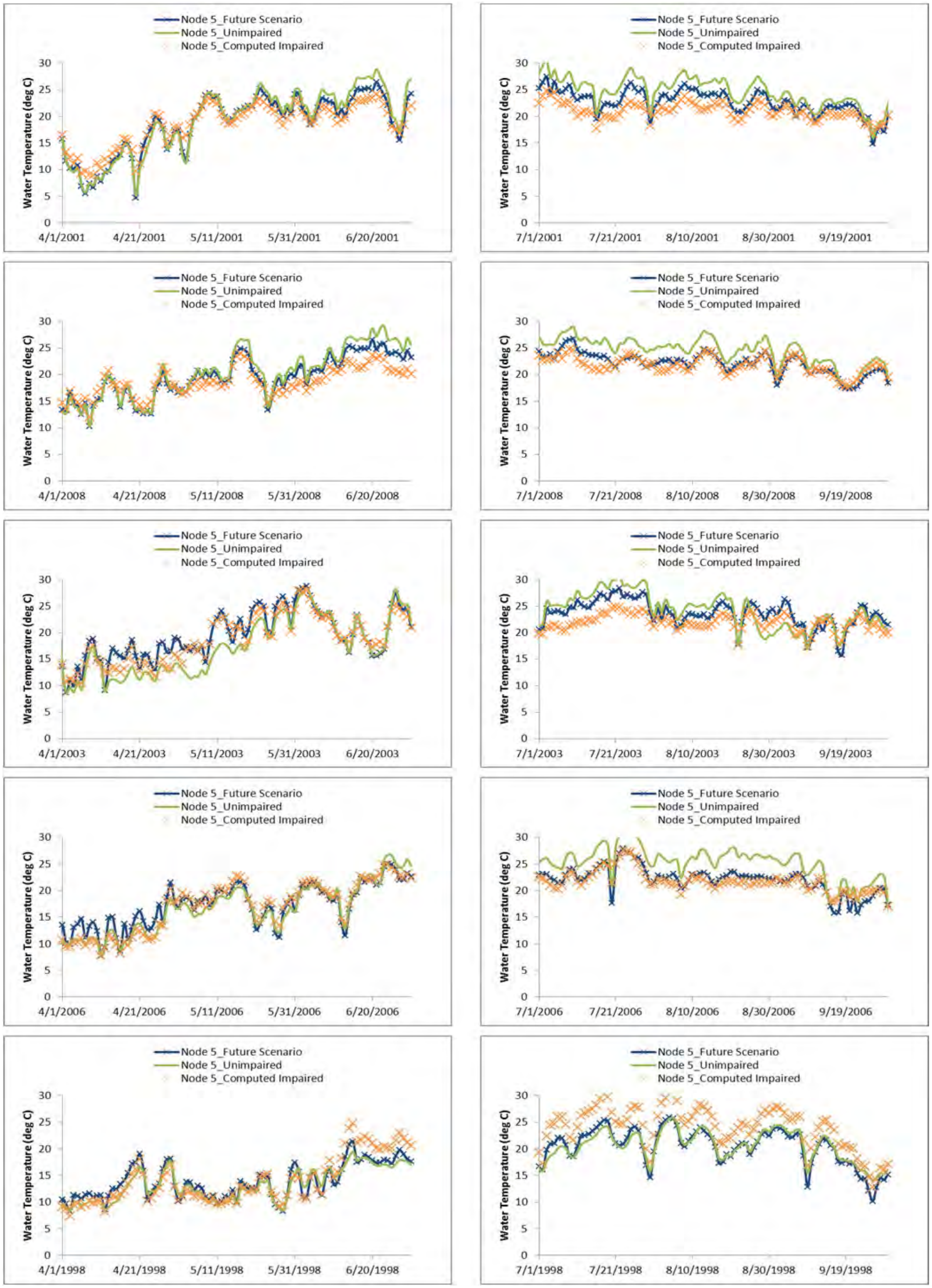

Figure 48. Water temperature at Node 5 for Scenario 2 (unimpaired), Scenario 5 (future), and Scenario 6 (computed impaired) from April to September for two Dry hydrologic years (2001, 2008), one hydrologic year on the Dry-Normal/Wet boundary (2003), and two Normal/Wet hydrologic years (2006, 1998).

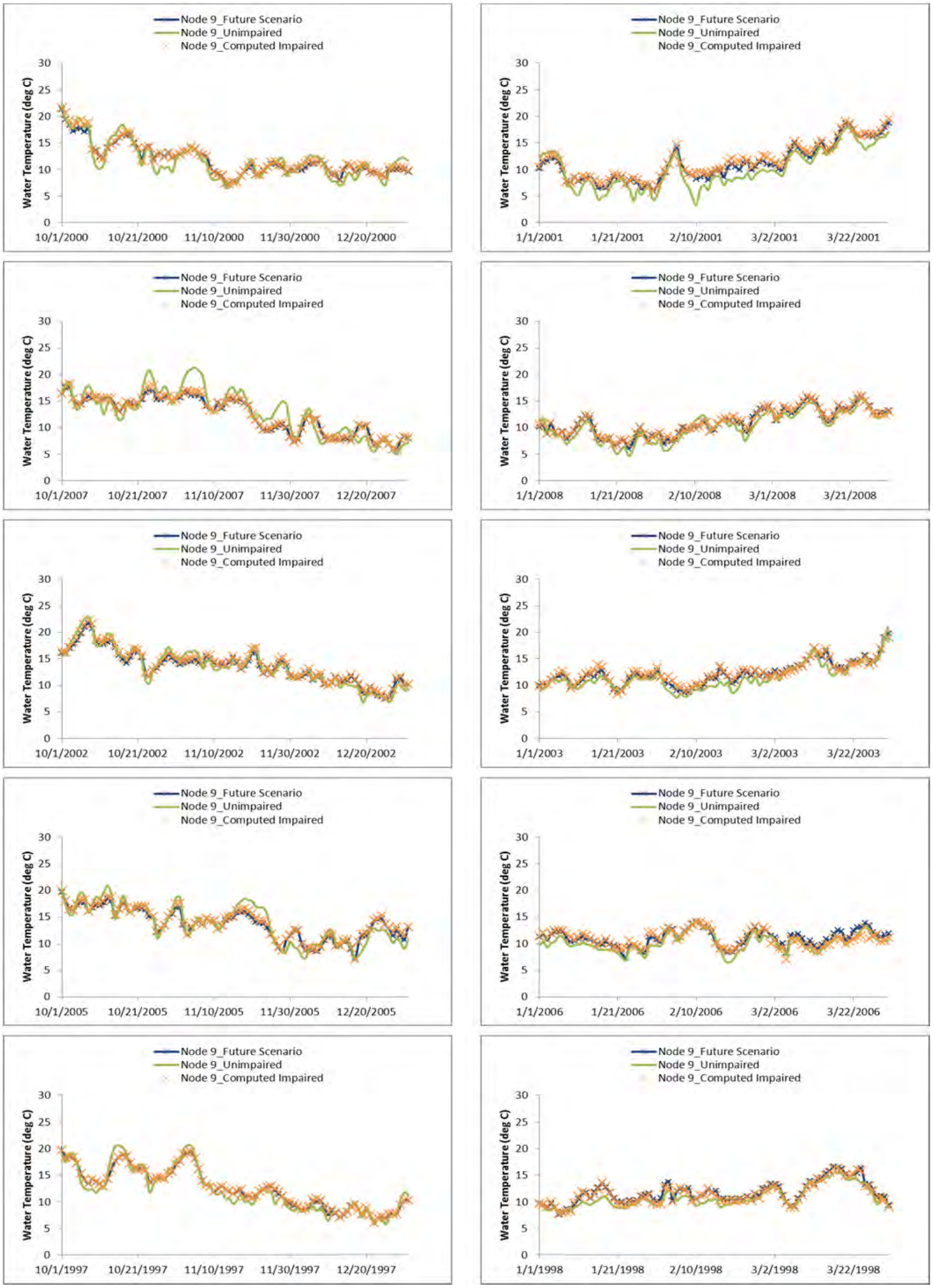

Figure 49. Water temperature at Node 9 for Scenario 2 (unimpaired), Scenario 5 (future), and Scenario 6 (computed impaired) from October to March for two Dry hydrologic years (2001, 2008), one hydrologic year on the Dry-Normal/Wet boundary (2003), and two Normal/Wet hydrologic years (2006, 1998).

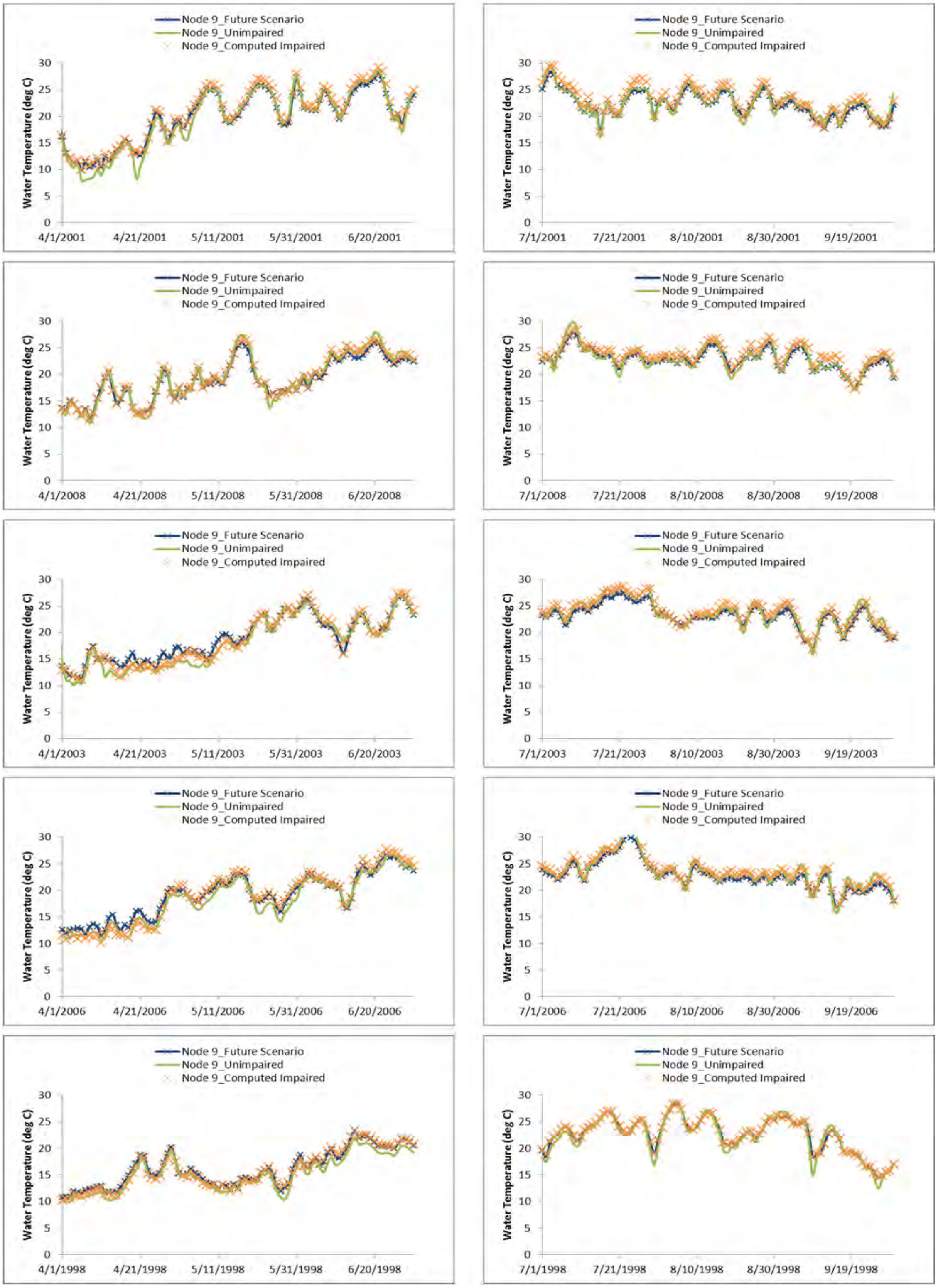

Figure 50. Water temperature at Node 9 for Scenario 2 (unimpaired), Scenario 5 (future), and Scenario 6 (computed impaired) from April to September for two Dry hydrologic years (2001, 2008), one hydrologic year on the Dry-Normal/Wet boundary (2003), and two Normal/Wet hydrologic years (2006, 1998).

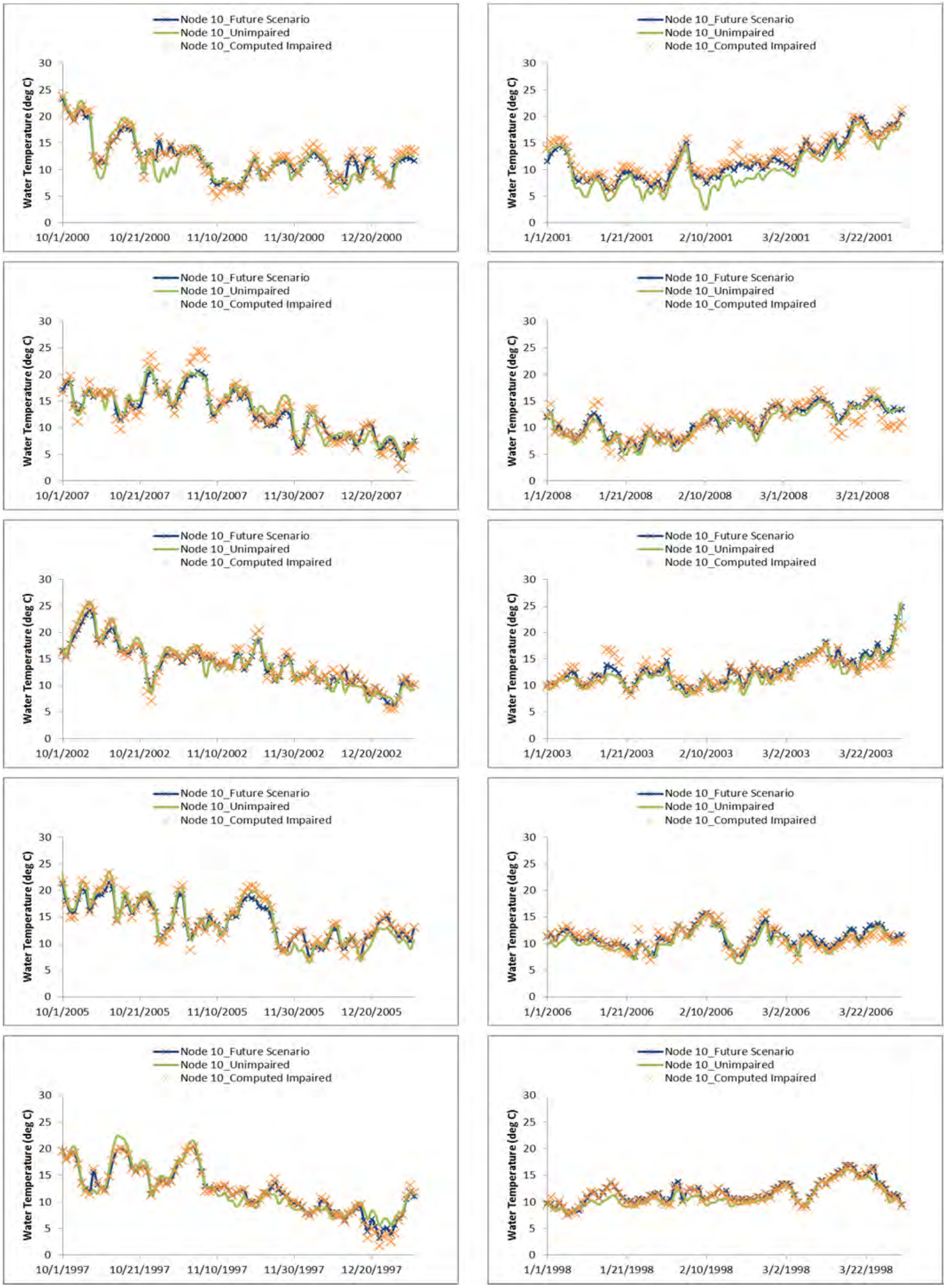

Figure 51. Water temperature at Node 10 for Scenario 2 (unimpaired), Scenario 5 (future), and Scenario 6 (computed impaired) from October to March for two Dry hydrologic years (2001, 2008), one hydrologic year on the Dry-Normal/Wet boundary (2003), and two Normal/Wet hydrologic years (2006, 1998).

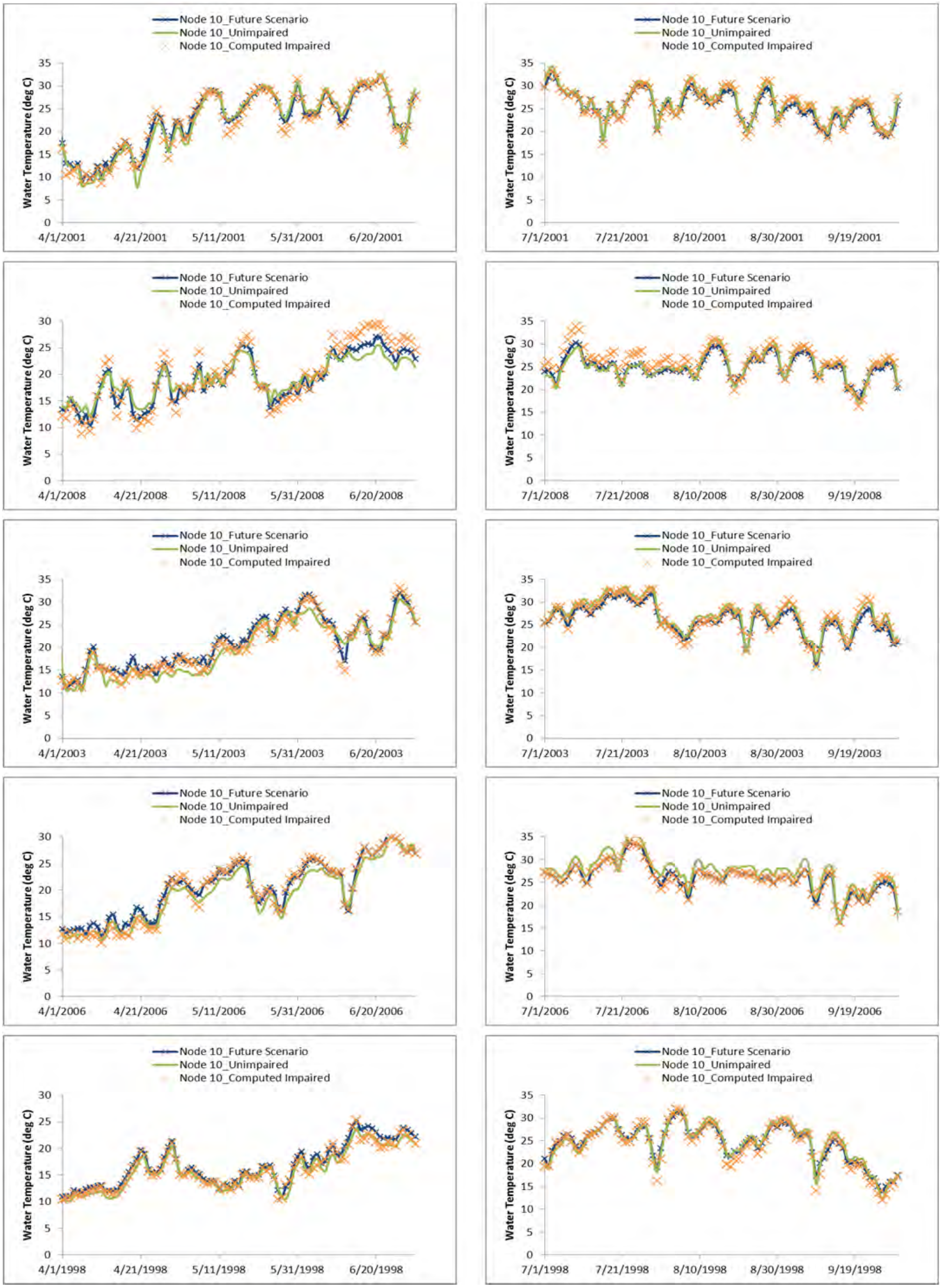

Figure 52. Water temperature at Node 10 for Scenario 2 (unimpaired), Scenario 5 (future), and Scenario 6 (computed impaired) from April to September for two Dry hydrologic years (2001, 2008), one hydrologic year on the Dry-Normal/Wet boundary (2003), and two Normal/Wet hydrologic years (2006, 1998).

3.3.2 Water temperature data reduction

Temperature output from the unsteady HEC-RAS model is used as input data for the EDT model, the bioenergetics growth model and the NGD model. The EDT model requires average water temperatures for each EDT segment, the NGD model requires temperature at four discrete modeling sites, and the bioenergetics model requires temperatures at each of its 500 ft computational sub-nodes. However, water temperature output from the unsteady HEC-RAS model was produced at the downstream cross section boundary of each computational cell in the model (see Section 3.3.1.1), which had variable lengths, and local variability due to predicted local tributary inputs and thermodynamic assumptions (incoming solar radiation, wind-speed, and other meteorological data). Therefore, the HEC-RAS output needed to be smoothed and standardized for use in the EDT, NGD, and bioenergetics models.

HEC-RAS cross sections representing each of the ASDHM nodes were identified, and a linear interpolation of water temperature between the cross sections representative of ASDHM nodes was developed to estimate temperature for the biological modeling efforts at 500 ft sub-node increments. The linear interpolation of water temperature between cross sections (near ASDHM nodes) provided a consistent temperature data output format for all the biological modeling efforts. Figure 53 shows an example comparison between the HEC-RAS unsteady water temperature output and the sub-node interpolations for 5/10/05. This interpolation was performed for sub-nodes for all scenarios over the HY1996-2009 time series and was provided to the various biological modeling teams.

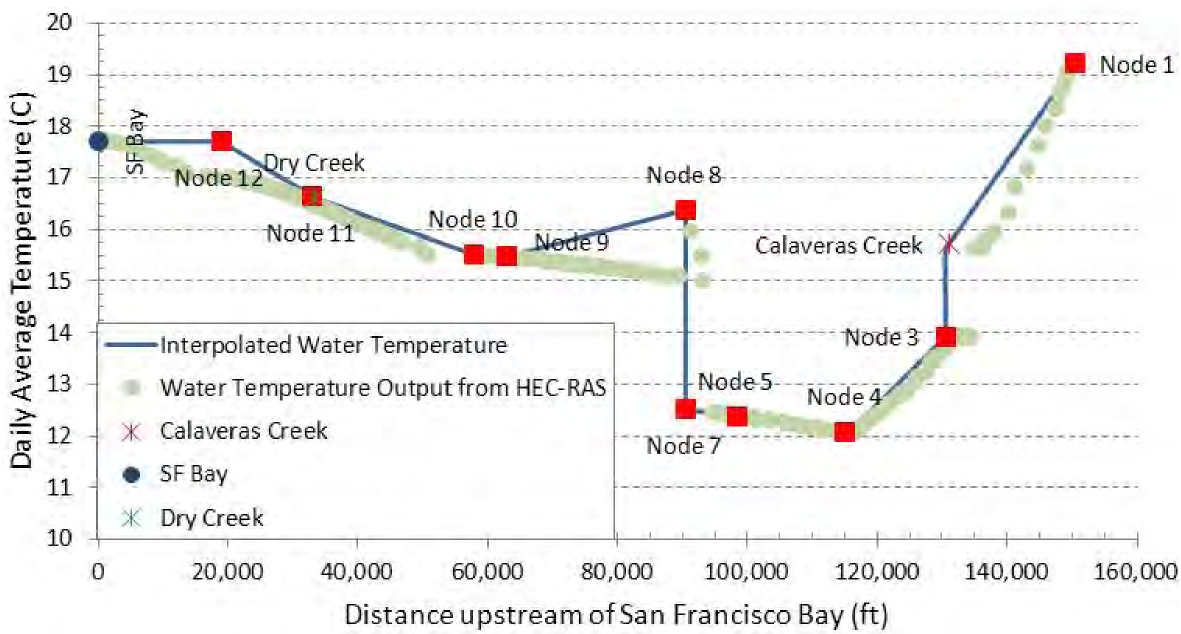

Figure 53. Example of HEC-RAS water temperature output and sub-node interpolations for Scenario 5 for 5/10/05.

4 RECOMMENDED NEXT STEPS

All of the output data from the analyses described in this report have been provided to the EDT and NGD/SRA modeling teams, so the primary purpose of this effort has been fulfilled. The modeling tools developed under this effort will likely continue to be refined by the ACWD and SFPUC as additional data become available. For example, additional cross sections and calibration data will likely be added to the steady state hydraulic model to improve its performance. The Fisheries Workgroup and individual agencies that have developed the modeling tools wanted consistency in the models, assumptions, and input data, such that all the Fisheries Workgroup participants were using the same data sets. This coordinated effort is expected to continue into the future, and the Fisheries Workgroup and agencies will need to decide upon a process to update the modeling tools so that improvements can be managed, and updated model versions can be documented and distributed in a structured way.

Improvements to these modeling tools will be driven by need. For example, per the 2008 Study Plan (M&T 2008), similar steelhead recovery efforts should be expanded into the Arroyo de la Laguna watershed, and specific improvements in the modeling tools may include:

- Incorporate dynamic flow loss assumptions for Sunol Valley into ASDHM as our understanding of infiltration loss mechanisms improves;
- Incorporate reservoir operations and dynamics at San Antonio Reservoir into ASDHM as was done with Calaveras Reservoir;
- Incorporate flow routing and storage dynamics between nodes into ASDHM;
- Continue the collaborative effort between Fisheries Workgroup agencies on additional data collection efforts to further refine the ASDHM and HEC-RAS modeling tools for common use in the Alameda Creek watershed;
- Expand the ASDHM model into the Arroyo de la Laguna watershed and its tributaries (rather than treating Arroyo de la Laguna as a single input to the model);
- Expand the HEC-RAS steady state model into the Arroyo de la Laguna watershed, focusing on key reaches where future restoration efforts will be prioritized. There are likely several HEC-RAS models already developed within the flood control system, so those should be utilized as much as possible to reduce costs and avoid redundancy; and
- Expand the HEC-RAS unsteady model into the Arroyo de la Laguna watershed to enable water temperature predictions in key reaches where future restoration efforts will be prioritized. Additional water temperature sensors should be installed within these key reaches to facilitate calibration of the water temperature model.

In addition, there may be additional informational needs within Alameda Creek that may benefit from improvements in the existing modeling tools. For example, the Sunol Valley Restoration Plan is investigating relationships between foothill yellow-legged frog breeding success as a function of flows, water temperatures, and channel morphology, which will likely require more detail and calibration in the hydraulic model to improve the accuracy of water surface elevation predictions at a few study sites where egg masses are likely to be found.

5 REFERENCES

Entrix, Inc. 2004. *Alameda Creek Juvenile Steelhead Downstream Migration Flow Requirements Evaluation*, Phase 1: Field Survey Results, 10 pp.

Erickson, T.R. and H.G. Stefan. 2000. Linear air/water temperature correlations for streams during open water periods. *Journal of Hydrologic Engineering* 5: 317-321.

Mann, M.P., Rizzardo, J., Satkowski, R. 2004. Evaluation of methods used for estimating selected streamflow statistics, and flood frequency and magnitude, for small basins in north coastal California. *USGS Scientific Investigations Report 2004-5068*. 92 pp.

McBain & Trush (M&T) 2008. *Alameda Creek population recovery strategies and instream flow assessment for steelhead trout, Final Study Plan.* Prepared for the Alameda Creek Fisheries Workgroup, January 2008, 56 pp.

Morrill, J.C., Bales, R.C., and M.H. Conklin. 2005. Estimating stream temperature from air temperature: Implications for future water quality. *Journal of Environmental Engineering* 131: 139-146.

National Marine Fisheries Service (NMFS), 2011. *Biological Opinion for Calaveras Dam Replacement Project in Alameda and Santa Clara Counties, California*, 83 pp.

Steiner, D.B 2007. *Water Supply System Modeling Report, Hetch Hetchy/Local Simulation Model,* Prepared by Daniel B. Steiner for the SFPUC, May 2007, 61 pp.

San Francisco Public Utilities Commission (SFPUC) 2010. *Alameda Creek Aquatic Resource Monitoring Report 1998 to 2007*, Vol. 1-2, San Francisco Public Utilities Commission, Water Enterprise, Natural Resources and Land Management Division Fisheries and Wildlife Section.

San Francisco Public Utilities Commission (SFPUC) 2011. *Final Environmental Impact Report, Vol. 1, Calaveras Dam Replacement Project,* San Francisco Public Utilities Commission.

Trihey & Associates, Inc., 2003. Sunol Valley Surface Flow Study fall 2001, Prepared for Office of the City Attorney, City and County of San Francisco

US Army Corps of Engineers (ACOE) 2008. HEC-RAS River Analysis System User's Manual v 4.0

Webb, B.W., P.D. Clack, and D.E. Walling. 2003. Water – air temperature relationships in a Devon river system and the role of flow. *Hydrological Processes* 17: 3069-3084.

6 APPENDIX A: ASDHM COMPUTATIONAL ASSUMPTIONS

Node 1

	Proposed Flow (Scenario 5)	Measured Impaired Flow (Scenario 4)	Unimpaired Flow (Scenario 1 and 2)
Primary data	Flow measured by USGS gage above ACDD (10/1/1995 – 9/30/2009)	Flow measured by USGS gage above ACDD (10/1/1995 – 9/30/2009)	Flow measured by USGS gage above ACDD (10/1/1995 – 9/30/2009)
ACDD tunnel capacity	370 cfs	650 cfs	N/A
ACDD tunnel operation period	As per BO (12/1-3/31)	No restriction. Historic record	N/A
Influence of Calaveras Reservoir being full	ACDD tunnel closed	ACDD tunnel operation based on historic record	N/A
Instream flow requirement	As per BO	None	N/A

*Impaired flow = measured impaired; assumptions for computed impaired is same as proposed flow except for instream flow

Node 2

	Proposed Flow (Scenario 5)	Measured Impaired Flow (Scenario 4)	Unimpaired Flow (Scenario 1 and 2)
Primary data	Instream flow from Calaveras Reservoir as per BO and simulated Calaveras level for Reservoir spill	Flow measured by USGS gage below Calaveras dam ACDD (05/23/2002 – 9/30/2009)	Flow measured by USGS gage at Arroyo Hondo scaled to DA at USGS gage below Calaveras Dam (10/01/1995 – 9/30/2009)
Calaveras Reservoir spillway rating and spill level	New dam spillway rating, spill elevation 756.2 ft (NGVD 1929)	Existing dam spillway rating, spill elevation 756.2 ft (NGVD 1929)	N/A
Calaveras transfer to San Antonio Reservoir and Sunol Valley Water Treatment Plant	Historical	Historical	N/A
Contribution from unregulated area between Calaveras Dam and the USGS gage site below Calaveras Dam	Omitted	Omitted	Included in USGS gage drainage area
Seepage from Calaveras Reservoir	0.1 cfs	N/A	N/A

Node 3

	Proposed Flow (Scenario 5)	Measured Impaired Flow (Scenario 4)	Unimpaired Flow (Scenario 1 and 2)
Primary data	Computed flow at Node 1 and Node 2 (10/01/1995 – 9/30/2009)	Computed flow at Node 1 and Node 2 (10/01/1999 – 9/30/2009)	Computed flow at Node 1 and Node 2 (10/01/1995 – 9/30/2009)
Contribution from unregulated area between Calaveras gage and the confluence of Alameda and Calaveras Creeks in Calaveras Creek watershed	Estimated based on drainage area ratio using Arroyo Hondo flow measured by USGS gage	Estimated based on drainage area ratio using Arroyo Hondo flow measured by USGS gage	Omitted
Contribution from unregulated area between upper Alameda Creek gage and the confluence of Alameda and Calaveras Creeks in Alameda Creek watershed	Estimated based on drainage area ratio using upper Alameda Creek flow measured by USGS gage	Estimated based on drainage area ratio using upper Alameda Creek flow measured by USGS gage	Estimated based on drainage area ratio using above ACDD USGS gage (10/1/1996-9/30/1999), computed from subtracting USGS gages on Calaveras and above ACDD from Confluence gage (10/1/1999-9/30/2009)

Node 4

	Proposed Flow (Scenario 5)	Measured Impaired Flow (Scenario 4)	Unimpaired Flow (Scenario 1 and 2)
Primary data	Computed flow at Node 3 (10/01/1995 – 9/30/2009)	Computed flow at Node 3 (10/01/1999 – 9/30/2009)	Computed flow at Node 3 (10/01/1995 – 9/30/2009),
Contribution from unregulated area between the confluence of Alameda and Calaveras Creeks and the confluence of Alameda and Welch Creeks	Estimated based on drainage area ratio using upper Alameda Creek flow measured by USGS gage	Estimated based on drainage area ratio using upper Alameda Creek flow measured by USGS gage	Estimated based on drainage area ratio using above ACDD USGS gage (10/1/1996-9/30/1999), computed from subtracting USGS Confluence gage from Welch Creek gage (10/1/1999-9/30/2009)

Node 5

	Proposed Flow (Scenario 5)	Measured Impaired Flow (Scenario 4)	Unimpaired Flow (Scenario 1 and 2)
Primary data	Computed flow at Node 3 (10/01/1995 – 9/30/2009)	Computed flow at Node 3 (10/01/1999 – 9/30/2009)	Computed flow at Node 4 (10/01/1995 – 9/30/2009)
Contribution from unregulated area between the confluence of Alameda and Calaveras Creeks and the confluence of Alameda and San Antonio Creeks	Estimated based on drainage area ratio using upper Alameda Creek flow measured by USGS gage	Estimated based on drainage area ratio using upper Alameda Creek flow measured by USGS gage	Estimated based on drainage area ratio using above ACDD USGS gage
Losses between Node 4 and Node 5	Constant loss with four options ranging from 0 cfs to 17 cfs. EDT run assumes 17 cfs constant loss.	Constant loss with four options ranging from 0 cfs to 17 cfs. EDT run assumes 17 cfs of constant loss.	No Loss
Recapture of water by filter gallery	Option of recapturing supplemental flow of up to 20 cfs. EDT run assumes no recapturing	N/A	N/A

Node 6

	Proposed Flow (Scenario 5)	Measured Impaired Flow (Scenario 4)	Unimpaired Flow (Scenario 1 and 2)
Primary data	Computed flow at Node 5 (10/01/1995 – 9/30/2009)	Computed flow at Node 5 (10/01/1999 – 9/30/2009)	Computed flow at Node 5 (10/01/1995 – 9/30/2009)
Spill from San Antonio Reservoir	Historical Observation by USGS gage 10/1/1999-09/30/2009. Historical spill empirically estimated from 10/1/1995 to 09/30/1999	Historical Observation by USGS gage 10/1/1999-09/30/2009. Historical spill empirically estimated from 10/1/1995 to 09/30/1999	Flow at the USGS gage site in San Antonio Cr. estimated based on monthly runoff volume ratio between above ACDD USGS gage and inflow into San Antonio Reservoir
Contribution from drainage areas below San Antonio dam to the USGS gage site, and USGS gage site to the confluence with Alameda Cr.	Provision of incorporating this using relationship between upper Alameda Cr. flow and San Antonio Creek flow when San Antonio dam is not spilling. However, EDT run neglects this component.	Provision of incorporating this using relationship between upper Alameda Cr. flow and San Antonio Creek flow when San Antonio dam is not spilling. However, EDT run neglects this component.	Omitted
Losses in San Antonio Creek	Provision of incorporating constant losses. However, EDT run neglects this component.	Provision of incorporating constant losses. However, EDT run neglects this component.	No Loss
Gain from Quarry Pits	Provision of incorporating historic data. However, EDT run neglects this component.	Historical data provided by Hansen is used to estimate inflow to Alameda Cr. from Quarry pits.	No Gain

Node 7

	Proposed Flow (Scenario 5)	Measured Impaired Flow (Scenario 4)	Unimpaired Flow (Scenario 1 and 2)
Primary data	Computed flow at Node 6 (10/01/1995 – 9/30/2009)	Computed flow at Node 6 (10/01/1999 – 9/30/2009)	Computed flow at Node 6 (10/01/1995 – 9/30/2009)
Contribution from unregulated area between the confluence of Alameda and San Antonio Creeks and the confluence of Alameda and Arroyo de la Laguna Creeks	Estimated based on drainage area ratio using upper Alameda Creek flow measured by USGS gage	Estimated based on drainage area ratio using upper Alameda Creek flow measured by USGS gage	Estimated based on drainage area ratio using above ACDD USGS gage

Node 8

	Proposed Flow (Scenario 5)	Measured Impaired Flow (Scenario 4)	Unimpaired Flow (Scenario 2)
Primary data	Computed flow at Node 7 (10/01/1995 – 9/30/2009)	Computed flow at Node 7 (10/01/1999 – 9/30/2009)	Computed flow at Node 7 (10/01/1995 – 9/30/2009)
Contribution from Arroyo de la Laguna	Historical Observation by USGS gage 10/1/1999-09/30/2009.	Historical Observation by USGS gage 10/1/1999-09/30/2009.	Winter flows computed based on drainage area ratio using Arroyo Mocho USGS gage, summer flows estimated from 1912-1930 flows at USGS Verona gage.
Water diverted to Vallecitos Cr. from South Bay Aqueduct for ACWD (cfs)	Historical data provided by ACWD	Historical data provided by ACWD	N/A
Additional Water Released to Vallicitos Cr. from SBA to release the pressure	Lack of data. Currently omitted.	Lack of data. Currently omitted.	N/A
Vallecitos Creek Natural Flow	Estimated based on drainage area ratio using upper Alameda Creek flow measured by USGS gage	Estimated based on drainage area ratio using upper Alameda Creek flow measured by USGS gage	Estimated based on drainage area ratio using Dry Creek flow measured by USGS gage
Sinbad Creek Natural Flow	Estimated based on drainage area ratio using upper Dry Creek flow measured by USGS gage	Estimated based on drainage area ratio using upper Dry Creek flow measured by USGS gage	Estimated based on drainage area ratio using upper Dry Creek flow measured by USGS gage

Node 9

	Proposed Flow (Scenario 5)	Measured Impaired Flow (Scenario 4)	Unimpaired Flow (Scenario 2)
Primary data	Computed flow at Node 8 (10/01/1995 – 9/30/2009)	Computed flow at Node 8 (10/01/1999 – 9/30/2009)	Computed flow at Node 8 (10/01/1995 – 9/30/2009)
Contribution from small Alameda Cr. watershed between Arroyo de la Laguna and Stonybrook Creek	Estimated based on drainage area ratio using upper Dry Creek flow measured by USGS gage	Estimated based on drainage area ratio using upper Dry Creek flow measured by USGS gage	Estimated based on drainage area ratio using upper Dry Creek flow measured by USGS gage
Stonybrook Creek Natural Flow	Estimated based on drainage area ratio using upper Dry Creek flow measured by USGS gage	Estimated based on drainage area ratio using upper Dry Creek flow measured by USGS gage	Estimated based on drainage area ratio using upper Dry Creek flow measured by USGS gage
Contribution from small Alameda Cr. watershed between Stonybrook and Niles Gage (cfs)	Estimated based on drainage area ratio using upper Dry Creek flow measured by USGS gage	Estimated based on drainage area ratio using upper Dry Creek flow measured by USGS gage	Estimated based on drainage area ratio using upper Dry Creek flow measured by USGS gage

Node 10 for Unimpaired

	Proposed Flow (Scenario 5)	Measured Impaired Flow (Scenario 4)	Unimpaired Flow (Scenario 2)
Primary data			Computed flow at Node 9 (10/01/1995 – 9/30/2009)
Instream flow requirement			N/A
PUC flows contributing to Niles			N/A
Niles Cone percolation			Assumed zero
Historical Old Alameda Cr. Diversion			N/A
Contribution from Natural Watershed Between Node 9 and Node 10			Estimated based on drainage area ratio using upper Dry Creek flow measured by USGS gage

Node 10 without ACWD bypass flow (calculated after Node 11 calculation; with ACWD bypass flow, Node 10 is estimated in ACWD bypass template)

	Proposed Flow (Scenario 5)	Measured Impaired Flow (Scenario 4)	Unimpaired Flow (Scenario 2)
Primary data	Computed flow at Node 11 (10/01/1995 – 9/30/2009)	Computed flow at Node 11 (10/01/1999 – 9/30/2009)	
Contribution from Natural Watershed Between Node 10 and Node 11	Estimated based on drainage area ratio using upper Dry Creek flow measured by USGS gage	Estimated based on drainage area ratio using upper Dry Creek flow measured by USGS gage	
Contribution from urban watershed between Node 10 and Node 11	Estimated based on drainage area ratio using San Lorenzo Cr. flow measured by USGS gages	Estimated based on drainage area ratio using San Lorenzo Cr. flow measured by USGS gages	
Old Alameda Cr. Diversion (cfs)	Maximum of 40 cfs for flows incrementally greater than 2640 cfs at Node 11.	Maximum of 40 cfs for flows greater than 2640 cfs at Node 11.	

Node 10 with ACWD bypass flow

	Proposed Flow (Scenario 5)	Measured Impaired Flow (Scenario 4)	Unimpaired Flow (Scenario 2)
Primary data	Computed flow at Node 9 (10/01/1995 – 9/30/2009)	Computed flow at Node 9 (10/01/1999 – 9/30/2009)	
Instream flow requirement	Provided by ACWD	N/A	
PUC flows contributing to Niles	Node 1 + Node 2 – Sunol valley loss. Assumes a day lag time	N/A	
Niles Cone percolation	A constant loss of 12 cfs	N/A	
Historical Old Alameda Cr. Diversion	Maximum of 40 cfs for flows incrementally greater than 2640 cfs for observed flow at Union city USGS gage.	Maximum of 40 cfs for flows incrementally greater than 2640 cfs for observed flow at Union city USGS gage.	
Contribution from Natural Watershed Between Node 10 and Node 11	Estimated based on drainage area ratio using upper Dry Creek flow measured by USGS gage	Estimated based on drainage area ratio using upper Dry Creek flow measured by USGS gage	
Contribution from urban watershed between Node 10 and Node 11	Estimated based on drainage area ratio using San Lorenzo Cr. flow measured by USGS gages	Estimated based on drainage area ratio using San Lorenzo Cr. flow measured by USGS gages	
ACWD historical observed diversions, percolation, storage, and runoff of Alameda Creek water	Estimated using observed flows at Nodes 9,11, and contribution from natural and urban watersheds, and diversions from Vallecitos and Old Alameda Creeks.	N/A	

Node 11 Unimpaired

	Proposed Flow (Scenario 5)	Measured Impaired Flow (Scenario 4)	Unimpaired Flow (Scenario 2)
Primary data			Computed flow at Node 10 (10/01/1995 – 9/30/2009)
Contribution from Natural Watershed Between Node 10 and Node 11			Estimated based on drainage area ratio using upper Dry Creek flow measured by USGS gage
Contribution from urban watershed between Node 10 and Node 11			N/A
Old Alameda Cr. Diversion			N/A

Node 11 without ACWD bypass flows

	Proposed Flow (Scenario 5)	Measured Impaired Flow (Scenario 4)	Unimpaired Flow (Scenario 2)
Primary data	Computed flow at Node 9 (10/01/1995 – 9/30/2009)	Computed flow at Node 9 (10/01/1999 – 9/30/2009)	
Historical contribution from watershed between Node 9 and Node 11	Estimated based on observed flows at USGS ALAMEDA Cr NR NILES (11179000) and USGS Alameda Cr at Flood Channel Union City USGS gage (11180700)	Estimated based on observed flows at USGS ALAMEDA Cr NR NILES (11179000) and USGS Alameda Cr at Flood Channel Union City USGS gage (11180700)	

Node 11 with ACWD bypass flows

	Proposed Flow (Scenario 5)	Measured Impaired Flow (Scenario 4)	Unimpaired Flow (Scenario 2)
Primary data	Computed flow at Node 10 (10/01/1995 – 9/30/2009)	Computed flow at Node 10 (10/01/1999 – 9/30/2009)	
Contribution from Natural Watershed Between Node 10 and Node 11	Estimated based on drainage area ratio using upper Dry Creek flow measured by USGS gage	Estimated based on drainage area ratio using upper Dry Creek flow measured by USGS gage	
Contribution from urban watershed between Node 10 and Node 11	Estimated based on drainage area ratio using San Lorenzo Cr. flow measured by USGS gages	Estimated based on drainage area ratio using San Lorenzo Cr. flow measured by USGS gages	
Old Alameda Cr. Diversion	Maximum of 40 cfs for flows incrementally greater than 2640 cfs at Node 11.	Maximum of 40 cfs for flows incrementally greater than 2640 cfs at Node 11.	

Node 12

	Proposed Flow (Scenario 5)	Measured Impaired Flow (Scenario 4)	Unimpaired Flow (Scenario 2)
Primary data	Computed flow at Node 11 (10/01/1995 – 9/30/2009)	Computed flow at Node 11 (10/01/1999 – 9/30/2009)	Computed flow at Node 11 (10/01/1995 – 9/30/2009)
Contribution from Natural Watershed Between Node 11 and Node 12	Estimated based on drainage area ratio using upper Dry Creek flow measured by USGS gage	Estimated based on drainage area ratio using upper Dry Creek flow measured by USGS gage	Estimated based on drainage area ratio using upper Dry Creek flow measured by USGS gage
Contribution from urban watershed between Node 10 and Node 11	Estimated based on drainage area ratio using San Lorenzo Cr. flow measured by USGS gages	Estimated based on drainage area ratio using San Lorenzo Cr. flow measured by USGS gages	N/A

7 APPENDIX B: CD OF FLOWS AND WATER TEMPERATURE DATA FOR 1996-2009 FOR SCENARIOS 1, 2, 4, 5, AND 6